METABOLIC ENGINEERING AND PROCESS DEVELOPMENT IN BUTANOL PRODUCTION WITH CLOSTRIDIUM TYROBUTYRICUM

by

CHAO MA

X MARGARET LIU, COMMITTEE CHAIR

STEPHEN M.C. RITCHIE
YONGHYUN KIM
RYAN SUMMERS
JANNA FIERST

A DISSERTATION

Submitted in partial fulfillment of the requirements
for the degree of Doctor of Philosophy
in the Department of Chemical and Biological Engineering
in the Graduate School of
The University of Alabama

TUSCALOOSA, ALABAMA

2016

ABSTRACT

As a sustainable and environmentally friendly biofuel, biobutanol is a potential substitute for gasoline without any engine modification. The multiple Omics studies were applied to evaluate the change of the expression of host protein and intracellular metabolism in *Clostridium tyrobutyricum* in response to butanol production. The key enzymes related to carbon balance (i.e. acid and solvent end products and carbohydrates in central pathway), redox balance, energy balance, and cell growth has been studied. It was found that rebalancing both carbon and redox was critical to improve butanol production. These findings were used to achieve high production of biobutanol via integrated metabolic cell-process engineering (MCPE).

In a comparative genomics study, the wild type *C. tyrobutyricum*, the metabolically engineered mutant with down-regulated acetate kinase and evolutionarily engineered strain showing fast cell growth were used to evaluated in butyrate fermentation at pH 6.0 and 37 ^{o}C. It was found that the cell growth rate was increased by 61-100% and butyrate productivity was improved by 44-102% by the evolutionarily engineered strain. To understand the mechanism of butyric acid production and cell growth regulation in engineered *C. tyrobutyricum* mutant, a comparative genomics study was performed. It was concluded that the genome mutations in transcription, translation, amino acid and phosphate transportation and cofactor binding might play important role in regulating cell growth and butyric acid production.

Comparative proteomics, which covered 78.1% of open reading frames and 95% of core enzymes, was performed using wild type, mutant producing 37.30 g/L of butyrate and mutant

producing 16.68 g/L of butanol. Carbon regulation enzymes in the central metabolic pathway that correlated with butanol production were identified, including thiolase (*thl*), acetyl-CoA acetyltransferase (*ato*), 3-hydroxybutyryl-CoA dehydrogenase (*hbd*) and crotonase (*crt*). The apparent imbalance of energy and redox was also observed due to the downregulation of acids production and the addition of butanol synthesis pathway. The understanding of the mechanism of carbon redistribution enabled the rational design of metabolic cell and process engineering strategies were revealed to achieve high butanol production in *C. tyrobutyricum*.

With the fundamental understanding, the *C. tyrobutyricum* was metabolically engineered by rebalancing carbon and redox simultaneously. The overexpression of aldehyde/alcohol dehydrogenase (*adhE2*) and formate dehydrogenase (*fdh*) improved butanol titer by 2.15 fold in serum bottle and 2.72 fold in bioreactor. In addition, the proteomics study and metabolite analysis showed that more than 90% of the amino acid in the medium was consumed before the cell entered the stationary phase and some enzymes involved in amino acid metabolism had low expression in butanol producing mutant. Extra yeast extract or casamino acids was fed to the free-cell fermentation the mid-log phase, improving the butanol titer to more than 18 g/L compared to 14 g/L without extra nitrogen supplement. The rational metabolic cell-process engineering facilitated with systems biology understanding was demonstrated a powerful approach in butanol production.

Finally, the *C. tyrobutyricum* was further rationally engineered by integrating multiple regualtors, including 1) heterologous NAD^+-fdh that provides extra reducing power, 2) the thiolase (*thl*) that redirects metabolic flux from C2 to C4, and 3) AdhE2. Two novel mutatns, ACKKO-*adhE2-fdh* and ACKKO-*thl-adhE2-fdh*, were constructed and produced 18.37 g/L and 19.41 g/L, respectively. This study demonstrated that systems biology-based metabolic cell-process engineering of *C. tyrobutyricum* enabled a high production of butanol

DEDICATION

This dissertation is dedicated to everyone who helped me and guided me through the trials and tribulations of creating this manuscript. In particular, my family and close friends who stood by me throughout the time taken to complete this masterpiece

LIST OF ABBREVIATIONS AND SYMBOLS

AA Amino acid

ABE Acetone-Butanol-Ethanol

ack Acetate kinase

adc Acetoacetate decarboxylase

adh Alcohol dehydrogenase

adhE2 Aldehyde/alcohol dehydrogenase

ato Acetyl-CoA acetyltransferase

bdh Butanol dehydrogenase

buk Butyrate kinase

CGM Clostridial Growth Medium

CID Collision-induced dissociation

Cm Chloramphenicol

ctf CoA-transferases

Em Erythromycin

EMP Embden-Meyerhof-Parnas

etf Electron transfer flavoproteins

FBB Fibrous-bed bioreactor

fdh Formate dehydrogenase

FdH_2 Reduced ferredoxi

fnor Ferredoxin NADH oxidoreductase

fpl Pyruvate-formate lyase

GC Gas chromatograph

glpA Glycerol-3-phosphate dehydrogenase

hbd 3-hydroxybutyryl-CoA dehydrogenase

HPLC High performance liquid chromatography

Hsp Heat shock protein expression

hydA Hydrogenase A

Kan Kanamycin

MS Mass Spectrometer

MVH Methyl viologen hydrate

NGS Next generation sequencing

OD_{600} Optical density at 600 nm

PAGE Polyacrylamide gel electrophoresis

pgk Phosphoglycerate kinase

pta Phosphotrans acetyrylase

ptb Phosphotransbutyrylase

pfor Pyruvate–ferredoxin oxidoreductase

pyk Pyruvate kinases

RCM Reinforced Clostridium Medium

SDS Sodium dodecyl sulfate

SF Sodium formate

solR Transcriptional activator protein

Spo0A Sporulation transcription factor

thl Thiolase

Tm Thiamphenicol

WT Wild type

ACKNOWLEDGMENTS

First of all, I am pleased to have this opportunity to thank my advisor, Dr. Xiaoguang (Margaret) Liu. Dr. Liu has maintained an excellent level of patience, inspiring advisement, and continuous encouragement throughout all of my study at The University of Alabama. She has been teaching me all about knowledge in laboratory work and in scientific communication. I am very grateful to have an opportunity to work in Dr. Liu's lab. She is not only an advisor of my research, but also a friend and mentor of my life.

I would like to thank all of my committee members, Dr. Stephen M.C. Ritchie, Dr. Yonghyun Kim, Dr. Ryan Summers, and Dr. Janna Fierst, for their invaluable suggestions and insightful recommendation for my academic research.

I would like to appreciate Dr. Shang-Tian Yang at the Ohio State University, Nigel P. Minton at the University of Nottingham, and Dr. E.T. Papoutsakis at University of Delaware, for their supports for this research.

I would also like to recognize my research group colleague, Jianfa Ou. Jianfa offered me a lot of useful and insightful suggestions in my research. I would also like to thank all the previous and current undergraduate research assistant in our lab, Robert Lind, Laruen Mathew, Carson Dietrich, Michael Leffler, Whitney Smith, Christine Gomez, Rebecca Beasley, Zac Gentle, Elizabeth Parcher, and Brittany A Artale.

The BRIGE grant (24512) from the National Science Foundation and the start-up fund from the University of Alabama are acknowledged

Finally, I would like to give my special thanks to my wife, Ningning Xu, and my parents, Mr. Yunqing Ma and Ms. Xiujuan Wang, for their enormous support in my life

CONTENTS

ABSTRACT ii

DEDICATION iv

LIST OF ABBREVIATIONS AND SYMBOLS v

ACKNOWLEDGMENTS viii

LIST OF TABLES xvi

LIST OF FIGURES xviii

CHAPTER 1 INTRODUCTION 1

1.1 Biobutanol Poduction through ABE Fermentation 2

1.1.1 Solventogenic Clostridial Strains 2

1.1.2 Strain Modification by Metabolic Engineering 3

1.2 *C. tyrobutyricum* and Butanol Biosynthesis in *C. tyrobutyricum* 4

1.2.1 Solvent Production in *C. tyrobutyricum* 4

1.2.2 Metabolic Engineering & Process Development in *C. tyrobutyricum* 5

1.3 Comparative Genomics and Proteomics 6

1.3.1 Comparative Genomics 6

1.3.2 Comparative Proteomics 7

1.4 Hypothesis of this study 8

1.5 References 11

CHAPTER 2 COMPARATIVE PROTEOMICS ANALYSIS 20

2.1. Introduction 21

2.2. Materials and Methods 22
2.2.1 Strains and Media 22
2.2.2 Fermentation Kinetics 23
2.2.3 Fermentation Products Titration 24
2.2.4 Proteomics: GeLC-MS/MS 24
2.2.5 Fatty Acid and Amino Acid Analysis 26
2.3. Results 27
2.3.1. Cell Growth 27
2.3.2. Acids and Alcohols Production 28
2.3.3. Comparative Proteomics 29
2.3.4. Carbon Metabolism 30
2.3.5. Energy Metabolism 32
2.3.6. Redox Metabolism 33
2.3.7. Cellular Responses to Metabolic Engineering 34
2.3.8. Metabolite Analysis 35
2.4. Discussion 37
2.4.1 Proteomics study of *C. tyrobutyricum* 37
2.4.2 Carbon Redistribution 38
2.4.3 Rational Metabolic Engineering 39
2.5. Conclusions 41
2.6. References 43
CHAPTER 3 HIGH PRODUCTION OF BUTYRIC ACID 56
3.1. Introduction 57

3.2. Materials and Methods 59
3.2.1 Cultures and Media 59
3.2.2 Fermentation Kinetic Study 59
3.2.3 Analytical Methods 59
3.2.4 Metabolic Flux Analysis 60
3.3. Results and Discussion 60
3.3.1 Kinetics of Free-cell Fermentation 60
3.3.2 Effect of pH on Butyric Acid Fermentation 62
3.3.3 Metabolic Flux Balance Analysis 63
3.4. Conclusion 64
3.5. References 66
CHAPTER 4 CHARACTERIZATION OF ENGINEERED MUTANT 77
4.1 Introduction 78
4.2 Materials and Methods 79
4.2.1 Strains, Cultures and Media 79
4.2.2 Butyrate Fermentation 80
4.2.3 Comparative Genomics Analysis 81
4.2.4 Analytical Methods 81
4.3 Results 82
4.3.1 Fermentation with PAK-Em 82
4.3.2 Characterization of Hyd-Em by Genomics Analysis 83
4.4 Discussion 85
4.4.1 Engineering of *C. tyrobutyricum* 85

4.4.2 Genomics of *C. tyrobutyricum* 86
4.4.3 Advantages of Immobilized-cell Butyrate Fermentation 87
4.5 Conclusions 87
4.6 References 88
CHAPTER 5 REBALANCING REDOX TO IMPROVE BIOBUTANOL PRODUCTION .. 95
5.1 Introduction 96
5.2 Materials and Methods 97
5.2.1 Strains and Media 97
5.2.2 Plasmid Construction 98
5.2.3 Mutant Construction 99
5.2.4 Butanol Fermentation 100
5.2.5 Activity Assay of Formate Dehydrogenase 100
5.2.6 Butanol Tolerance 101
5.2.7 NADH Assay 101
5.2.8 Analytical Methods 102
5.3 Results 102
5.3.1 Construction and Evaluation of Redox Engineered Mutant 102
5.3.2 Evaluation of Medium Supplements 104
5.3.3 Butanol Fermentation 106
5.3.4 Butanol Tolerance 107
5.4 Discussion 108
5.4.1 Improvement of Butanol Production by Rebalancing Redox 108
5.4.2 Comparison with Previous Studies 109

5.5 Conclusions 111
5.6 Reference 112
CHAPTER 6 METABOLIC-PROCESS ENGINEERING 127
6.1 Introduction 128
6.2 Materials and Methods 129
6.2.1 Strain, culture and Media 129
6.2.2 Fermentation Kinetics 129
6.2.3 Fermentation Products Titration 130
6.2.4 Amino Acid Analysis 130
6.2.5 Proteomics: GeLC-MS/MS 131
6.3 Results 131
6.3.1 Butanol Fermentation in Wild Type and Butanol Producing Mutant 131
6.3.2 Comparative Proteomics Related to Amino Acid Mechanism 132
6.3.3 Extra Amino Acid Feeding in Butanol Production 133
6.3.4 Amino Acid Analysis 135
6.4 Discussion 136
6.4.1 Understanding of Amino Acid Metabolism via Comparative Proteomics 136
6.4.2 Effect of Amino Acid Addition on Butanol Production 137
6.4.3 How to Improve the Butanol Production 138
6.5 Conclusions 139
6.6 References 140
CHAPTER 7 CONCLUSIONS AND FUTURE WORK 151
7.1 Conclusions 151

7.2 Future Works 153
7.2.1 Metabolic engineering strategy 153
7.2.2 Immobilized-cell Fermentation and Online Butanol Recovery 154
7.3 Reference 156
APPENDIX I Gene sequences 161
I.1 Gene *adhE2* sequence 161
I.2 Gene *fdh* sequence 162
I.3 Gene *thl* sequence 165
APPENDIX II HPLC operation for substrate and products 167
APPENDIX III HPLC operation for amino acids 173
APPENDIX IV *Clostridium tyrobutyricum* transformation 179
APPENDIX V Proteomics sample preparation 183
APPENDIX VI High performance liquid chromatography (HPLC) diagrams 184
APPENDIX VII.1 HPLC standard diagram for substrate and products 184
APPENDIX VII.2 HPLC standard diagram for amino acids 185
APPENDIX VII CGM medium formula 186
APPENDIX VIII Diagram of free-cell fermentation 187
APPENDIX IX Flow chat of FBB 189
APPENDIX X List of publications 191

LIST OF TABLES

Table 1.1. Properties of fuels.....16

Table 2.1 Physiological characteristics of WT, ACKKO and ACKKO *adhE2*…….....46

Table 2.2 Comparison of fermentation production by WT, ACKKO and ACKKO-*adhE2*.....47

Table 2.3 Comparison of the expression of glycolytic proteins in different strains..... 48

Table 2.4 Comparison of expression of enzymes catalyzing core pathway in different strains…49

Table 2.5 Comparison of enzymes expression involved in energy & redox balance in strains…50

Table 2.6 Comparison of the expression of butanol stress related proteins in strains……...51

Table 2.7 Fatty acid, amino acids and succinate with significant change…….52

Table 3.1 Recent progresses of butyric acid production from sugar…….69

Table 3.2 Stoichiometric equations used in the FBA modeling of *C. tyrobutyricum*…70

Table 3.3 Comparison of fermentation products by wild type (control) and PAK-Em……71

Table 3.4 Effect of pH on acids production in immobilized-cell fermentations by PAK-Em…..72

Table 3.5 Effect of pH on acids production in immobilized-cell fermentations by wide type…..73

Table 4.1. Kinetics of *C. tyrobutyricum* wild type and mutants in free cell fermentation……91

Table 4.2. Kinetics of *C. tyrobutyricum* in immobilized-cell fermentations…….92

Table 4.3. Gene variations between PAK-Em and Hyd-Em…….…….....93

Table 5.1. Strains and plasmids used in this study…….....115

Table 5.2. Medium components screening to rebalance redox and carbon…….…….116

Table 5.3. Butanol fermentations using metabolically engineered *C. tyrobutyricum* ……117

Table 5.4. Recent progresses of butanol production with *C. tyrobutyricum*……...118

Table 6.1. Comparison of TCA-related proteins among different strains …….……..…...…..142

Table 6.2. Comparison of representative aa proteins among *C. tyrobutyricum* ……..143

Table 6.3. Comparison of cell growth, product concentrations, and yield ……..144

Table 6.4. Comparison of aa consumption from *C. tyrobutyricum* butanol producing mutant …145

Table 7.1. Strains and plasmids used in this study……..……157

Table 7.2. Butanol fermentations using metabolically engineered *C. tyrobutyricum* ……158

LIST OF FIGURES

Fig. 1.1. Metabolic pathway of *Clostridium acetobutylicum* ATCC 824……17

Fig. 1.2. Metabolic pathway of *Clostridium tyrobutyricum* ATCC 25755…….……18

Fig. 1.3. Plasmid pMTL007…….…….....……19

Fig. 2. 1. Metabolic pathway in ACKKO-*adhE2*……..53

Fig. 2.2. Fermentation kinetics of *C. tyrobutyricum* ATCC 25755 ……..54

Fig. 2.3. Heat map of protein expression level in different strains. ...……...55

Fig 3.1. Kinetics of free-cell fermentations ……....74

Fig 3.2. Kinetics of immobilized-cell fermentations by PAK-Em …….75

Fig. 3.3. *C. tyrobutyricum* metabolic flux distribution ……...76

Fig. 4.1. Butyric acid production improvement by cell adaptation ……94

Fig. 5.1. Butanol producing metabolic pathway in *C. tyrobutyricum*……...…...119

Fig. 5.2. Plasmid construction…….....…..120

Fig. 5.3. NADH assay…….……121

Fig. 5.4. Kinetics butanol fermentation by *C. tyrobutyricum* in serum bottles…….……...…122

Fig. 5.5. Medium components screening to rebalance carbon and redox flux ……123

Fig. 5.6. Kinetics of butanol fermentation by *C. tyrobutyricum* ……..……....124

Fig. 5.7. Improvement of n-butanol selectivity by rebalancing carbon and redox flux…..……..125

Fig. 5.8. Butanol tolerance study of *C. tyrobutyricum* in serum bottles…….……126

Fig. 6.1. Fermentation kinetics of *C. tyrobutyricum* ……...146

Fig. 6.2. Metabolic pathway of TCA and related aa mechanism …….147

Fig. 6.3. Metabolic pathway of butanol related aa mechanism ……...…148

Fig. 6.4. Heat map of protein expression level in different strains……149

Fig. 6.5. Fermentation kinetics of *C. tyrobutyricum* butanol producing mutant…….…….150

Fig. 7.1. Plasmid construction…….…….159

Fig. 7.2. Fermentation kinetics of *C. tyrobutyricum* mutants……..…….160

CHAPTER 1

INTRODUCTION

Butanol is an important raw material in the production of lacquer and latex surface coating, a widely used solvent in the manufacturing of hormones and vitamins, and a superior liquid biofuel with great potential to directly replace gasoline due to its excellent fuel properties. Butanol was predominately produced from Acetone-Butanol-Ethanol (ABE) fermentation and used as a solvent before 1980, but the biological production gradually slowed down because of high cost fermentation [1,2,3,4,5]. However, the renewed trends towards using green energy have been increasing due to the high price of crude oil, the environmental concern about using fossil fuel, and the growing demand for non-fossil based bio-products. Compared to ethanol and methanol, butanol is a better fuel candidate due to the higher energy density and lower volatility (Seen in Table 1.1). Importantly, butanol can directly replace gasoline or work as an energy alternative in the current vernicle without any modification.

1.1 Biobutanol Poduction through ABE Fermentation

Because of all the great features of biobutanol as a potential next generation liquid bioenergy and raw material in biotechnology, the renew interest in ABE fermentation recently has made a significant progress in the bioproduction of butanol. Novel strain construction and high-efficient process development can significantly improve butanol titer and productivity, while the application of low-cost biomass as substrate and the development of high-efficiency solvent recovery techniques can greatly reduce the cost of butanol production. Developing a high butanol producing strain is the first key step to achieve high biobutanol production. Metabolic engineering has been used to reprogram the microorganism metabolic pathways using genetic engineering tools [6,7,8], and synthetic biology is another efficient cell engineering strategy which introduces a series of heterologous enzymes or metabolic pathway to produce biochemical or biofuel [9,10,11]. With engineered strain, further fermentation process development can achieve high-productivity, high-quality, robust and scalable butanol production. Various powerful process development strategies have been applied in butanol and other biochemical production, including bioreactor parameters optimization via precise bioreactor controllers, dynamically monitoring metabolic parameters with in situ sensors, and rational process development based on the knowledge of systems biology [12,13,14,15].

1.1.1 Solventogenic Clostridial Strains

The solvents, such as butanol, acetone, ethanol and isopropanol, can be produced by Clostridia strains [16]. The solvent fermentation processes have been developed using *C. acetobutylicum* ATCC 824, *C. carboxidivorans* P7, *C. saccharoperbutylacetonicum* N1-4, *C. saccharobutylicum* NCP 262, *C. butylicum* NRRL B592, *C. beijerinckii* NCIMB 8052, *C. aurantibutyricum* ATCC 17777, and *C. pasteurianum* ATCC 6013 [17,18,19,20,21,22,23,24,25]. ABE fermentation using

Clostridia is a biphasic process, in which acids and energy are first produced in the acidogenic phase, and solvents are generated from acids in the following solventogenic phase [4,16,26]. A detailed metabolic pathway in *C. acetobutylicum* ATCC 824 with genes and enzymes for reactions during acidogenesis and solventogenesis is shown in Fig. 1.1. Acids (e.g. acetate and butyrate) and carbon dioxide are produced as the main products at low pH during the acidogenic phase. The produced acids are converted to solvents after the solventogenic phase is triggered by a series of gene regulations [5,27].

1.1.2 Strain Modification by Metabolic Engineering

As a cytotoxin, butanol can alter cell membrane structure, compromise membrane fluidity, and affect many membrane-bound transport activities [4,26], resulting in severe inhibition to fermentation [28]. Various cell engineering strategies, such as genetic engineering and metabolic engineering, have been developed to enhance the butanol tolerance and thereby improve butanol production.

The ratio of butanol to acetone was increased by knocking out acetoacetate decarboxylase (*adc*) and altering electron flow with the addition of methyl viologen, while the ethanol productivity was increased [29,30,31]. Instead of enhancing butanol titer and yield by overexpressing aldehyde/alcohol dehydrogenase (*aad*) and thiolase (*thl*) coupled with down-regulating CoA transferase in *C. acetobutylicum*, ethanol concentration was largely increased [32,33,34]. Due to the complex metabolic system, little progress in enhancing butanol productivity and selectivity in *C. acetobutylicum* has been made using traditional metabolic engineering method.

1.2 *C. tyrobutyricum* and Butanol Biosynthesis in *C. tyrobutyricum*

Clostridium tyrobutyricum ATCC 25755 is a gram-positive, rod-shaped, and anaerobic bacterial [35]. Historically, butyric acid fermentation in cheese (late blowing) caused by the outgrowth of Clostridial spores present in raw milk, most commonly originating from silage, can result in considerable product loss [36]. On the other hand, butyric acid has many applications in chemical, food, and pharmaceutical industries [37,38,39].

1.2.1 Solvent Production in *C. tyrobutyricum*

C. tyrobutyricum natively produces butyric acid, acetic acid, carbon dioxide, and hydrogen, as shown in Fig. 1.2 [40, 41, 42]. It is thus of interest to also produce hydrogen from low-cost renewable biomass by anaerobic fermentation with *C. tyrobutyricum* to add value to the butyric acid fermentation process. The production of butyric acid and hydrogen from renewable resources has become an increasingly attractive alternative to petroleum-based processes because of public concerns about the environmental pollution caused by the petrochemical industry and consumers' preference for bio-based natural ingredients in foods, cosmetics, and pharmaceuticals.

C. tyrobutyricum can produce butyric acid, acetic acid, hydrogen, and carbon dioxide as the end products. As shown in Fig. 1.2, Embden-Meyerhof-Parnas (EMP) pathway leads to the formation of pyruvate from glucose. Pyruvate is catalyzed by pyruvate–ferredoxin oxidoreductase (*pfor*) to form acetyl-CoA, carbon dioxide, and reduced ferredoxin (FdH_2) [42]. Reduced Fd can supply electrons to protons to produce H_2. In the central metabolic pathway, acetyl-CoA are converted to butyryl-CoA through thiolase (*thl*), acetyl-CoA acetyltransferase (*ato*), 3-hydroxybutyryl-CoA dehydrogenase (*hbd*), and crotonase (*crt*). Two similar pathways directed to the convert of acetic acid from acetyl-CoA and butyric acids from butyryl-CoA. In an acetic acid biosynthesis pathway,

acetyl-CoA was converted to acetyl-phosphate first via phosphotransacetylase (*pta*) and to acetic acid via acetate kinase (*ack*). Butyric acid was produced via phosphotransbutyrylase (*ptb*) and butyrate kinase (*buk*) in a similar pathway. The features of the relatively simple metabolic pathway (no acetone production), high C4 products generation (butyric acid > 40 g/L in free-cell fermentation) [43], and high tolerance of butanol (higher than 1.5% (v/v) butanol) [44] enabled *C. tyrobutyricum* as an interesting alternative host for butanol production.

Recently *C. tyrobutyricum* mutants were constructed based on an advanced metabolic engineering strategy to produce butanol. In the wild-type of *C. tyrobutyricum*, no solvent (i.e., acetone, ethanol and butanol) is produced, but homogenous alcohol dehydrogenase (*adh*) and butanol dehydrogenase (*bdh*) genes exist, thus introducing heterologous alcohol/aldehyde dehydrogenase (*ahdE2*) gene from *C. acetobutylicum* to *C. tyrobutyricum* could complete both butanol pathway and ethanol pathway. However, *C. tyrobutyricum* has a favorable metabolic pathway from carbon direction toward butyryl-CoA (C4) not acetyl-CoA (C2). The butyryl-CoA is key intermediate note and plays an important role in butanol production. Therefore, butanol production in *C. tyrobutyricum* solvent-producing mutant was much higher (~ 10 g/L in serum bottle) than ethanol production (~ 1 g/L) [45,46,47].

1.2.2 Metabolic Engineering & Process Development in *C. tyrobutyricum*

Recently, a novel butanol-producing strain has been developed by introducing a butanol synthesis pathway into *C. tyrobutyricum* with plasmid pMTL007 system (Fig. 1.3) increased butanol production [44]. Butanol titer of 10.0 g/L and butanol yield of about 27.0% have been achieved with this mutant. However, the butanol production has not arrived at the desired value for application in industry (>20g/L). In order to solve the problem of low butanol production brought by acid accumulation, the metabolic pathway need to be re-modified with molecular biology

technology. For instance, the genes in acetic acid biosynthesis pathway could be knocked down to increase the C4 production.

Most recent butanol production research in *C. tyrobutyricum* has only focused on the carbohydrate metabolic pathway. However, it has been previously reported that excess nitrogen source, especially the amino acid, was necessary and improved butanol production with *C. beijerinckii*, *C.acetobutylicum*, and *C. saccharobutylicum* [48,49,50]. Because amino acid mechanism were correlated to ATP & NADH consumption and carbon redistribution in the metabolic pathway. It is important to investigate the effect of nitrogen source on butanol production with process development.

Recently, the fibrous-bed bioreactor (FBB) has been developed for immobilized-cell fermentations to produce several organic acids with significantly improved productivity, yield, and final product concentration [51,52,53,54]. With the FBB, a much higher final product concentration that is 2 to 3-fold higher than those previously attained can be achieved, not only because of the higher cell density in the FBB, but also through the adaptation of the culture to become more tolerant of the fermentation product [38,55]. For the economical production of butanol from biomass, it is desirable to further improve the final product concentration and productivity of the fermentation process.

1.3 Comparative Genomics and Proteomics

1.3.1 Comparative Genomics

The reducing cost enhanced a large range of applications of next generation sequencing (NGS) technology in genomics study [56]. The genome sequences of clostridia can supply us the genetic

information to better understand the metabolic pathway and facilitate high product generation mutant with advanced metabolic engineering technology.

Recently the draft genome sequences of *C. tyrobutyricum* strains were published [57,58,59] and supplied the genome information for mutant characterization in our study. For instance, gene mutations, including stop codon insertion, stop codon deletion, and non-synonymous coding mutations, could be detected and evaluated in genetically engineered or evolutionary engineered *C. tyrobutyricum* strains.

The published genome information also benefits genetic engineering of *C. tyrobutyricum*, including ClosTron technology. Recently developed ClosTron, a Group II intron directed mutagenesis system, can address the low efficiency of homogenous integration and the instability of mutation in gene knockout. The ClosTron plasmid contains a mini-intron derivative and element facilitating plasmid conjugal transfer. The ClosTron was already successfully applied in *C. acetobutylicum*, *C. difficile*, *C. botulinum* and *C. sporogenes* [60].

1.3.2 Comparative Proteomics

In addition to genomics, the proteomics, an advanced qualitative and quantitative tool, has been applied to analyze the expression of a large number of proteins using SELDI-TOF-MS, UPLC-MS/MS and MALDI-TOF-MS [61]. Integrated with genome data base, proteome study has been widely used to identify the host cell mechanism, including the cell growth, amino acid, and butanol production.

Proteomics study meets the need for evaluating global changes of protein expression and identifying the key regulators to further construct high-production mutants. Proteomics study of *clostridia* have been reported recently based on advanced mass spectrum technology. Maps of

acidogenic and solventogenic proteins have been compared in *C. acetobutylicum* ATCC824 to evaluate effects of different pH values on butanol production [62]. To understand the relationship between butanol tolerance and butanol production, a comparative proteomics study was performed to find the key up-regulated and down-regulated enzymes between the wild type strain DSM 1731 and its enhanced-butanol-tolerance mutant [63]. Proteomic analysis was also applied in *C. beijerinckii* NCIMB 8052 to investigate the role of Ca^{2+} in cell growth, carbon source utilization, and butanol fermentation [64].

As compared to *E. coli* and other Clostridial strains, *C. tyrobutyricum* has multiple advantages. For example, the simpler metabolic pathway in *C. tyrobutyricum* can produce higher titer of butanol without acetone byproduct. However, none of the advanced Omics studies in *C. tyrobutyricum*, e.g. transcriptomics, proteomics and metabolomics, has been reported so far. In this study, we built a global proteomics database of *C. tyrobutyricum* using the advanced GeLC-ESI-MS/MS technique.

1.4 Hypothesis of this study

Recently n-Butanol has become an important energy substitute for fossil fuel. Previous studies have demonstrated that *C. tyrobutyricum* could be used as a suitable host cell for the biobutanol production. Therefore, further improvement of butanol yield to approach the theoretical yield of 0.4g/g glucose could be achieved in *C. tyrobutyricum* by affective metabolic cell and process engineering. To reach the goal of high biobutanol production, two hypothesis were proposed in this study in metabolic cell and process engineering of *C. tyrobutyricum*. The first hypothesis was that advanced Omics technology must be applied to further rationally engineer *C. tyrobutyricum*. The second hypothesis was that Biobutanol production must be improved by carbon, redox, and amino acid rebalance strategy.

Metabolically engineered *C. tyrobutyricum* can produce butanol, butyrate, acetate, ethanol from carbon sourceAcetyl-CoA and butyryl-CoA are key intermediate chemicals in carbon flux from C2 to C4. . Although completing butanol pathway to rebalance carbon flux from acid to solvent in *C. tyrobutyricum*, the unbalance of carbon has still limited further improvement of biobutanol production. Increasing the butyryl-CoA pool is a straightforward strategy to improve butanol production in *C. tyrobutyricum*. Therefore, overexpressing native thiolase (*thl*) in *C. tyrobutyricum* must redistribute more carbon flux from acetyl-CoA to butyryl-CoA and increase butanol production furtherly.

Butanol production is ATP and NADH consumption process. ATP generation, involved in the formation pathways of acetic and butyric acids, can supply the energy pool to butanol production. The convert from glucose to pyruvate can form two molecules of NADH, but four molecules NADH are needed to form one molecules of butanol from the glucose [46]. So the unbalance of NADH is one of the limiting steps in butanol production. It has been reported that NADH availability can be improved through the redox engineering [47]. Therefore, introducing heterologous formate dehydrogenase (*fdh*) and extracellular electron carrier addition (methyl viologen) in *C. tyrobutyricum* must increase NADH pool and improve the butanol production.

Our proteomics study has shown most enzymes involved in amino acid metabolism had significantly lower expressions in the butanol producing *C. tyrobutyricum* strain at the mid-log phase, compared with wild type, which were attributed to a larger amount of amino acids consumption and less substrates left for the reaction catalyzed by these enzymes and resulted in more carbon flux flowing to amino acid production not butanol production. This phenomenon suggested that amino acid feeding was a limiting factor in butanol production with *C.*

tyrobutyricum. Therefore, changing amino acid feeding must be an effective method to improve butanol production in *C. tyrobutyricum*.

1.5 References

[1] T.C. Ezeji, N. Qureshi, H.P. Blaschek, "Butanol fermentation research: upstream and downstream manipulations", Chem. Rec., vol. 4, pp. 305-314, 2004.

[2] T.C. Ezeji, N. Qureshi, H.P. Blaschek, "Bioproduction of butanol from biomass: from genes to bioreactors", Curr. Opin. Biotechnol., vol. 18, pp. 220-227, 2007.

[3] V. Garćia, J. Päkkilä, H. Ojamo, E. Muurinen, R.L. Keiski, "Challenges in biobutanol production: How to improve the efficiency", Renew. Sustain. Ener., vol. 15, pp. 964-980, 2011.

[4] M. Kumar, K. Gayen, "Developments in biobutanol production: New insights", Appl. Ener., vol. 88, pp. 1999-2012, 2011.

[5] S.T. Lee, J.H. Park, S.H. Jang, L.K. Nielsen, J. Kim, K.S. Jung, "Fermentive butanol production by Clostridia", Biotechnol. Bioeng., vol. 101, pp. 209-228, 2008.

[6] W. Higashide, Y. Li, Y. Yang, J.C. Liao, "Metabolic engineering of *Clostridium cellulolyticum* for production of isobutanol from cellulose", Appl. Environ. Microbiol., vol. 77, pp. 2727-2733, 2011.

[7] D. Amador-Noguez, I.A. Brasg, X.J. Feng, N. Roquet, J.D., "Rabinowitz, Metabolome remodeling during the acidogenic-solventogenic transition in *Clostridium acetobutylicum*", Appl. Environ. Microbiol., vol. 77, pp. 7984-7997, 2011.

[8] E.T. Papoutsakis, "Engineering solventogenic clostridia", Curr. Opin. Biotechnol.,vol. 19, pp. 420-429, 2008.

[9] D.R. Nielsen, E. Leonard, S.H. Yoon, H.C. Tseng, C. Yuan, K.L. Prather, "Engineering alternative butanol production platforms in heterologous bacteria", Metab. Eng., vol. 11, pp. 262-273, 2009.

[10] S. Atsumi, A.F. Cann, M.R. Connor, C.R. Shen, K.M. Smith, M.P. Brynildsen, et al., "Metabolic engineering of *Escherichia coli* for 1-butanol production", Metab. Eng., vol. 10, pp. 305-311, 2008.

[11] C.R. Shen, J.C. Liao, "Metabolic engineering of *Escherichia coli* for 1-butanol and 1-propanol production via the keto-acid pathways", Metab. Eng., vol. 10, pp. 312-320, 2008.

[12] H. Heluane, M.R. Evans, S.F. Dagher, J.M. Bruno-Barcena, "Meta-analysis and functional validation of nutritional requirements of solventogenic Clostridia growing under butanol stress conditions and coutilization of D-glucose and D-xylose", Appl. Environ. Microbiol., vol. 77, pp. 4473-4485, 2011.

[13] Y. Wang, X. Li, H.P. Blaschek, "Effects of supplementary butyrate on butanol production and the metabolic switch in *Clostridium beijerinckii* NCIMB 8052: genome-wide transcriptional analysis with RNA-Seq", Biotechnol. Biofuels., vol. 6, pp. 138, 2013.

[14] P.S. Nigam, A. Singh, "Production of liquid biofuels from renewable resources", Prog. Ener. Combust. Sci., vol. 37, pp. 52-68, 2011.

[15] J. Swana, Y. Yang, M. Behnam, R. Thompson, "An analysis of net energy production and feedstock availability for biobutanol and bioethanol", Bioresour. Technol., vol. 102, pp. 2112-2117, 2011.

[16] D.T. Jones, D. Woods, "Acetone-butanol fermentation revisited", Microbiol. Reviews., vol. 50, pp. 484-524, 1986.

[17] T. Lutke-Eversloh, H. Bahl, "Metabolic engineering of *Clostridium acetobutylicum*: recent advances to improve butanol production", Curr. Opin. Biotechnol., vol. 22, pp. 634-647, 2011.

[18] N. Qureshi, I.S. Maddox, "Reduction in butanol inhibition by perstraction: Utilization of concentrated lactose/whey permeate by *Clostridium acetobutylicum* to enhance butanol fermentation economics", Food. and. Bioproducts. Processing., vol. 83, pp. 43-52, 2005.

[19] G. Bruant, M.J. Levesque, C. Peter, S.R. Guiot, L. Masson, "Genomic analysis of carbon monoxide utilization and butanol production by *Clostridium carboxidivorans* strain P7", PLoS. One., vol. 5, pp. 13033, 2010.

[20] V.H. Thang, K. Kanda, G. Kobayashi, "Production of acetone-butanol-ethanol (ABE) in direct fermentation of cassava by *Clostridium saccharoperbutylacetonicum* N1-4", Appl. Biochem. Biotechnol., vol 161, 157-170, 2010.

[21] T. Ezeji, H.P. Blaschek, "Fermentation of dried distillers' grains and solubles (DDGS) hydrolysates to solvents and value-added products by solventogenic clostridia", Bioresour. Technol., vol. 99, pp. 5232-5242, 2008.

[22] T.W. Jesse, T.C. Ezeji, N. Qureshi, H.P. Blaschek, "Production of butanol from starch-based waste packing peanuts and agricultural waste", J. Ind. Microbiol. Biotechnol., vol. 29, pp. 117-123, 2002.

[23] W. Somrutai, M. Takagi, T. Yoshida, "Acetone-butanol fermentation by *Clostridium aurantibutyricum* ATCC 17777 from a model medium for palm oil mill effluent", J. Ferment. Bioeng., vol. 81, pp. 543-547, 1996.

[24] H. Biebl, "Fermentation of glycerol by *Clostridium pasteurianum*--batch and continuous culture studies", J. Ind. Microbiol. Biotechnol., vol. 27, pp. 18-26, 2001.

[25] K.A. Taconi, K.P. Venkataramanan, D.T. Johnson, "Growth and solvent production by *Clostridium pasteurianum* ATCC 6013TM utilizing biodiesel-derived crude glycerol as the sole carbon source", Environ. Prog., Sustainable. Energy., vol. 28, pp. 100-110, 2009.

[26] T. Ezeji, C. Milne, N.D. Price, H.P. Blaschek, "Achievements and perspectives to overcome the poor solvent resistance in acetone and butanol-producing microorganisms", Appl. Microbiol. Biotechnol., vol. 85, pp. 1697-1712, 2010.

[27] J.C. Gottschalk, M. J.G., "The induction of acetone and butanol production in cultures *Clostridium acetobutylicum* by elevated concentrations of acetate and butyrate", FEMS. Microb. Letters., vol. 12, pp. 385-389, 1981.

[28] E.P. Knoshaug, M. Zhang, "Butanol tolerance in a selection of microorganisms", Appl. Biochem. Biotechnol., vol. 153, pp. 13-20, 2009.

[29] J. Formanek, R. Mackie, H.P. Blaschek, "Enhanced Butanol Production by *Clostridium beijerinckii* BA101 Grown in Semidefined P2 Medium Containing 6 Percent Maltodextrin or Glucose", Appl. Environ. Microbiol., vol. 63, pp. 2306-2310, 1997.

[30] Y.L. Lin, H.P. Blaschek, "Butanol Production by a Butanol-Tolerant Strain of *Clostridium acetobutylicum* in Extruded Corn Broth", Appl. Environ. Microbiol., vol. 45, pp. 966-973, 1983.

[31] N. Qureshi, H.P. Blaschek, "Recent advances in ABE fermentation: hyper-butanol producing *Clostridium beijerinckii* BA101", J. Ind. Microbiol. Biotechnol., vol. 27, pp. 287-291, 2001.

[32] L.M. Harris, N.E. Welker, E.T. Papoutsakis, "Northern, morphological, and fermentation analysis of spo0A inactivation and overexpression in *Clostridium acetobutylicum* ATCC 824", J. Bacteriol., vol. 184, pp. 3586-3597, 2002.

[33] Y.N. Zheng, L.Z. Li, M. Xian, Y.J. Ma, J.M. Yang, X. Xu, et al., "Problems with the microbial production of butanol", J. Ind. Microbiol. Biotechnol., vol. 36, pp. 1127-1138, 2009.

[34] Y. Jiang, C. Xu, F. Dong, Y. Yang, W. Jiang, S. Yang, "Disruption of the acetoacetate decarboxylase gene in solvent-producing *Clostridium acetobutylicum* increases the butanol ratio", Metab. Eng., vol. 11, pp. 284-291, 2009.

[35] Y. Zhu, Z. Wu, S.T. Yang, “Butyric acid production from acid hydrolysate of corn fiber by *Clostridium tyrobutyricum* in a fibrous-bed bioreactor”, Process Biochem., vol. 38, pp. 657-666, 2002.

[36] N. Klijin, F.F.J. Nieuwenhof, J.D. Hoolwerf, C.B. Van Der Waals, A.H. Weerkam, “Identification of *Clostridium tyrobutyricum* as the causative agent of late blowing in cheese by species-specific PCR amplification”. Appl. Environmental. Microbiol., vol. 61, pp. 2919-2924, 1995.

[37] J. Zigova, E. Sturdik, D. Vandak, S. Schlosser. “Butyric acid production by *Clostridium butyricum* with integrated extraction and pertraction”. Proc Biochem., vol. 34, pp. 835-843, 1999.

[38] D. Vandak, J. Zigova, E. Sturdik, S. Schlosser. “Evaluation of solvent and pH for extractive fermentation of butyric acid”. Process Biochem., vol. 32, pp. 245-251, 1997.

[39] E.A. Williams, J.M. Coxhead, J.C. Mathers. “Anti-cancer effects of butyrate: use of microarray technology to investigate mechanisms”. Proc. Nutr. Soc., vol. 62, pp. 107-115, 2003.

[40] M. Momirlan, T. Veziroglu. “Recent directions of world hydrogen production”. Energy Rev., vol. 3, pp. 219-231, 1999.

[41] D. Das, T.N. Veziroglu. “Hydrogen production by biological processes: a survey of literature”. Int. J. Hydrogen Energy., vol. 26, pp. 13-28, 2001.

[42] X. Liu, Y. Zhu, S.T. Yang. “Construction and characterization of ack deleted mutant of *Clostridium tyrobutyricum* for enhanced butyric acid and hydrogen production”. Biotechnol. Prog., vol. 2, pp. 1265-1275, 2006.

[43] Y. Zhu, S.T. Yang. "Adaptation of *Clostridium tyrobutyricum* for enhanced tolerance to butyric acid in a fibrous-bed bioreactor". Biotechnol. Prog., vol. 19, pp. 365-372, 2003.

[44] M. Yu, Y. Zhang, I. C. Tang, S. T. Yang, "Metabolic engineering of *Clostridium tyrobutyricum* for n-butanol production". Metab. Eng., vol. 13, pp. 373-382, 2011.

[45] M. Yu, Y. Du, W. Jiang, W.L. Chang, S.T Yang, I.C. Tang. "Effects of different replicons in conjugative plasmids on transformation efficiency, plasmid stability, gene expression and n-butanol biosynthesis in *Clostridium tyrobutyricum*". Appl. Microbiol. Biotechnol., vol. 93, pp.881-889, 2012.

[46] C.R. Shen, E.I. Lan, Y. Dekishima, A. Baez, K.M. Cho, J.C. Liao. "Driving forces enable high-titer anaerobic 1-butanol synthesis in *Escherichia coli*". Appl. Environ. Microbiol., vol. 77, pp. 2905-2915, 2011.

[47] B.B. Bond-Watts, R.J. Bellerose, M.C.Y. Chang. "Enzyme mechanism as a kinetic control element for designing synthetic biofuel pathways". Nat. Chem. Biol., vol. 7, pp. 222-227, 2011.

[48] J.C. Gottschal, J.G. Morris. "Non-production of acetone and butanol by *C. acetobutylicum* during glucose- and ammonium-limitation in continuous culture". Biotech. Lett., vol. 3, pp. 525-530, 1982.

[49] W. Andersch, H. Bahl, G. Gottschalk. "Acetono-butanol production by *Clostridium acetobutylicum* in an ammonium-limited chemostat at low pH values". Biotech. Lett., vol. 4, pp. 29-32, 1982.

[50] S. Long, D.T. Jones, D.R. Woods. "Initiation of solvent production, clostridial stage and endospore formation in *Clostridium acetobutylicum* P262". Appl. Microbiol. Biotechnol., vol. 20, pp. 256-261, 1982.

[51] V.P. Lewis, S.T. Yang. "Continuous propionic acid fermentation by immobilized *Propionibacterium acidipropionici* in a novel packed-bed bioreactor" Biotechnol. Bioeng., vol. 40, pp. 465-474, 1992.

[52] Y. Huang, S.T. Yang. "Acetate production from whey lactose using co-immobilized cells of homolactic and homoacetic bacteria in a fibrous-bed bioreactor". Biotechnol. Bioeng., vol. 60, pp. 499-507, 1998.

[53] E.M. Silva, S.T. Yang. "Kinetics and stability of a fibrous bed bioreactor for continuous production of lactic from unsupplemented acid whey". J. Biotechnol., vol. 41, pp. 59-70, 1995.

[54] X. Liu, S.T Yang. "Kinetics of butyric acid fermentation of glucose and xylose by *Clostridium tyrobutyricum* wild type and mutant". Process Biochem., vol. 41, pp. 801-808, 2006.

[55] S.T. Yang. "Extractive fermentation using convoluted fibrous bed bioreactor". U. S. Patent No. 5563069. 1996.

[56] L. Liu, Y. Li, S. Li, N. Hu, Y. He, R. Pong, D. Lin, L. Lu, M. Law. "Comparison of next-generation sequencing systems". J. Biomed. Biotechnol., 2012.

[57] Y. Zhang. "Metabolic engineering of Clostridium tyrobutyricum for production of biofuels and bio-based chemicals". PhD diss., The Ohio State University, 2009.

[58] L. Jiang, L. Zhu, X. Xu, Y. Li, S. Li, H. Huang. "Genome sequence of *Clostridium tyrobutyricum* ATCC 25755, a butyric acid-overproducing strain". Genome Announcements, vol. 271, pp. e00308-13, 2013.

[59] D. Bassi, C. Fontana, S. Gazzola, E. Pietta, E. Puglisi, F. Cappa, P.S. Cocconcelli. "Draft genome sequence of *Clostridium tyrobutyricum* strain UC7086, isolated from Grana Padano cheese with late-blowing defect". Genome announcements, vol. 29, pp. e00614-13, 2013.

[60] S.A. Kuehne, N.P. Minton. "ClosTron-mediated engineering of *Clostridium*". Bioengineered, vol. 3, pp. 247-54, 2012.

[61] Mao, S., Jia, K., Zhang, Y., Li, Y. "Use of proteomic tools in microbial engineering for biofuel production". Methods. Mol. Biol., vol. 834, pp. 137-51, 2012.

[62] H. Janssen, C. Doring, A. Ehrenreich, B. Voigt, M. Hecker, H. Bahl, R.J. Fischer. "A proteomic and transcriptional view of acidogenic and solventogenic steady-state cells of *Clostridium acetobutylicum* in a chemostat culture". Appl. Microbiol. Biotechnol., vol. 87, pp. 2209-26, 2010.

[63] S. Mao, Y. Luo, T. Zhang, J. Li, G. Bao, Y. Zhu, Z. Chen, Y. Zhang, Y. Li, Y. Ma. "Proteome reference map and comparative proteomic analysis between a wild type *Clostridium acetobutylicum* DSM 1731 and its mutant with enhanced butanol tolerance and butanol yield". J. Proteome Res., vol. 9, pp. 3046-61, 2010.

[64] B. Han, V. Ujor, L.B. Lai, V. Gopalan, T.C. Ezeji. "Use of proteomic analysis to elucidate the role of calcium in acetone-butanol-ethanol fermentation by *Clostridium beijerinckii* NCIMB 8052". Appl. Environ. Microbiol., vol. 79, pp. 282-93, 2013.

Table 1.1. Properties of fuels [5]

Properties	Butanol	Gasoline	Ethanol	Methanol
Energy density (MJ/L)	29.2	32	19.6	16
Air-fuel ratio	11.2	14.6	9	6.5
Heat of evaporation (MJ/kg)	0.43	0.36	0.92	1.2
Research octane number	96	91-99	129	136
Motor octane number	78	81-89	102	104

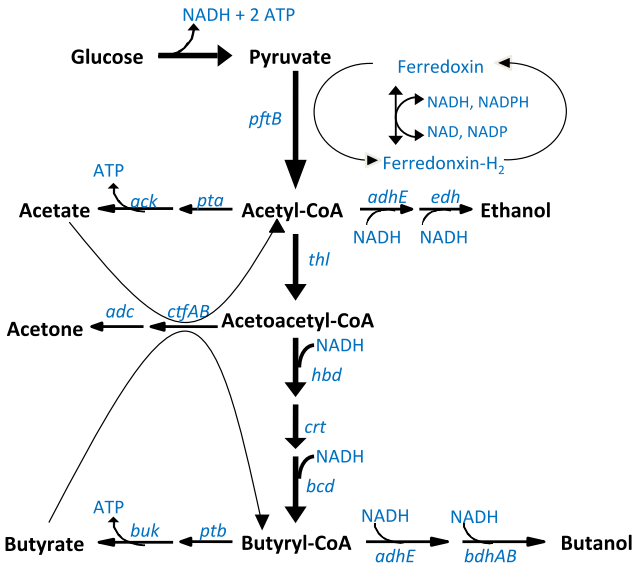

Figure 1.1. Metabolic pathway of *Clostridium acetobutylicum* ATCC 824 [5]. *pftB*: pyruvate-ferredxin oxidoreductase; *ack*: acetate kinase; *pta*: phosphotrans acetylase; *adhE*: aldehyde dehydrogenase; *edh*: ethanol dehydrogenase; *thl*: thiolase; *adc*: acetoacetate decarboxylase; *ctfAB*: CoA-transferase; *hbd*: 3-hydroxybutyryl-CoA dehydrogenase; *crt*: crotonase; *bcd*: butyryl-CoA dehydrogenase; *buk*: butyrate kinase; *ptb*: phosphotrans butyrylase; *bdh*: butanol dehydrogenase.

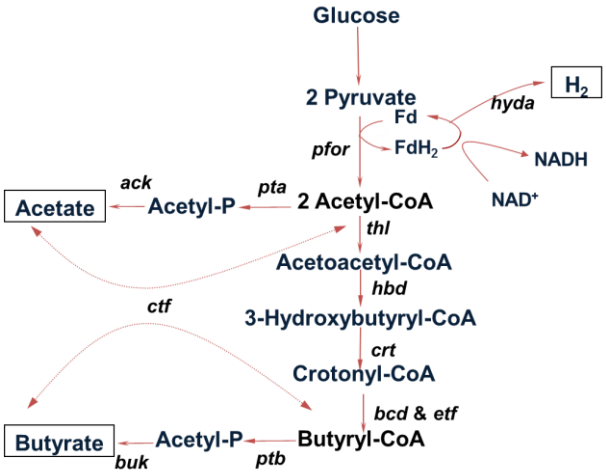

Figure 1.2. Metabolic pathway of *Clostridium tyrobutyricum* ATCC 25755 [40]. *pfor*: pyruvate: ferredoxin oxidoreductase; *hyda:* hydrogenase*; ack*: acetate kinase; *pta*: phosphotrans acetylase; *thl*: thiolase; etf: electron transfer flavoprotein; *ctf*: CoA-transferase; *hbd*: 3-hydroxybutyryl-CoA dehydrogenase; *crt*: crotonase; *bcd*: butyryl-CoA dehydrogenase; *buk*: butyrate kinase; *ptb*: phosphotrans butyrylase.

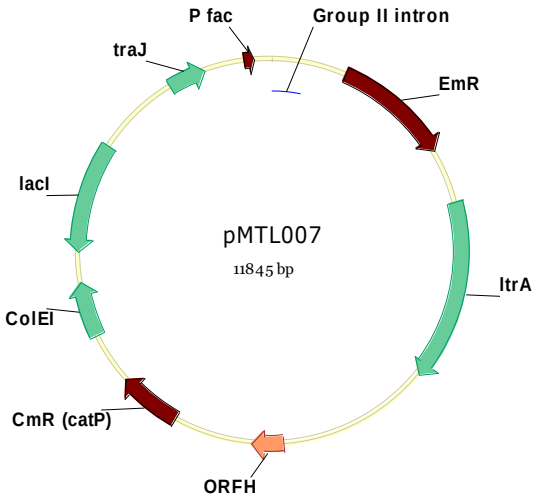

Figure 1.3. Plasmid pMTL007 [55]. (*CatP*: chloramphenicol resistance gene; *lacI*: lac repressor; *ORFH*: gram-postive replicon; P*fac:* artificial Clostridium promoter; *ColEI*: gram-negative replicon; traJ: TraJ protein for conjugation; ItrA Group II intron-encoded protein; EmR: erythromycin resistance gene)

CHAPTER 2

COMPARATIVE PROTEOMICS ANALYSIS

Abstract

Clostridium tyrobutyricum strains have been metabolically engineered to produce n-butanol. The objective of this study was to obtain a comprehensive understanding as to how butanol production was regulated in *C. tyrobutyricum* to guide the engineering of next-generation strains. A comparative proteomics analysis was performed, covering 78.1% of open reading frames, using wild type, ACKKO mutant (Δ*ack*) producing 37.30 g/L of butyrate and ACKKO-*adhE2* mutant (Δ*ack*-*adhE2*) producing 16.68 g/L of butanol. In ACKKO-*adhE2*, the expression of most glycolytic enzymes was decreased, the thiolase (*thl*), acetyl-CoA acetyltransferase (*ato*), 3-hydroxybutyryl-CoA dehydrogenase (*hbd*) and crotonase (*crt*) that convert acetyl-CoA to butyryl-CoA were increased, and the heterologous bifunctional acetaldehyde/alcohol dehydrogenase (*adhE2*) catalyzing butanol formation was highly expressed. The apparent imbalance of energy and redox was observed due to the downregulation of acids production and the addition of a butanol synthesis pathway. This study revealed the mechanism of carbon redistribution from C2 to C4 and its limiting factors to direct rational engineering for high butanol production

2.1. Introduction

The increasing price of crude oil and growing concern over national security have driven an appreciable investment toward the development of novel sustainable fuels. Among various alternatives, n-butanol has been identified as an efficient substitute for gasoline without any modification of today's engines. Butanol can also be converted to high-energy jet fuel (JP8) and diesel fuels. It is reported that the current market price of butanol is $6.75/gal in a market of 1.4 B gal/yr with an estimated annual growth rate predicted to increase upwards of 11% (http://elcriton.com/Markets.html). Most butanol has been manufactured using the petroleum refinery route since 1950s, but the biobutanol produced by microorganisms has drawn significant attention due to the advantages of environmentally benign [1].

Clostridium tyrobutyricum is a gram-positive, anaerobic and acidogenic bacterium that naturally produces butyric acid and acetic acid (Fig. 2.1). A advanced metabolic engineering and synthetic biology technologies have enabled high butanol production using *C. tyrobutyricum.* Recently, a novel high butanol-producing mutant strain, ACKKO-*adhE2*, has been developed by introducing a butanol synthesis pathway into the high butyrate-producing mutant ACKKO [2,3]. The ACKKO with downregulated acetate formation pathway produced >50 g/L of butyrate from free-cell fermentation and >80 g/L of butyrate from immobilized-cell fermentation. The synthesis of a heterologous butanol pathway in ACKKO-*adhE2* produced > 12 g/L of butanol from free-cell fermentation. Despite the achievement in biobutanol production, the lack of fundamental understanding in the regulation mechanism that drives butanol production has hindered the development of more efficient strains. The current advances in Omics technologies, e.g. genomics, transcriptomics, proteomics and metabolomics, offer powerful research tools to overcome this challenge.

The genome sequences of microorganisms can provide us the genetic background to facilitate the construction of metabolically engineered strains. From that perspective, comprehensive genomics studies have been completed for multiple Clostridia, such as *C. acetobutylicum* ATCC 824 [4], *C. carboxidivorans* $P7^T$ [5], and *C. thermocellum* ATCC 27405 [6]. Multiple genomics studies of *C. tyrobutyricum* ATCC 25755 have also been performed, including a shotgun or complete genome sequencing with annotation, which are available on NCBI or IMG [7,8,9]. Integrated with genomics, proteomics has been applied to analyze the expression of a large number of intracellular proteins and identify the host cell regulators involved in cell growth, sporulation, carbohydrate metabolism, and solvent tolerance. Proteomics databases of a few solventogenic Clostridia, such as *C. acetobutylicum, C. thermocellum,* and *Clostridium sp.,* have been reported [10,11,12,13]. However, the protein map of *C. tyrobutyricum* ATCC 25755 has not been created.

The goals of this study were to establish a comprehensive understanding of butanol production and identify the limiting factors for butanol production in *C. tyrobutyricum*. The global intracellular maps of three strains cultivated in fermentation bioreactors were established. The expression of key enzymes in glycolysis, products formation, metabolism of energy and redox, and cellular responses to butanol stress were analyzed and compared. The key enzymes that correlated to high butanol production were identified. In addition, the amino acids and fatty acids involved in the core metabolic pathway were also investigated. Finally, the strategies of rational construction of next-generation *C. tyrobutyricum* for high butanol production were discussed.

2.2. Materials and Methods

2.2.1 Strains and Media

Three *C. tyrobutyricum* ATCC 25755 strains, including wild type, mutant ACKKO (*a.k.a.* ACK-Em), and mutant ACKKO-*adhE2*, were analyzed in this study. The wild type strain was

purchased from ATCC (Manassas, VA); ACKKO was developed by downregulating the acetate pathway in Yang's lab [14]; and ACKKO-*adhE2* was constructed by overexpressing bifunctional aldehyde/alcohol dehydrogenase (*adhE2*) in ACKKO in Yang's lab [3]. The seed culture was maintained anaerobically at 37 ^{o}C in Reinforced Clostridial Medium (RCM; Difco, Kansa City, MO) supplemented with 30 μg/mL of erythromycin (Em) for ACKKO and 30 μg/mL of Em plus 30 μg/mL of thiamphenicol (Tm, Alfa Aesar, Ward Hill, MA) for ACKKO-*adhE2*. In fermentation, cells were cultivated in Clostridial Growth Medium (CGM) as reported previously[14,15]. All chemical reagents were purchased from Sigma-Aldrich (St. Louis, MO), unless otherwise specified.

2.2.2 Fermentation Kinetics

The free-cell fermentations of all three strains were performed in stirred-tank bioreactors (FS-01-A; Major science, Saratoga, CA). After autoclaving at 121 ^{o}C for 60 mins, the anaerobiosis of the fermentation medium was reached by sparging with nitrogen gas at a flow rate of 10 mL/min for 3 hrs. Each bioreactor contains 2 liters of CGM, ~40 g/L of glucose, no addition of antibiotics for wild type and ACKKO but 30 μg/mL of Tm for ACKKO-*adhE2*. Fresh seed culture with optical density at 600 nm (OD_{600}) of 1.5 was used to inoculate the 2-L fermentation medium to reach seeding density OD_{600} of ~0.04. One unit of OD_{600} corresponded to 0.34 g-dry cell/L. All fermentations were operated in fed-batch mode at Temp 37 ^{o}C, agitation 100 rpm, and pH controlled at 6.0±0.1 with 5 N NaOH. The concentrated glucose stock (400 g/L) was fed to fermentation broth when the sugar level decreased below 10 g/L. The bioreactors were sampled at regular intervals (twice a day) to monitor cell growth and titrate substrate and products. Although the samples to analyze the expression of intracellular proteins and test metabolites were archived, only the mid-log phase samples were applied in proteomics and metabolite analysis in this study.

All fermentations were carried out in duplicate and data were presented as the average of biological replicates with standard deviation.

2.2.3 Fermentation Products Titration

The cell density was measured by the OD_{600} of cell suspension using a spectrophotometer (Biomate3; Thermo Fisher Scientific, Waltham, MA). The concentrations of fermentation products, including butanol, butyrate, acetate and ethanol, were analyzed using high performance liquid chromatography (HPLC, Shimadzu, Columbia, MD). The HPLC system was equipped with an automatic sampler (Shimadzu SIL-20A), a solvent delivery unit (Shimadzu LC-20AT), an organic acid and solvent analysis column (Rezex RHM-Monosaccharide H^+, Phenomenex, Torrance, CA), a column oven at 78 ^oC (CTO-20A), and a refractive index detector (Shimadzu RID-10A). The eluent was HPLC-grade H_2O at a flow rate of 0.6 mL/min. The glucose was analyzed using both a YSI 2700 Select Biochemistry Analyzer (YSI Life Sciences, Yellow Springs, OH) and HPLC.

2.2.4 Proteomics: GeLC-MS/MS

The cells of all three strains at 30 min post inoculation to evaluate the baseline and the fermentations were sampled in mid-log phase to prepare the proteomics samples. The protein content in the lag phase samples was minimal and ignored in the proteomics study. At sampling point of mid-log phase, the OD_{600} were 3.94 at time of 11 h, 5.82 at time of 22 h and 4.51 at time of 30.5 h, and specific cell growth rate were 0.21 h^{-1}, 0.13 h^{-1} and 0.16 h^{-1}, for the wild type, ACKKO and ACKKO-*adhE2*, respectively. The summarized physiological characteristics of the cells at sampling points were summarized in Table 2.1. The cells were collected from fermentors and centrifuged at 14,000 rpm for 10 mins at 4 ^oC. The cell pellets were washed for three times

using PBS buffer and stored at -80 ºC. The extract of the lysed cell pellets was prepared for denaturing 1D-PAGE (polyacrylamide gel electrophoresis). SDS (sodium dodecyl sulfate)-sample buffer was added to the IP (immunoprecipitation) beads, boiled and run into a 10% SDS Bis-Tris PAGE (Life Technologies, Carlsbad, CA) for 5 mins as a short stack, stained overnight with colloidal blue (Life Technologies), and destained with water for 3 hrs. The entire band containing protein was excised and equilibrated in 100 mM ammonium bicarbonate, then reduced, carbidomethylated, dehydrated and digested with Trypsin Gold (Promega, Madison, WI). Following digestion, peptides were concentrated under vacuum and resolubilized in 0.1% formic acid prior to 1D reverse phase nLC-ESI-MS (liquid chromatography-electrospray ionization-tandem mass spectrometry) analysis.

Digested peptides were separated using a Surveyor HPLC plus (Thermo Fisher Scientific) using a split flow configuration on the back end of a 100 micron I.D. x 13 cm pulled tip C-18 column (Jupiter C-18 300 Å, 5 micron, Phenomenex). The column was on-line with a Thermo Orbitrap Velos Pro hybrid mass spectrometer equipped with a nano-electrospray source (Thermo Fisher Scientific). All data were collected in CID (collision-induced dissociation) mode. Peptide fractions were directly sprayed into the mass spectrometer over a 1 hr gradient set to increase from 0%-30% acetonitrile in D.I. H_2O containing 0.1% formic acid with a flow rate of 0.3 µL/min. Following each parent ion scan, fragmentation data were collected on the top most intense 18 ions. During data collection, the instrument is configured as follows: spray voltage 1.9 kV, capillary temperature 170 °C, 1 microscan for all scans, with a maximum inject time set for full MS scan in FT mode at 500 ms, and for fragmentation (MSn) in the Ion Trap at 100 ms. The parent ion scans were obtained at 60 K resolution in FT mode with a minimum signal threshold of 2000 counts for MSn activation. The activation settings were at charge state 3, isolation width 2.0 m/z, normalized

collision energy 30.0, activation Q 0.250 and activation time 25 ms. For the dependent scans, both the charge state screening and dynamic exclusion were enabled with these settings: repeat count 2, repeat duration 30 secs, exclusion list size 500 and exclusion duration 60 secs.

The XCalibur RAW files collected in profile mode were centroided and converted to MzXML using ReADW v. 3.5.1. The .mgf files were created using MzXML2Search for all scans with a precursor mass between 300 Da and 1,200 Da. The data were searched using SEQUEST set for three maximum missed cleavages, a precursor mass window of 20 ppm, trypsin digestion, variable modification C at 57.0293 and M at 15.9949. For the fragment-ion mass tolerance, 0.0 Da was used. Searches were performed with a Clostridial subset of the UniRef100 database, which includes common contaminants such as digestion enzymes and human keratin, and the in-house *C. tyrobutyricum* genome database. The resulting list of the generated peptide IDs was filtered using Scaffold (Proteomesoftware, Portland, OR). The filter cut-off values were set with peptide length (>5 AA's), peptide probability set to >90% C.I., ≥2 peptides/protein, and protein probabilities set to >99% C.I., with a final FDR of <1.0%. The protein expression was described using spectra count normalized to total protein in the samples.

2.2.5 Fatty Acid and Amino Acid Analysis

The same sampling points described in Section 2.2.4 were used to collect and prepare the metabolomics samples. The sampled cell pellets were used to prepare intracellular metabolite samples, and the supernatants were used to prepare the extracellular metabolite samples. The intracellular and extracellular metabolite samples were prepared as described in the literature [16,17]. The dried extracts were derivatized and subjected to gas chromatograph-Time of Flight Mass Spectrometer (GC-TOFMS) consisting of Agilent 6890 GC with split/spliless injector (Agilent Technologies, Wilmington, DE) and Leco Pegasus IV TOFMS (Leco, St. Joseph, MI)

[18]. The mass spectra data, the total ion current produced by all ions, were exported to BinBase for data processing as described by the Fiehn group [19]. The data mining was carried out using the statistical language R and normalized by dividing the area of each peak (component) by the total area of the metabolites with known structure in the same samples [20].

2.3. Results

2.3.1. Cell Growth

As presented in Fig. 2.2, the wild type grew immediately after inoculation and almost reached stationary phase by end of the first batch, whereas the ACKKO grew slower and the ACKKO-*adhE2* grew the slowest with a lag phase of ~10 hrs and ~20 hrs, respectively. The longer lag phase in ACKKO-*adhE2* fermentation was caused by the gene manipulation or antibiotics addition. Fermentations were stopped when the production of main C4 products stopped or glucose was no longer consumed. The total fermentation timeline was ~80 hrs, 140 hrs and 90 hrs for wild type, ACKKO and ACKKO-*adhE2*, respectively. The ACKKO mutant had an extended fermentation timeline that allows the third batch with glucose feed. As shown in Table 2.2, both mutants had a lower specific growth rate than the wild type, i.e. 0.21± 0.006 h^{-1}, μ = 0.13± 0.001 h^{-1} and 0.16± 0.002 h^{-1} by wild type, ACKKO, and ACKKO-*adhE2*, respectively. The yields of biomass were 0.06± 0.005 g/g-glucose for wild type, 0.04± 0.006 g/g for ACKKO, and 0.06± 0.004 g/g for ACKKO-*adhE2* (Table 2.2). The downregulation of *ack* reduced the yield of biomass, but the overexpression of *adhE2* led to an improved yield in biomass relative to the parental mutant ACKKO.

2.3.2. Acids and Alcohols Production

In the fermentations of wild type and ACKKO, the acetate production leveled off by the end of the first batch, much sooner than butyrate that reached the maximum concentration in the last batch (Fig. 2.2). Table 2.2 showed that the final concentrations of butyrate reached 19.28 g/L by wild type, 37.30 g/L by ACKKO, and 5.06 g/L by ACKKO-*adhE2*. The yields of butyrate were 0.35 g/g, 0.43 g/g, and 0.16 g/g, and productivities were 0.39 g/L/h, 0.45 g/L/h and 0.13 g/L/h, by wild type, ACKKO and ACKKO-*adhE2*, respectively. As compared to ACKKO, the butyrate production was significantly decreased but a high concentration of butanol was produced in the fermentation by ACKKO-*adhE2*, indicating that the carbon flux was redistributed from butyrate to butanol. The cell growth of ACKKO-*adhE2* slowed down from 33 h to 51 h, but the concentrations of butyrate and butanol increased. After OD_{600} reached the maximum value of 7.94 at 51 h, the butyrate production stopped while the butanol concentration increased until 78 h. This result could indicate that the gene complement for cell growth correlated with butanol concentration. For acid byproduct, a certain amount of acetate was produced by ACKKO (6.76 g/L) although the ratio of butyrate/acetate was increased. However, the acetate production by ACKKO-*adhE2* was minimal, only 0.47 g/L, which would benefit the downstream product separation.

Fig. 2.2 showed that only ACKKO-*adhE2* produced solvents (butanol and ethanol) starting from the log phase. The butanol production sped up from the midpoint of the first batch and continued increasing until the end of the second batch. The overexpression of the *adhE2* gene led to the production of a high level of butanol. The high butanol concentration of 16.68 g/L and overall yield of 0.32 g/g were achieved by ACKKO-*adhE2*. The traditional ABE fermentation by *C. acetobutylicum* produced butanol with yield of ~0.2 g/g, titer of ~12 g/L and productivity of

<0.5 g/L·h [21,22]. As compared to *C. acetobutylicum*, the higher butanol concentration and yield by ACKKO-*adhE2* were attributed to the high butanol tolerance and less byproducts by *C. tyrobutyricum*. It is noted that the productivity of butanol was low (0. 28 g/L/h) due to the slow cell growth rate and long lag phase, but it could be improved by cell adaptation using a fibrous-bed bioreactor [23]. Although ethanol production was observed in the fermentation by ACKKO-*adhE2*, its production was low, with a final concentration of 1.26 g/L, yield of 0.011 g/g, and productivity of 0.01 g/L/h.

It is noted that both wild type and ACKKO produced butyrate as the main product, with the selectivity of 0.82 g-product/g-total products and 0.85 g/g, respectively. Among the fermentations by the three strains, ACKKO-*adhE2* generated the highest selectivity of C4 products, i.e. 0.92 g/g including 0.71 g/g of butanol and 0.22 g/g of butyrate. Acetate was the single C2 byproduct by wild type and ACKKO, while two C2 products (acetate and ethanol) were produced by ACKKO-*adhE2*. The selectivity of C2 was 0.18 g/g, 0.15 g/g, and 0.07 g/g by wild type, ACKKO, and ACKKO-*adhE2*, respectively. These results indicated that carbon flux was redistributed from C2 to C4 due to the overexpression of the heterologous *adhE2* gene. Differently from the acetone-butanol-ethanol (ABE) fermentation by *C. acetobutylicum* which had metabolic shift from acidogenesis to solventogenesis, ACKKO-*adhE2* produced butanol from the beginning of exponential phase without a true acidogenic phase. Actually ACKKO-*adhE2* had a mixed phase to produce solvent and acid simultaneously followed by a solventogenic phase.

2.3.3. Comparative Proteomics

As described in Section 2.2.4, the cells used for proteomics analysis were collected at the mid-log phase for all three strains. The proteomics data were presented as the mass spectra normalized by the total protein in the same sample. Therefore, the proteomics data collected in this study can

reveal the difference of protein expression caused by the metabolic engineering. A total of 2374 intracellular proteins were detected by GeLC-ESI-MS/MS, which covered 78.1% of the open reading frames (3,040) in *C. tyrobutyricum*. The more important enzymes involved in the metabolism of carbon, energy and redox, and cellular responses to butanol stress were also analyzed. The expression data of the proteins from the log-phase cells were summarized in Tables 2.3-6. The relative change of the enzyme expression was described in the metabolic pathway in Fig. 2.1. The key findings of energy, redox and carbon balance were summarized and presented in the heat map in Fig. 2.3.

2.3.4. Carbon Metabolism

The fermentation substrate, glucose, was metabolized to pyruvate via the Embden-Meyerhof-Parnas (EMP) pathway. As shown in Table 2.3, most glycolytic enzymes in wild type had expression levels that were higher than or similar to the mutant strains. This result explained the faster conversion rate of glucose to pyruvate in wild type, 0.81 g/L/h (65 g/L of glucose within 80 hrs), than that in the mutants, ~0.62 g/L/h. A Similar proteomics result was observed in *C. thermocellum,* showing that the expression of glycolytic proteins decreased with ethanol stress [24].

For solvents production, the enzymes were analyzed involved in butanol and ethanol formation pathways. The wild type expressed native NAD(P)H-dependent butanol dehydrogenase (*bdh*) and alcohol dehydrogenase (*adh*) (Table 2.4), so the overexpression of the heterologous *adhE2* gene in ACKKO-*adhE2* enabled complete solvent formation pathways (Fig. 2.1). In the butanol synthesis pathway, both Aadh (*adhE2*) and Bdh had high MS spectra count, 209 and 95, respectively, indicating the active conversion from butyryl-CoA to a high level of butanol (16.68 g/L). In the ethanol formation pathway, the low expression of Adh (SC of 3) repressed ethanol

production (1.26 g/L) although *adhE2* gene had a high expression. Neither wild type nor ACKKO produced butanol because of the incomplete solvent generation pathways. Several proteome studies of *C. acetobutylicum* also demonstrated a higher expression of *adhE2* and *bdh* genes in the solventogenic phase [13,25,26].

In the butyrate generation pathway, only two spectral counts of phosphotransbutyrylase (*ptb*) were detected in wild type while the butyrate kinase (*buk*) was detected in none of the three strains (Table 2.4). The absence or the low level of these enzymes could be caused by the glitch in LC-MS/MS detection or the uncompleted annotation of the genome sequence of *C. tyrobutyricum*. The published genome database of *C. tyrobutyricum* ATCC 25755 [8,9] does not contain *ptb* and *buk* DNA sequences. Both butyrate and butanol were produced from butyryl-CoA through the butyrate pathway of butyryl-CoA→butyryl-P→butyrate and the butanol pathway of butyryl-CoA→butyraldehyde→butanol, respectivey. The reassimilation of butyrate catalyzed by acetoacetyl-CoA:acyl-CoA transferase and acetoacetate decarboxylase was reported in *C. acetobutylicum* [27], but neither genomics and proteomics indicated these two genes/enzymes in this study. In addition, the metabolic pathway of *C. tyrobutyricum* ACKKO-*adhE2* in literature [23] showed that ctfAB interact the acetate pathway and butyrate pathway, but our proteomics did not reveal obvious expression of this enzyme.

For the acetate formation pathway, the MS spectral count of phosphotransacetylase (*pta*) in wild type, ACKKO and ACKKO-*adhE2* was 5, 6 and 1.5, respectively (Table 2.4). Two acetate kinase (*ack*) enzymes were identified in *C. tyrobutyricum*. The Ack with ID of D8GRZ3 had low SC, i.e. 3 in wild type, 0 in ACKKO, and 1 in ACKKO-*adhE2*. Another Ack with ID of GB000761/CTYR_1364 had high SC, i.e. 102 in wild type, 68 in ACKKO, and 92 in ACKKO-*adhE2*. The published *ack* DNA sequences in *C. tyrobutyricum* ATCC 25755 (GI: 516360615,

Protein ID: WP_017750648.1) [8,9] showed the same DNA sequence and also matched with the sequence of CTYR_1364.

In the core metabolic pathway (Fig. 2.1), both acetyl-CoA and butyryl-CoA were key intermediates that controlled the carbon distribution between C2 and C4 products. Table 2.4 showed that the expression of thiolase (*thl*), acetyl-CoA acetyltransferase (*ato*), 3-hydroxybutyryl-CoA dehydrogenase (*hbd*), and crotonase (*crt*) in ACKKO-*adhE2* was significantly increased as compared to wild type and ACKKO. All these enzymes played important roles in directing the carbon from acetyl-CoA to butyryl-CoA. The carbon redirection resulted in the low production of C2 biochemicals (acetate and ethanol) and the high selectivity of C4 biochemicals (butanol and butyrate) in ACKKO-*adhE2*. Previous study of *C. acetobutylicum* [12,13,26] showed higher expression of enzymes in the catabolism of pyruvate in response to solvent production.

As the precursor of butanol and butyrate, butyryl-CoA dictated the distribution of carbon flux to C4 products. Therefore, the expression of the enzymes were analyzed prior to butyryl-CoA, i.e. butyryl-CoA dehydrogenase (*bcd*) and electron transfer flavoproteins (*etf*). As compared to wild type, the expression of Bcd was decreased by 0.8 fold and all three EtfA/B were decreased in ACKKO-*adhE2*. These results suggested that the flux flowed from crotonyl-CoA to butyryl-CoA was not efficient, which could impact the synthesis of butanol.

2.3.5. Energy Metabolism

In glycolysis pathway, the expressions of two ADP-dependent enzymes, phosphoglycerate kinase (*pgk*, CTYR_2948 and O52632) and pyruvate kinases (*pyk*, CTYR_387 and D8GLL2), significantly (> 80%) decreased in ACKKO-*adhE2* compared to wild type. The phosphoglycerate kinase catalyzed the formation of 3-phosphoglycerate and ATP from 1,3-biphosphoglycerate and ADP, and pyvuvate kinase catalyzed the conversion from phosphoenolpyruvate and ADP to

pyruvate and ATP. The downregulated ADP-dependent enzymes may slow the flux of carbon through glycolysis, unless pyruvate pyrophosphate dikinase or other isoenzymes are used as reported in *C. thermocellum* [28]. The catabolism of acetyl-CoA and butyryl-CoA to generate acetate and butyrate, respectively, was also important for energy conservation by providing ATP. In ACKKO, the lower expression of acetate kinase (*ack*) could cause lower ATP production, but the higher butyrate production could generate more ATP (Fig. 2.1 and Fig. 2.3A). In ACKKO-*adhE2*, both the acids formation metabolic pathways and glycolysis were obviously repressed. Table 2.5 showed that the overall expression level of ATP synthase in ACKKO was higher than other two strains.

2.3.6. Redox Metabolism

NAD(P)H is an important cofactor in the production of butanol. In the glycolysis and core metabolic pathways, the expression of the NAD(P)H-dependent Aadh (*adhE2*), Adh, Bdh, and Hbd in ACKKO-*adhE2* were significantly upregulated as compared to ACKKO, but restored to the same or higher levels of wild type except Aadh (Fig. 2.3B). In addition, an obvious correlation between the expression of NADH-dependent hydrogenases and the high butanol production was observed in ACKKO-*adhE2*. Two NAD^+-dependent triosephosphate isomerase (*tpi*) proteins (IDs of D8GUR1 and A0MJQ4) in glycolysis were detected. As compared to wild type, the expression of both *tpi* genes in ACKKO was significantly downregulated. Different from ACKKO, ACKKO-*adhE2* showed that the expression of *tpi* (D8GUR1) was zero but the SC of the *tpi* (A0MJQ4) was increased to 51 from 21 in wild type. Most NAD(P)H consuming enzymes had a higher expression in ACKKO-*adhE2* than that in ACKKO. Taken together, the overexpressed *adhE2* gene in the synthesized butanol pathway in ACKKO-*adhE2* increased the requirement for reducing power and

also resulted in the upregulation of other NADH consuming enzymes, which could hamper the further improvement of butanol production.

2.3.7. Cellular Responses to Metabolic Engineering

In solventogenic Clostridia, butanol stress induced multiple cellular responses, such as the expression changes of heat shock protein expression (Hsp), glycerolipid and sporulation. Although the low levels of butanol and butyrate production might not cause stress (Table 2.1), the protein expressions of Hsp, glycerolipid and sporulation in wild type and the two metabolically engineered strains were compared (Table 2.6). First, the expression of molecular chaperone proteins, including Hsp60 (SC of 63), GroEL (SC of 478) and GroES (SC of 34) in ACKKO-*adhE2*, was much higher than that in wild type and ACKKO. The Hsp assisted proper folding, stabilization and degradation, so the upregulation of these proteins could be caused by the production of butanol in the synthesized butanol pathway. Other studies showed that HSP18 [12], Hsp60 [1], GroEL [12,29], and GroES [12,30] were upregulated in solventogenic Clostridia. We also observed the downregulation of some Hsp in the mid-log phase of the fermentation by ACKKO-*adhE2*, including Hsp90, HslO, two putative DnaK isozymes, ClpB and HipG. To better understand the correlation between Hsp expression and butanol stress, the proteomics analysis using the cells from late stage of fermentation is highly needed. Second, the ACKKO-*adhE2* showed higher expression of glycerol-3-phosphate dehydrogenase (*glpA*), which might enhance the phospholipid bilayer of the cell membrane. Third, the expression of spore coat protein (*cotL*, CTYR_2314), spore germination protein (*gerKC*) and sporulation integral membrane protein (*ytvI*) was higher in ACKKO-*adhE2* than in other two strains. Very interestingly, the expression of sporulation transcription factor Spo0A (*spo0A*) was silent from SC of 45 in wild type to SC of 0 in ACKKO-*adhE2*. The shutdown of *spo0A* expression in ACKKO-*adhE2* demonstrated that the high butanol

production did not associate with sporulation. This feature could allow for the strict regulation of the metabolic shift to butanol production.

2.3.8. Metabolite Analysis

The metabolite analysis was performed in three strains. At the sampling point, the wild type produced 0 g/L of butanol, 2.65 g/L of butyrate and 0.21 g/L of acetate; the ACKKO produced 0 g/L of butanol, 6.25 g/L of butyrate and 2.27 g/L of acetate; and ACKKO-*adhE2* produced 3.44 g/L of butanol, 1.36 g/L of butyrate, 0.98 g/L of acetate and 1.30 g/L of ethanol. These end-products data indicated that the cell engineering manipulation significantly affect the metabolic activities. To understand the effect of metabolic engineering on metabolism, the normalized ion current reading in GC-TOFMS of both intracellular and extracellular metabolites with obvious changes were summarized in Table 2.7.

Three fatty acids with obvious changes, including stearate (KEGG C01539, C18:0), palmitate (KEGG C00249, C16:0) and myristate (KEGG C06424, C14:0), were identified. As compared to wild type, the concentrations of these three fatty acids in the mutants decreased by 0.5 fold or maintained at similar levels, both intracellular and extracellular. The fatty acids could be synthesized from acetyl-CoA and malony-CoA precursor, and the C2/C4 end-products were also produced from acetyl-CoA, indicating that the synthesis of fatty acids could compete with the bioproducts production. At the time points to take metabolite samples, the concentrations of end-products in ACKKO (4.83 g/L of C4 and 1.24 g/L of C2) and ACKKO-*adhE2* (4.80 g/L of C4 and 2.28 g/L of C2) were higher than that in wild type (0.21 g/L of C4 and 2.65 g/L of C2). The higher production of C4 by mutants indicated higher consumption and synthesis of acetyl-CoA, and thereby lower levels of fatty acids.

The extracellular concentrations of three amino acids (i.e. alanine, oxoproline and leucine) in the ACKKO-*adhE2* fermentation liquor were significantly higher than wild type and ACKKO. Since no amino acid supplement was added to fermentation broth, the increased extracellular alanine was secreted by the ACKKO-*adhE2* mutant. The first metabolite in the core pathway (Fig. 2.1), pyruvate, was correlated with succinate (non amino acid), tyrosine and alanine. The concentration of extracellular alanine in ACKKO-*adhE2* increased by 11.79 fold but its intracellular concentration slightly decreased as compared to wild type. The highly secreted alanine was not observed in the ACKKO fermentation broth. The high level of secreted alanine by ACKKO-*adhE2* suggested that the alanine had been actively synthesized intracellularlly. The alanine aminotransferase (*alt*) could catalyze the reaction of glutamate + pyruvate $\rightleftharpoons$ alanine + α-ketoglutamate, but our proteomics data showed 0.5-fold reduced expression of alanine aminotransferases (CTYR_1910 and CTYR_2567) in ACKKO-*adhE2*, so the intracellular alanine in ACKKO-*adhE2* could be produced by multiple reactions besides the synthesis pathway from pyruvate. It was found that the intracellular alanine in all three strains were similar but much lower than the extracellular alanine in ACKKO-*adhE2* fermentation. The reaction of alanine + H_2O + NAD^+ $\rightleftharpoons$ pyruvate + NH_3 + NADH + H^+ catalyzed by alanine dehydrogenase could synthesize pyruvate from alanine and also balance the reducing power. The high production of end-products in ACKKO and ACKKO-*adhE2* mutants consumed more pyruvate and alanine than wild type, meanwhile the synthesis of pyruvate from alanine increased the production of NADH and compensate the apparent redox imbalance caused by the synthesized butanol pathway. A recent study reported that the *C. thermocellum* mutant strains with disrupted end-product pathways (deleted *ldh* and *pta* genes) secreted higher amounts of alanine, valine, isoleucine, proline,

glutamine, and threonine because the production of amino acids could recycle $NADP^+$ to relieve the intracellular redox imbalance [31].

In our study, the ACKKO mutant of *C. tyrobutyricum* with deleted *ack* gene and downregulated acetate pathway did not show obvious increase of extracellular amino acids because the increased butyrate production did not need a higher level of NADH. In the middle of the core pathway, leucine and oxoproline provided a carbon source to the formation of acetyl-CoA. The higher extracellular concentration of leucine indicated its higher intracellular synthesis and higher cross-membrane transportation by ACKKO-*adhE2*. In the end of the core pathway, the α-ketoglutamate and succinate had lower concentrations in mutants. The high production of butyrate from butyryl-CoA in ACKKO and the high conversion of butanol from butyryl-CoA in ACKKO-*adhE2* might consume more α-ketoglutamate and succinate than wild type.

2.4. Discussion

2.4.1 Proteomics study of *C. tyrobutyricum*

As compared to *E. coli* and other Clostridia strains, *C. tyrobutyricum* showed multiple advantages, such as the relatively simple metabolic pathway and high butanol tolerance [3]. To date, the advanced Omics studies in *C. tyrobutyricum*, such as transcriptomics, proteomics and metabolomics, had not been reported. In this study, the global proteomic profiling of *C. tyrobutyricum* were analyzed using GeLC-ESI-MS/MS. It was found that the genome sequence of *C. tyrobutyricum* contains 3,040 open reading frames (ORFs) [8]. 2,374 cytoplasmic proteins were identified, which accounted for 78.1% of the predicted ORFs in the genome. More than 95% of the reported proteins catalyzing glycolysis, core metabolic pathway and products formation pathways, except butyrate kinase and acetate/butyrate CoA transferase, were detected. The

coverage percentage of our proteomics study was much higher than the reported coverage of other Clostridial proteome maps, including 21.0-23.9% in *C. acetobutylicum* ATCC 824 [12,13]and 14.7% in *C. acetobutylicum* DSM 1731 [26].

Facilitated with in-house genomic database, the comparative proteomics of the strains with different phenotypes made it possible to identify the host cell regulators of the desired phenotype. Specifically, the downregulation of ATP generation pathways in ACKKO-*adhE2*, i.e. glycolysis pathway and acids formation pathways could cause the slow cell growth rate and the carbon flux through glycolysis. The addition of a butanol synthesis pathway and other consequently unregulated NADH consuming pathways caused obvious redirection of electrons. The findings of apparent imbalanced energy and redox and the carbon regulators could provide the right direction to engineer the next-generation *C. tyrobutyricum* strain. In addition, the effect of metabolic engineering on the carbohydrate metabolism and enzymes expression in ACKKO mutant was more pronounced than that in ACKKO-*adhE2*.

2.4.2 Carbon Redistribution

As a key node in the metabolic network, both acetyl-CoA and butyryl-CoA played a critical role in redistributing carbon and energy. Specifically, acetyl-CoA was generated from pyruvate, and consumed by three downstream metabolic pathways that produced acetate, ethanol and acetoacetyl-CoA. The butyryl-CoA was synthesized from crotonyl-CoA, and converted to butyrate and butanol. In ACKKO-*adhE2*, the acetate formation from acetyl-CoA was minimal (0.47 g/L), small amount of ethanol was generated (1.26 g/L), and carbon flux was redirected from acetyl-CoA to acetoacetyl-CoA by the enzymes with increased expression. The efficiency of butyryl-CoA synthesis from crotonyl-CoA could be low due to the decreased expression of butyryl-CoA

dehydrogenase (*bcd*) and electron transfer flavoproteins (*etf*), the butyrate production was low (5.06 g/L), and butanol production was high (16.68 g/L).

Consistent with the fermentation results, the heat map (Fig. 2.3C) showed the upregulation of the enzymes that catabolized acetyl-CoA and the upregulation of the enzymes involved in butanol synthesis in ACKKO-*adhE2*. Thus it is hypothesized that the carbon reflux in ACKKO-*adhE2* was regulated via an integrated mechanism to achieve high butanol production. First, the decreased expression of phosphotransacetylase (*pta*) reduced the carbon flux distribution to acetate production. Second, the low expression of alcohol dehydrogenase (*adh*) generated a low ethanol production even though the bifunctional acetaldehyde/alcohol dehydrogenase (*adhE2*) expression was overexpressed. Third, the high expression of thiolase (*thl*) and acetyl-CoA acetyltransferase (*ato*) redirected carbon from C2 to C4, resulting in a high C4 selectivity. Finally, the overexpression of *adhE2* and *bdh* genes led to high production of butanol.

2.4.3 Rational Metabolic Engineering

Molecular biology tools for Clostridia are still in their infancy but tremendous progress has been made recently by a number of academics such as the Minton group, Yang group and Papoutsakis group [15,32,33,34]. For example, the gene knockout technology (ClosTron), gene integration (ACE), unique methylation and efficient replicon have been demonstrated on a wide range of *Clostridium* sp. Although promising butanol production has been achieved by *C. tyrobutyricum* mutant, the butanol production needs to be further improved to reduce the butanol cost to $3/gal gasoline equivalent (BETO 2022 cost target). Our study indicated some rationally metabolic engineering strategies, including carbon redistribution, redox redirection and process engineering.

The proteomics data in this study explained the fermentation observation that most carbon was redistributed from C2 to C4, so the downregulation of C2 production would not be an efficient strategy to improve butanol production. Since a certain level of butyrate was still produced by ACKKO-*adhE2*, the knockout of butyrate pathways could increase the selectivity and concentration of butanol but energy need be redirected. The comparative proteomics showed that the high expression of acetyl-CoA acetyltransferase (*ato*) correlated with high concentration of butanol, so overexpressing *ato* gene might aid in higher flux from acetyl-CoA to butyryl-CoA. Because the expression of butyryl-CoA dehydrogenase in ACKKO-*adhE2* was 80% lower than that in wild type, so replacing *bcd* gene with other gene, such as trans-enoyl-CoA reductase (*ter*) that catalyzes the formation of butyryl-CoA from crotonyl-CoA, should be able to improve butanol production efficiency.

Previous study suggested that the solventogenic transition involved global remodeling of metabolism in *C. tyrobutyricum* such as carbon and reducing power [35]. This study showed that the high production of butanol required more NAD(P)H, but the expression of NAD(P)H-dependent enzymes increased in *C. tyrobutyricum*, so a complete redox balance analysis is highly needed with hydrogen pathway analysis in the future. It was found that the change of NADH/NAD^+ ratio redistributed the metabolic flux and product formation in *E. coli* and *C. acetobutylicum* [36,37]. However, the redox redistribution in *C. tyrobutyricum* had not been reported. Several strategies could be applied to engineer redox in *C. tyrobutyricum*, including the upregulation of the NAD(P)H formation pathway, downregulation of the NAD(P)H consumption pathway, and the addition of a heterologous NAD(P)H generation pathway. As shown in Fig. 2.1, in the hydrogen production pathway, the formation of the oxidized ferredoxin from the reduced ferredoxin that is catalyzed by ferredoxin NADH oxidoreductase (*fnor*) can generate NADH, but

the upregulation of *fnor* could cause the decrease of carbon flux distribution to butanol, so it's complicated to increase both NADH and butanol production via manipulating the enzyme in the hydrogen pathway. Although the formation of one ethanol consumes two NADH, ethanol production is low, so the NADH accumulation by downregulating the ethanol pathway might be very limited. Therefore, the effective way to engineer redox in *C. tyrobutyricum* could be the addition of a new NADH generation reaction, such as the overexpression of heterologous format dehydrogenase and/or native pyruvate-formate lyase. The proteomics data showed certain level of pyruvate-formate lyase (*fpl*, CRYR_71), with SC of 8.5 in wild type, 2 in ACKKO and 8.5 in ACKKO-*adhE2*.

In addition to metabolic cell engineering, the output of proteomics integrated with metabolite analysis could facilitate metabolic process engineering. the metabolite analysis revealed that a couple of amino acids had changed metabolite profiles in the fermentations by mutants. This result indicated that the fermentation medium could be optimized by optimizing amino acids to improve butanol production. The supplement of the reducing power can also be increased by medium component optimization.

2.5. Conclusions

In this study, it is built a comprehensive dataset of the intracellular protein expression of *C. tyrobutyricum* using GeLC-MS/MS, identified the key enzymes regulating carbon, energy and redox balance in the core metabolic pathway using comparative proteomics, and investigated the host cell regulators in response to butanol production. This study represents the most extensive proteome investigation of *C. tyrobutyricum* to date, which greatly advances understanding of the regulating mechanisms driving butanol production. The findings in this proteomics study also suggested some strategies to rationally engineer *C. tyrobutyricum* by redirecting carbon and

electron flux for the improvement of biobutanol production. In addition, the intracellular and extracellular metabolite analysis revealed the changes of the metabolic activities and suggested the butanol production improvement by metabolic process engineering.

2.6. References

[1] K.V.Alsaker, C. Paredes, E.T. Papoutsakis. "Metabolite stress and tolerance in the production of biofuels and chemicals: gene-expression-based systems analysis of butanol, butyrate, and acetate stresses in the anaerobe *Clostridium acetobutylicum*". Biotechnol. Bioeng., vol. 105, pp. 1131-1147, 2010.

[2] X. Liu, Y. Zhu, S.T. Yang. "Butyric acid and hydrogen production by *Clostridium tyrobutyricum* ATCC 25755 and mutants". Enzyme Microbiol. Tech., vol. 38, pp. 521-528, 2006.

[3] M. Yu, Y. Zhang, I.C. Tang, S.T. Yang. "Metabolic engineering of *Clostridium tyrobutyricum* for n-butanol production". Metab. Eng., vol. 13, pp. 373-382, 2011.

[4] J. Nolling, G. Breton, M.V. Omelchenko, K.S. Makarova, Q. Zeng, R. Gibson, H.M. Lee, J. Dubois, D. Qiu, J. Hitti, Y.I. Wolf, R.L. Tatusov, F. Sabathe, L. Doucette-Stamm, P. Soucaille, M.J. Daly, G.N. Bennett, E.V. Koonin, D.R. Smith. "Genome sequence and comparative analysis of the solvent-producing bacterium *Clostridium acetobutylicum*". J. Bacteriol. Vol. 183, pp. 4823-4838, 2001.

[5] G. Bruant, M.J. Levesque, C. Peter, S.R. Guiot, L. Masson. "Genomic analysis of carbon monoxide utilization and butanol production by *Clostridium carboxidivorans* strain P7". PLoS One, vol. 5, pp. e13033, 2010.

[6] B. Raman, C.K. McKeown, M.Jr. Rodriguez, S.D. Brown, J.R. Mielenz. "Transcriptomic analysis of *Clostridium thermocellum* ATCC 27405 cellulose fermentation". BMC Microbiol., vol. 11, pp. 134, 2011.

[7] Y. Zhang. "Metabolic Engineering of *Clostridium tyrobutyricum* for Production of Biofuels and Bio-based Chemicals". The Ohio State University, 2009.

[8] L. Jiang, L. Zhu, X. Xu, Y. Li, S. Li, H. Huang. "Genome Sequence of *Clostridium tyrobutyricum* ATCC 25755, a Butyric Acid-Overproducing Strain". Genome Announc., vol. 1, 2013.

[9] D. Bassi, C. Fontana, S. Gazzola, E. Pietta, E. Puglisi, F. Cappa, P.S. Cocconcelli. Draft genome sequence of *Clostridium tyrobutyricum* strain UC7086, isolated from Grana Padano Cheese with Late-Blowing defect". Genome Announc., vol. 1, 614–613, 2013.

[10] E. Burton, V.J.Martin. "Proteomic analysis of *Clostridium thermocellum* ATCC 27405 reveals the upregulation of an alternative transhydrogenase-malate pathway and nitrogen assimilation in cells grown on cellulose". Can. J. Microbiol., vol. 58, pp. 1378-1388, 2012.

[11] N. Comba Gonzalez, A.F. Vallejo, M. Sanchez-Gomez, D. Montoya. Protein identification in two phases of 1,3-propanediol production by proteomic analysis. J. Proteomics., vol. 89, pp. 255-64, 2013.

[12] H. Janssen, C. Doring, A. Ehrenreich, B. Voigt, M. Hecker, H. Bahl, R.J. Fischer. "A proteomic and transcriptional view of acidogenic and solventogenic steady-state cells of *Clostridium acetobutylicum* in a chemostat culture". Appl. Microbiol. Biotechnol., vol. 87, pp. 2209-2226, 2010.

[13] K. Sivagnanam, V.G. Raghavan, M. Shah, R.L. Hettich, N.C. Verberkmoes, M.G. Lefsrud. "Shotgun proteomic monitoring of *Clostridium acetobutylicum* during stationary phase of butanol fermentation using xylose and comparison with the exponential phase". J. Ind. Microbiol. Biotechnol., vol. 39, pp. 949-955, 2012.

[14] H. Dong, W. Tao, Z. Dai, L. Yang, F. Gong, Y. Zhang, Y. Li. "Biobutanol". Adv. Biochem. Eng. Biotechnol., vol. 128, pp. 85-100, 2012.

[15] S.W. Jones, B.P. Tracy, S.M. Gaida, E.T. Papoutsakis. "Inactivation of sigmaF in *Clostridium acetobutylicum* ATCC 824 blocks sporulation prior to asymmetric division and abolishes sigmaE and sigmaG protein expression but does not block solvent formation". J. Bacteriol., vol. 193, pp. 2429-2440, 2011.

[16] O. Fiehn. "Extending the breadth of metabolite profiling by gas chromatography coupled to mass spectrometry". Trends Analyt. Chem., vol. 27, pp. 261-269, 2008.

[17] S.G. Villas-Boas, J. Hojer-Pedersen, M. Akesson, J. Smedsgaard, J. Nielsen. "Global metabolite analysis of yeast: evaluation of sample preparation methods". Yeast, vol. 22, pp. 1155-1169, 2005.

[18] S. Kim, Y. Lee do, G. Wohlgemuth, H.S. Park, O. Fiehn, K.H. Kim. "Evaluation and optimization of metabolome sample preparation methods for *Saccharomyces cerevisiae*". Anal. Chem., vol. 85, pp. 2169-2176, 2013.

[19] T. Kind, G. Wohlgemuth, Y. Lee do, Y. Lu, M. Palazoglu, S. Shahbaz, O. Fiehn. "FiehnLib: mass spectral and retention index libraries for metabolomics based on quadrupole and time-of-flight gas chromatography/mass spectrometry." Anal. Chem., vol. 81, pp. 10038-10048, 2009.

[20] M. Gobel, K. Kassel-Cati, E. Schmidt, W. Reineke. "Degradation of aromatics and chloroaromatics by Pseudomonas sp. strain B13: cloning, characterization, and analysis of sequences encoding 3-oxoadipate:succinyl-coenzyme A (CoA) transferase and 3-oxoadipyl-CoA thiolase". J. Bacteriol., vol. 184, pp. 216-23, 2002.

[21] R. Gheshlaghi, J.M. Scharer, M. Moo-Young, C.P. Chou. "Metabolic pathways of clostridia for producing butanol". Biotechnol. Adv., vol. 27, pp. 764-781, 2009.

[22] S.Y. Lee, J.H. Park, S.H. Jang, L.K. Nielsen, J. Kim, K.S. Jung. "Fermentative butanol production by Clostridia". Biotechnol. Bioeng., vol. 101, pp. 209-228, 2008.

[23] D. Wei, X. Liu, S.T. Yang. "Butyric acid production from sugarcane bagasse hydrolysate by *Clostridium tyrobutyricum* immobilized in a fibrous-bed bioreactor". Bioresour. Technol., vol. 129, pp. 553-60, 2013.

[24] S. Yang, R.J. Giannone, L. Dice, Z.K. Yang, N.L. Engle, T.J. Tschaplinski, R.L. Hettich, S.D. Brown. "*Clostridium thermocellum* ATCC27405 transcriptomic, metabolomic and proteomic profiles after ethanol stress". BMC Genomics., vol. 13, pp. 336, 2012.

[25] S. Hu, H. Zheng, Y. Gu, J. Zhao, Zhang, W., Yang, Y., Wang, S., Zhao, G., Yang, S., Jiang, W., 2011. Comparative genomic and transcriptomic analysis revealed genetic characteristics related to solvent formation and xylose utilization in Clostridium acetobutylicum EA 2018. BMC Genomics. 12, 93.

[26] S. Mao, Y. Luo, T. Zhang, J. Li, G. Bao, Y. Zhu, Z. Chen, Y. Zhang, Y. Li, Y. Ma. "Proteome reference map and comparative proteomic analysis between a wild type *Clostridium acetobutylicum* DSM 1731 and its mutant with enhanced butanol tolerance and butanol yield". J. Proteome Res., vol. 9, pp. 3046-3061, 2010.

[27] D. Lehmann, N. Radomski, T. Lütke-Eversloh. "New insights into the butyric acid metabolism of *Clostridium acetobutylicum*". Appl. Microbiol. Biotechnol., vol. 96, pp. 1325-1339, 2012.

[28] T. Rydzak, P.D. McQueen, O.V. Krokhin, V. Spicer, P. Ezzati, R.C. Dwivedi, D. Shamshurin, D.B. Levin, J.A. Wilkins, R. Sparling. Proteomic analysis of *Clostridium thermocellum* core metabolism: relative protein expression profiles and growth phase-dependent changes in protein expression. BMC Microbiol. 12, 214, 2012.

[29] J. Yuan, L. Zhu, X. Liu, T. Li, Y. Zhang, T. Ying, B. Wang, J. Wang, H. Dong, E. Feng, Q. Li, J. Wang, H. Wang, K. Wei, X. Zhang, C. Huang, P. Huang, L. Huang, M. Zeng, H. Wang. "A proteome reference map and proteomic analysis of Bifidobacterium longum NCC2705". Mol. Cell Proteomics., vol. 5, pp. 1105-1118, 2006.

[30] C.A. Tomas, J. Beamish, E.T. Papoutsakis. "Transcriptional analysis of butanol stress and tolerance in *Clostridium acetobutylicum*". J. Bacteriol., vol. 186, pp. 2006-2018, 2004.

[31] D. Van der Veen, J. Lo, S.D. Brown, C.M. Johnson, T.J. Tschaplinski, M. Martin, N.L. Engle, R.A. van den Berg, A.D. Argvros, N.C. Caiazza, A.M. Guss, L.R. Lynd. "Characterization of *Clostridium thermocellum* strains with disrupted fermentation end-product pathways". J. Ind. Microbiol. Biotechnol., vol. 40, pp. 725-734, 2013.

[32] J.T. Heap, S.A. Kuehne, M. Ehsaan, S.T. Cartman, C.M. Cooksley, J.C. Scott, N.P. Minton. "The ClosTron: Mutagenesis in Clostridium refined and streamlined". J. Microbiol. Methods., vol. 80, pp. 49-55, 2010.

[33] M. Yu, Y. Du, W. Jiang, W.L. Chang, S.T. Yang, I.C. Tang. "Effects of different replicons in conjugative plasmids on transformation efficiency, plasmid stability, gene expression and n-butanol biosynthesis in *Clostridium tyrobutyricum*". Appl. Microbiol. Biotechnol., vol. 93, pp. 881-889,2012.

[34] T. Lütke-Eversloh. "Application of new metabolic engineering tools for *Clostridium acetobutylicum*". Appl. Microbiol. Biotechnol., vol. 98, pp. 5823-5837, 2014.

[35] D. Amador-Noguez, I.A. Brasg, X.J. Feng, N. Roquet, J.D. "Rabinowitz. Metabolome remodeling during the acidogenic-solventogenic transition in *Clostridium acetobutylicum*". Appl. Environ. Microbiol., vol. 77, pp. 7984-7997, 2011.

[36] S.J. Berrios-Rivera, G.N. Bennett, K.Y. San. "Metabolic engineering of *Escherichia coli*: increase of NADH availability by overexpressing an NAD(+)-dependent formate dehydrogenase". Metab. Eng., vol. 4, pp. 217-229, 2002.

[37] S. Nakayama, T. Kosaka, H. Hirakawa, K. Matsuura, S. Yoshino, K. Furukawa. "Metabolic engineering for solvent productivity by downregulation of the hydrogenase gene cluster hupCBA in *Clostridium saccharoperbutylacetonicum* strain N1-4". Appl. Microbiol. Biotechnol., vol. 78, pp. 483-493, 2008.

Table 2.1 Physiological characteristics of wild type (WT), ACKKO and ACKKO-*adhE2* of *C. tyrobutyricum* at the sampling point for proteomics analysis.

Products	**WT**	**ACKKO**	**ACKKO-*adhE2***
Time (h)	11	22	30.5
OD_{600}	3.94	5.82	4.51
Cell growth (h^{-1})	0.21	0.13	0.16
Glucose (g/L)	32.94	26.27	25.53
Acetate (g/L)	2.65	1.24	0.98
Butyrate (g/L)	0.21	4.83	1.36
Ethanol (g/L)	0	0	1.30
Butanol (g/L)	0	0	3.44

Table 2.2 Comparison of fermentation production by WT, ACKKO and ACKKO-*adhE2* of *C. tyrobutyricum*.

Products		**WT**	**ACKKO**	**ACKKO-*adhE2***
Cell growth (h^{-1})		0.21±0.006	0.13±0.001	0.16±0.002
Biomass yield (g/g)		0.06±0.005	0.04±0.006	0.06±0.004
Concentration (g/L)	Butanol	0	0	16.68±0.58
	Butyrate	19.28±0.04	37.30±1.07	5.06±0.82
	Acetate	4.21±0.05	6.76±0.36	0.47±0.05
	Ethanol	0	0	1.26±0.07
Yield (g/g-glucose)	Butanol	0	0	0.32±0.11
	Butyrate	0.35±0.01	0.43±0.01	0.16±0.01
	Acetate	0.074±0.0015	0.072±0.0024	0.0052±0.0001
	Ethanol	0	0	0.011±0.002
Productivity (g/L/h)	Butanol	0	0	0.28±0.01
	Butyrate	0.39±0.005	0.45±0.03	0.13±0.01
	Acetate	0.18±0.01	0.15±0.001	0.05±0.001
	Ethanol	0	0	0.01±0.001
Selectivity (g/g-total product)	Butanol	0	0	0.71±0.04
	Butyrate	0.82±0.04	0.85±0.01	0.22±0.03
	Acetate	0.18±0.07	0.15±0.01	0.02±0.003
	Ethanol	0	0	0.05±0.00
Carbon balance		0.62	0.70	0.83

Table 2.3 Comparison of the expression of glycolytic proteins in WT, ACKKO, and ACKKO-*adhE2*.

Function	Protein		Spectral Count[a]		
	ID[b]	Name	WT	ACKKO	ACKKO -*adhE2*
Carbon: glycolysis	GB001058	Glucokinase (ATP) (*gck*)	112	60	74
	GB000442	Glucose-6-phosphate isomerase (*gpi*)	65	22	72
	GB002422	1-Phosphofructokinase (ATP) (*pfk1*)	16	12	9
	GB002868	6-Phosphofructokinase (*pfk6*)	69	42	44
	D8GLG9	Fructose-bisphosphate aldolase (*aldoa*)	8	9	5
	D8GUR1	Triosephosphate isomerase (NAD^+) (*tpi*)	9	3	0
	A0MJQ4	Triosephosphate isomerase (NAD^+) (*tpi*)	31	16	51
	Q59309	Glyceraldehyde-3-phosphate dehydrogenase (*gapdh*)	43	18	40
	O52631	Glyceraldehyde-3-phosphate dehydrogenase (*gapdh*)	55	31	1
	GB000935	Glyceraldehyde-3-phosphate dehydrogenase (*gapdh*)	136	70	116
	GB000936	Phosphoglycerate kinase (ADP) (*pgk*)	101	84	8
	O52632	Phosphoglycerate kinase (ADP) (*pgk*)	17	16	0
	C6PSA3	Phosphoglycerate mutase (*pgm*)	8	5	3
	D8GUQ9	Enolase (*neo*)	7	8	12
	E9SM07	Phosphoenolpyruvate carboxykinase (*pck*)	1	1	0
	GB002867	Pyruvate kinase (ADP) (*pyk*)	66	30	11
	D8GLL2	Pyruvate kinase (ADP) (*pyk*)	5	1	1
	GB001253	Malate dehydrogenase (*mdh*)	7	4	2

Note:

[a] The average spectral count data from the duplicated injection in triplicated experiments were presented.

[b] Annotation was performed using in-house *C. tyrobutyricum* genome sequence database (ID is described as CTYR_Number) and the Clostridial UniRef100 database (ID is described as published ID).

Table 2.4 Comparison of the expression of the enzymes catalyzing the core pathway in WT, ACKKO, and ACKKO-*adhE2*.

Function	Protein		Spectral Count		
	ID	Name	WT	ACKKO	ACKKO *-adhE2*
Carbon: core pathway and products formation pathways	GB001798	Pyruvate:ferredoxin (flavodoxin) oxidoreductase (*pfor*)	112	60	74
	GB000374	Pyruvate:ferredoxin (flavodoxin) oxidoreductase (*pfor*)	4	4	2
	Q6PWX1	Phosphotransacetylase (ADP) (*pta*)	5	6	1.5
	D8GRZ3	Acetate kinase (ADP) (*ack*)	3	0	1
	GB000761	Acetate kinase (ADP) (*ack*)	102	68	92
	GB002960	Alcohol dehydrogenase (NAD(P)H) (*adh*)	2	0	3
	E3VJQ0	Thiolase (*thl*)	216	150	342
	GB002225	Acetyl-CoA acetyltransferase (*ato*)	294	221	425
	GB000459	3-hydroxybutyryl-CoA dehydrogenase (NADH) (*hbd*)	290	176	438
	Q891F6	3-hydroxybutyryl-CoA dehydrogenase (NADH) (*hbd*)	17	14	26
	GB000464	Crotonase (*crt*)	81	40	98
	G7M3R4	Butyryl-CoA dehydrogenase (*bcd*)	10	3	2
	GB000461	Electron transfer flavoprotein alpha-subunit (*etfA*)	5	9	1
	GB000446	Electron transfer flavoprotein alpha-subunit (*etfA*)	27	18	19
	GB000448	Electron transfer flavoprotein beta-subunit (*etfB*)	18	7	12
	Q890T9	Phosphotransbutyrylase (ADP) (*ptb*)	2	0	0
	NA	Butyrate kinase (ADP) (*buk*)	NA	NA	NA
	GB002080	Butanol dehydrogenase (NADPH) (*bdh*)	109	50	95
	GB001335	Butanol dehydrogenase (NADH) (*bdh*)	3	1	1
	F7ZYF5	Bifunctional acetaldehyde/ alcohol dehydrogenase (NAD(P)H) (*adhE2*)	0	0	209
	NA	Acetate/butyrate CoA transferase (*ctf*)	NA	NA	NA

Note: NA means data are not available.

Table 2.5 Comparison of the expression of the enzymes involved in energy and redox balance in WT, ACKKO, and ACKKO-*adhE2*.

Function	Protein		Spectral Count		
	ID	Name	WT	ACKKO	ACKKO-*adhE2*
Energy	The expression data of glucokinase (ATP) (*gck*) and phosphofructokinase (ATP) (*pfk*), phosphoglycerate kinase (ADP) (*pgk*), pyruvate kinase (ADP) (*pyk*), phosphotransacetylase (ADP) (*pta*), acetate kinase (ADP) (*ack*), phosphotransbutyrylase (ADP) (*ptb*) and butyrate kinase (ADP) (*buk*) see Tables 2.3&2.4.				
	Q93Q46	ATP synthase, alpha subunit (*atpA*)	11	12	4
	Q9Z689	ATP synthase, alpha subunit (*atpA*)	23	25	7
	F1TDP6	ATP synthase F1, alpha subunit (*atpA*)	9	13	0
	GB000859	ATP synthase F1, alpha subunit (*atpA*)	66	78	79
	D8GL00	ATP synthase, beta subunit (*atpD*)	31	33	0
	C6PVC7	ATP synthase, beta subunit (*atpD*)	33	31	39
	GB000861	ATP synthase F1, beta subunit (*atpD*)	74	92	89
	GB000858	ATP synthase F1, delta subunit (*atpH*)	4	2	4
	GB000862	ATP synthase F1, epsilon subunit (*atpC*)	4	3	5
	GB000860	ATP synthase F1, gamma subunit (*atpG*)	3	2	6
NAD(P)H	The NADH related enzymes in carbohydrate metabolism, including triosephosphate isomerase (NAD^+) (*tpi*), 3-hydroxybutyryl-CoA dehydrogenase (NADH) (*hbd*), bifunctional acetaldehyde/alcohol dehydrogenase (NAD(P)H) (*adhE2*), alcohol dehydrogenase (NAD(P)H) (*adh*), and butanol dehydrogenase (NAD(P)H) (*bdh*), see Tables 2.3&2.4.				
	A6LR69	Glutamate synthase (NAD(P)H) (*glt*)	16	13	4
	GB000457	Glutamate synthase (NAD(P)H), homotetrameric (*glt*)	78	63	13
	GB002494	Glutamate dehydrogenase ($NAD(P)^+$) (*glud*)	31	22	62
	GB002725	Glycerol dehydrogenase (NAD^+)	27	17	50
	GB002047	Glycerol-3-phosphate dehydrogenase ($NAD(P)^+$) (*gpd*)	7	8	21
	GB000310	FMN reductase (NAD(P)H)	8	8	8
	GB002389	Isocitrate dehydrogenase ($NAD(P)^+$) (*idh*)	25	18	4
	GB000455	Fe-Hydrogenase (NADH)	38	41	27

Table 2.6 Comparison of the expression of butanol stress related proteins in WT, ACKKO, and ACKKO-*adhE2*.

Function	Protein		Spectral Count		
	ID	Name	WT	ACKKO	ACKKO *-adhE2*
Heat shock	Electron transfer flavoprotein alpha-subunit (*etf*) see Table 2.4.				
	A6LQ87	Molecular chaperone, HSP 60 family (*hsp 60*)	29	21	63
	GB001545	Molecular chaperone, HSP 90 family (*hsp 90*)	80	2	6
	GB000336	Co-chaperone GrpE *(grpE*)	1	0	0
	GB000246	Chaperonin HslO (*hslO*)	9	0	0
	GB000244	Chaperone protein DnaJ (*dnaJ*)	21	23	26
	B2TLZ7	Chaperone protein DnaK (*dnaK*)	9	5	2
	GB000245	Chaperone protein DnaK (*dnaK*)	91	57	28
	GB000451	Chaperonin GroEL (*groEL*)	323	259	478
	GB000452	Chaperonin GroES (*groES*)	23	21	34
	GB002403	ATP-dependent chaperone ClpB (*clpB*)	39	42	24
	Q97E05	Chapersone protein htpG (*htpG*)	5	0.4	0
Glycerol	A0Q1Z8	1-acyl-sn-glycerol-3-phosphate acyltransferase (*plsC*)	2	2	0
	GB000477	Glycerol uptake facilitator protein (*glpF*)	1	0	0
	GB001791	Glycerol kinase (*glpK*)	3	1	0
	GB002047	Glycerol-3-phosphate dehydrogenase (*glpA*)	10	13	22
	GB000936	Phosphoglycerate kinase (*pgk*)	91	97	3
	O52632	Phosphoglycerate kinase (*pgk*)	14	14	0
Sporulation	GB002192	Spore coat protein (*cotL*)	2	2	10
	GB002194	Spore coat protein (*cotL*)	5	7	3
	GB001225	Spore germination protein (*gerKC*)	0	1	6
	GB001365	Sporulation integral membrane protein Ytvl (*ytvl*)	0	6	8
	GB002116	Sporulation transcription factor Spo0A (*spo0A*)	45	10	0
	GB000710	RNA polymerase sigma-E factor (*sigE*)	0	3	0
	GB001297	RNA polymerase sigma-F factor (*sigF*)	3	1	2
	GB000711	RNA polymerase sigma-G factor (*sigG*)	2	3	2
	GB000704	RNA polymerase sigma-K factor (*sigK*)	3	2	0

Table 2.7 Fatty acid, amino acids and succinate with significant change.

FA and AA	KEGG ID	Intracellular			Extracellular		
		WT	ACKKO	ACKKO-*adhE2*	WT	ACKKO	ACKKO-*adhE2*
Stearate	C01539	13769±138	12231±297	7901±670	39979±2037	21433±1872	18084±1834
Palmitate	C00249	1962±135	1604±199	1135±17	3412±342	1848±265	1553±419
Myristate	C06424	178±9	163±7	132±3	314±54	181±43	184±56
α-Ketoglut.	C00026	86±42	58±22	35±12	1684±48	563±17	603±53
Leucine	NA	121±3	125±32	132±17	51±7	55±15	425±12
Tyrosine	C00082	1007±66	476±68	478±172	6167±1735	2560±36	2365±134
Oxoproline	C01879	909±223	808±225	1250±208	2449±452	613±262	6987±176
Alanine	NA	333±42	414±43	297±5	87±21	42±10	1113±34
Succinate	C00042	158±12	108±18	69±3	380±63	220±13	241±28

Note: (FA) fatty acid; (AA) amino acid; (α-Ketoglut) α-Ketoglutarate. The unit of metabolites is normalized total ion current.

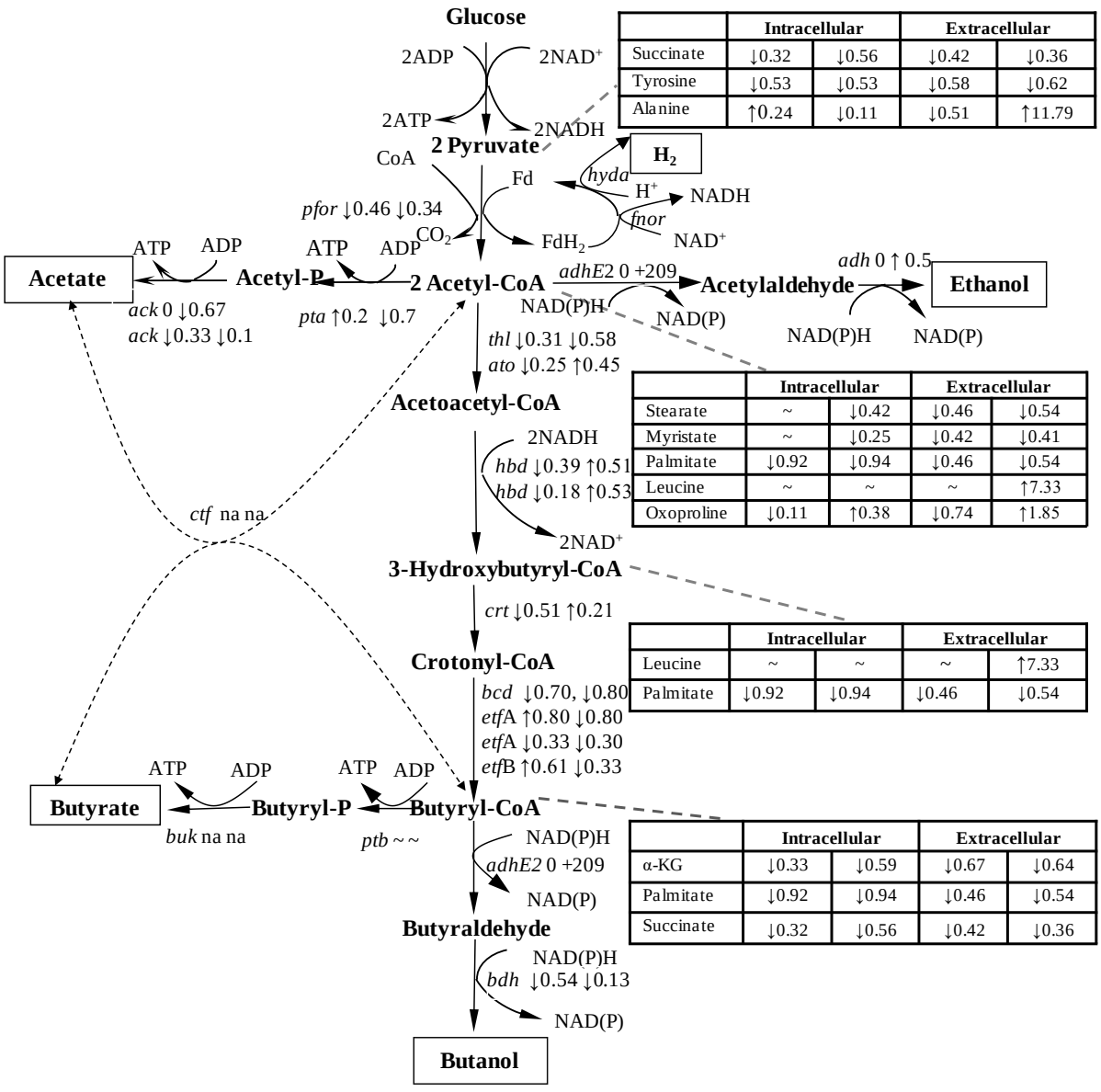

	Intracellular		Extracellular	
Succinate	↓0.32	↓0.56	↓0.42	↓0.36
Tyrosine	↓0.53	↓0.53	↓0.58	↓0.62
Alanine	↑0.24	↓0.11	↓0.51	↑11.79

	Intracellular		Extracellular	
Stearate	~	↓0.42	↓0.46	↓0.54
Myristate	~	↓0.25	↓0.42	↓0.41
Palmitate	↓0.92	↓0.94	↓0.46	↓0.54
Leucine	~	~	~	↑7.33
Oxoproline	↓0.11	↑0.38	↓0.74	↑1.85

	Intracellular		Extracellular	
Leucine	~	~	~	↑7.33
Palmitate	↓0.92	↓0.94	↓0.46	↓0.54

	Intracellular		Extracellular	
α-KG	↓0.33	↓0.59	↓0.67	↓0.64
Palmitate	↓0.92	↓0.94	↓0.46	↓0.54
Succinate	↓0.32	↓0.56	↓0.42	↓0.36

Fig. 2. 1. Metabolic pathway in ACKKO-*adhE2*. Abbreviations: *pta*, phosphotransacetylase; *ack*, acetate kinase; *ptb*, phosphotransbutyrylase; *buk*, butyrate kinase; *thl*, thiolase; *hbd*, beta-hydroxbutyryl-CoA dehydrogenase; *pfor*, pyruvate: ferredoxin oxidoreductase; *hyda*, hydrogenase; *ctf A/B*, CoA transferase; *adhE2*, bifunctional acetaldehyde/ alcohol dehydrogenase; *crt*, 3-hydroxybutyryl-CoA dehydratase; *bcd*, butyryl-CoA dehydrogenase; *etf*, electron transfer flavoprotein. The relative changes of protein expression in two mutants were calculated by "fold change = (ACKKO or ACKKO-*adhE2* – WT)/WT".

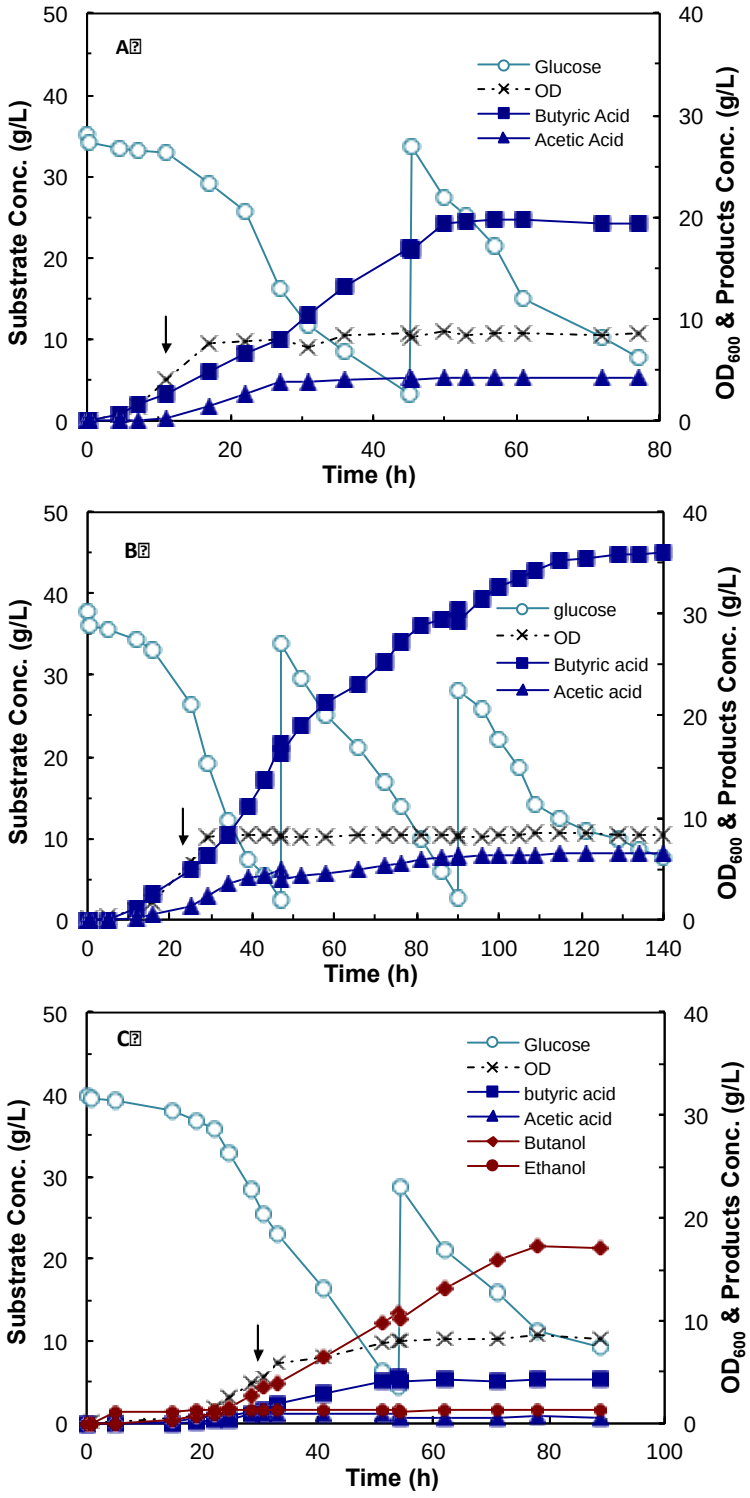

Fig. 2.2. Fermentation kinetics of *C. tyrobutyricum* ATCC 25755 wild type (A), ACKKO (B), and ACKKO-*adhE2* (C) in 2 L bioreactor using glucose as substrate at pH 6.0, temperature 37°C, and 100rpm. ○: Glucose, ×OD, ■: Butyric acid, ▲: Acetic acid, ♦: Butanol, ●: Ethanol.

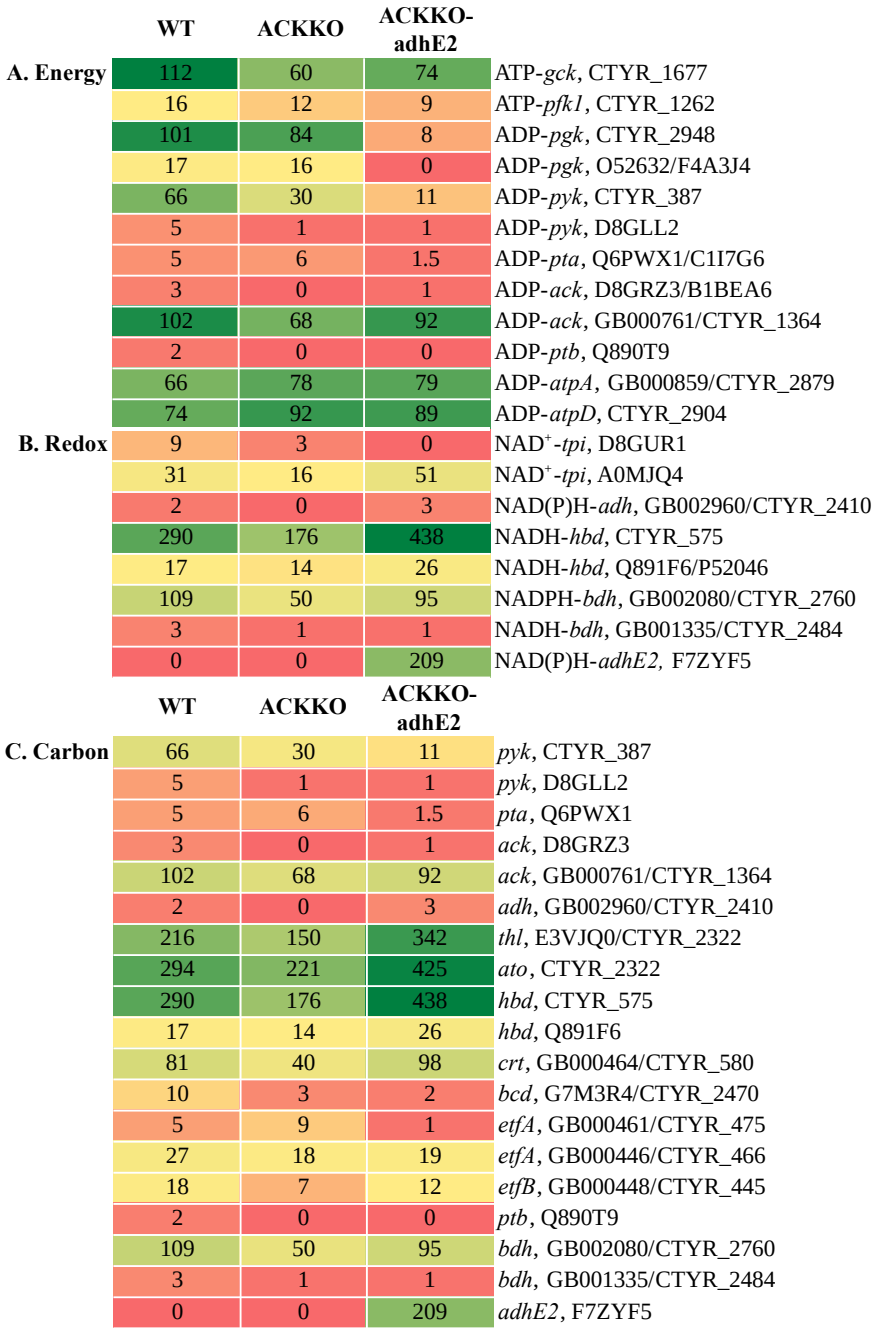

Fig. 2.3. Heat map of protein expression level in different strains. Red color: high expression, Yellow color: medium expression, and Green color: low expression.

CHAPTER 3

HIGH PRODUCTION OF BUTYRIC ACID

Abstract

The objective of this study was to improve the production of butyric acid by process optimization using the metabolically engineered mutant of *Clostridium tyrobutyricum*, PAK-Em. First, the free-cell fermentation at pH 6.0 produced butyric acid with concentration of 40.10 g/L and yield of 0.42 g/g. Second, the immobilized-cell fermentations using a fibrous-bed bioreactor (FBB) were run at pHs of 5.0, 5.5, 6.0, 6.5 and 7.0 to improve the butyric acid production. It was found that the highest titer of butyric acid, 63.02 g/L, was achieved at pH 6.5. Finally, the metabolic flux balance analysis was performed to investigate the carbon rebalance in *C. tyrobutyricum*. The results showed both gene manipulation and fermentation pH redistributed carbon between biomass, acetic acid and butyric acid. This study demonstrated that high butyric acid production could be obtained by integrating metabolic engineering and fermentation process optimization.

3.1. Introduction

Butyric acid, a four-carbon short-chain fatty acid, has been widely used in chemical, food, and pharmaceutical industries. For example, butyric acid has been used as an additive in the manufacturing of plastic and fiber products to enhance their hydrophobicity, flexibility, as well as light and heat resistance [1]. The ester of butyric acid is used as a fruit-flavour fragrant reagent in beverages, food, and cosmetics [2]. Butyric acid has a great potential to treat colorectal cancer, hemoglobinopathies, and insulin resistance [3,4,5]. In addition, butyric acid can be used as a raw material to synthesize biofuel. During the last two decades, there has been an increasing interest to produce butyric acid from microbial fermentation because of the growing demand for bio-based natural foods, cosmetics, and pharmaceuticals [6].

The anaerobic Clostridial strains, such as *C. butyricum* [7], *C. tyrobutyricum* [8], and *C. thermobutyricum* [9], have been predominantly used in butyric acid production. *C. tyrobutyricum* ATCC 25755, a gram-positive, rod-shaped, and anaerobic bacterium, produces butyric acid as the main product from various carbohydrates, such as glucose and xylose [10]. The recent progresses of butyric acid production are summarized in Table 3.1 [11–21]. Compared with other strains, the wild type *C. tyrobutyricum* produced higher levels of butyric acid in the fed-batch free-cell fermentation. Both metabolic engineering and fermentation process development have been applied to improve butyric acid production by *C. tyrobutyricum*. For example, one engineered mutant, *C. tyrobutyricum* PAK-Em, has been constructed by downregulating the acetate kinase gene (ack) involved in the acetic acid formation pathway [22]. Although this mutant showed improved butyric acid production compared to wild type, the cell growth rate was reduced significantly. In addition, the metabolic flux analysis is an important tool to analyze the carbon

redistribution caused by genetic engineering or fermentation process, but it has not been applied to investigate the mutant PAK-Em.

The major fermentation process parameters that affect butyric acid production include fermentation mode, agitation, temperature, pH, nutrient feeding strategy [10]. A novel fibrous-bed bioreactor (FBB) has been developed to produce organic acids and biofuel in immobilized-cell fermentations, which can significantly improve the productivity, yield, and final product concentration [23,24,25,26]. In FBB fermentation, the butyric acid concentration has been improved by 2 to 3 fold because of the high cell density and the high butyric acid tolerance of the immobilized *C. tyrobutyricum* cell inside the FBB [27,28]. As shown in Table 3.1, 49.9 g/L and 86.9 g/L of butyric acids have been produced by *C. tyrobutyricum* mutant from fed-batch FBB fermentation and repeated fed-batch FBB fermentation, respectively [19,20]. It has been reported that pH can significantly affect the butyric acid production [29], but its effect on PAK-Em has not been reported so far.

The main objective of this work was to achieve high butyric acid production by *C. tyrobutyricum* mutant. The free-cell fermentation was performed to build the baseline of butyric acid production. The immobilized-cell fermentations using a FBB were applied to improve the butyric acid production through pH optimization. The metabolic flux balance analysis was used to understand the carbon redistribution caused by metabolic engineering and fermentation parameters. This work demonstrated the great potential to produce high-level butyric acid using the metabolically engineered *C. tyrobutyricum* combined with fermentation optimization.

3.2. Materials and Methods

3.2.1 Cultures and Media

The wild type *C. tyrobutyricum* ATCC 25755 was maintained on the Reinforced Clostridial Medium (RCM; Difco, Kansa City, MO) plates in an anaerobic chamber (95% N_2, 5% H_2). The metabolically engineered mutant, PAK-Em with inactivated *ack* gene, was obtained from the Yang Lab [30]. The seed colony of PAK-Em mutant was maintained on RCM plates containing 40 μg/mL erythromycin (Em). Unless otherwise noted, all liquid cultures were grown at 37°C in a modified Clostridial Growth Medium (CGM) with glucose as substrate following the protocol described previously [20].

3.2.2 Fermentation Kinetic Study

The kinetics of both free-cell and immobilized-cell fermentations of *C. tyrobutyricum* were carried out in a stirred-tank bioreactor. The detailed fermentation operation was described in previous studies [10,11]. To identify the optimal fermentation pH, the immobilized-cell fermentations using FBB were operated at different pH values, including 5.0, 5.5, 6.0, 6.5, and 7.0. The fermentation samples were taken twice a day from the fermentor to analyze the cell growth and titrate the substrate and products (i.e. butyrate and acetate).

3.2.3 Analytical Methods

The cell growth of *C. tyrobutyricum* was analyzed by measuring the OD_{600} of the cell suspension using a spectrophotometer (Biomate3; Thermo Fisher Scientific, Waltham, MA). A high performance liquid chromatography (HPLC, Shimadzu, Columbia, MD) system was used to analyze the concentration of glucose, butyrate, and acetate in the fermentation broth. The detailed methods can be found in our previous study [10].

3.2.4 Metabolic Flux Analysis

A constraint-based metabolic model of the central metabolism of *C. tyrobutyricum* [20] was constructed to perform flux balance analysis (FBA) of carbon and energy. A stoichiometric matrix, was constructed to mathematically represent the set of chemical reactions composing the central metabolism of *C. tyrobutyricum*. Each of the rows of the matrix corresponded to a chemical species present in the bacterial cell while each column corresponded to a reaction occurring in the cell. Entries of the matrix were stoichiometric coefficients. Columns were added to the matrix to represent the transportation of glucose into the cell and the transportation of acetic acid, butyric acid, ethanol, and butanol out of the cell. Two additional columns were added to represent biomass synthesis and biomass "exportation", since biomass was produced by the cell but not consumed by it. The microorganism was assumed to operate at steady state, so the product of the stoichiometric matrix and the flux vector containing all of the unknown fluxes was set equal to zero, forming a linear programming problem. The data collected from butyric acid fermentations in the pH optimization study were used as the input of the FBA model. A total of nine biochemical reactions were included into the FBA model and are displayed, alongside their functions, in Table 3.2.

3.3. Results and Discussion

3.3.1 Kinetics of Free-cell Fermentation

Fig. 3.1 shows the kinetics of the free-cell fermentations at pH 6.0 and 37 °C by the wild type (control) and mutant PAK-Em. The wild type entered the exponential phase at 7 h while the PAK-Em entered the exponential phase at 13 h post inoculation. Because the same operation in seed culture preparation and bioreactor inoculation were used, the longer lag phase in the fermentation

by PAK-Em was caused by gene manipulation in metabolic engineering. Energy (ATP) is generated during the formation of acetate, so the downregulation of the acetate pathway reduced energy efficiency and thus slowed down the cell growth that consumed energy. As shown in Table 3.2, PAK-Em had a lower growth rate (0.14 h^{-1}) than that of the wild type (0.21 h^{-1}). As discussed before [11], both the low ATP production and the metabolic burden caused by high production of butyrate reduced the cell growth rate. In addition, the yield of biomass in the PAK-Em fermentation was 0.04 g/g, lower than that of 0.06 g/g in the wild type.

As shown in Fig. 3.1, both strains started to produce butyrate and acetate very slowly at the beginning of the free-cell fermentation, then the production of acids sped up from the log phase. The wild type stopped producing butyrate after 60 h while PAK-Em stopped after 100 h. The PAK-Em mutant generated butyrate at a final concentration of 38.44 g/L and acetate at 7.16 g/L, while the final concentrations of butyrate and acetate from the wild type fermentation were 19.24 g/L and 4.22 g/L, respectively. Butyrate titer produced by PAK-Em was much higher than that by wild type. This carbon rebalance between acetate and butyrate has been also observed in previous study [11] by downregulation of ack gene in PAK-Em.

As shown in Table 3.3, the butyrate yield was increased from 0.34 g/g glucose by wild type to 0.42 g/g glucose by PAK-Em. The butyrate/acetate ratios were 4.56 g/g and 5.36 g/g by the wild type and PAK-Em. It is clear that the PAK-Em mutant is a better butyrate producer than the wild type. The butyrate baseline study was similar to the butyrate production in previous study [11].

The free-cell fermentation showed that the downregulation of acetate pathway increased the production of butyrate due to the carbon flux redistribution from C2 to C4 in the metabolically engineered strain. Because the acetate pathway is more efficient in energy production, the PAK-Em had a significantly reduced cell growth rate and biomass yield. These results indicated that the

regulation of C2 pathway caused the global carbon redistribution and energy redistribution. Further evaluation of carbon and energy balancescould reveal the whole picture of the metabolic flux shift in butyrate production, which would be discussed in the following flux balance analysis.

3.3.2 Effect of pH on Butyric Acid Fermentation

The immobilized-cell fermentation by PAK-Em using fibrous-bed bioreactor (FBB) was performed To increase the butyrate production. It was reported that the wild type *C. tyrobutyricum* could grow at pH values between 5.0 and 7.0 [29], so the immobilized-cell fermentations were run at pHs of 5.0, 5.5, 6.0, 6.5, and 7.0 to evaluate the effect of pH on the butyrate production by PAK-Em. The time-course data is presented in Fig. 3.2 and the acids production data are summarized in Table 3.4.

As shown in Fig. 3.2, the glucose consumption rates in the immobilized-cell fermentation at all pHs was slow in the lag phase, increased greatly after cell growth entered the log phase, and decreased in the late stationary phase. When strains stopped producing butyrate and acetate, there was no significant glucose consumption. The production of acids (butyrate and acetate) started at the beginning of the first batch and increased afterwards in the log phase. The production of acetate stopped in the early stationary phase and the butyrate concentration reached the maximum value at the end of fermentation. It is noted that the fermentation timeline was significantly extended from 140-200 h at high fermentation pHs (6.5 and 7.0) compared with that at low pHs (5.0, 5.5 and 6.0). Fig. 3.2 also showed that the butyrate concentration was increased with the increase of fermentation pH.

As summarized in Table 3.4, the butyrate concentration was 14.79 g/l, 23.18 g/L, 50.11 g/L, 63.02 g/L and 61.01 g/L, and the butyrate yield was 0.37 g/g, 0.38 g/g, 0.45 g/g, 0.45 g/g and 0.42 g/g at pH of 5.0, 5.5, 6.0, 6.5 and 7.0, respectively. It is clear that the immobilized-cell fermentation

by PAK-Em produced the highest concentration of butyrate, i.e. 63.02 g/L, at pH 6.5. The butyrate/acetate ratio was also increased at high pHs (6.5 and 7.0). These results indicated that the uptake and conversion efficiency of glucose were upregulated by higher pH and more carbon flux was redistributed from C2 to C4.

The results in pH optimization demonstrated that the fermentation pH is an important process parameter in order to achieve high butyrate production. To rational optimize fermentation process, it is very important to understand how the pH correlates with the intracellular metabolic flux distribution. Moreover, the high concentration of butyrate produced at the optimized fermentation condition would greatly reduce the product extraction cost of butyrate, which could make the biobutyrate production more competitive compared to the traditional butyrate production from petroleum.

3.3.3 Metabolic Flux Balance Analysis

The metabolic flux distribution in the immobilized PAK-Em mutant of *C. tyrobutyricum* has not been investigated. The effect of fermentation pH on the metabolic flux balance of PAK-Em has not been analyzed. In this study, it was constructed a flux balance analysis (FBA) model and analyzed the biomass and acids production data collected in the immobilized-cell fermentations by wild type (shown in Table 3.5) and PAK-Em at various pHs from 5.0 to 7.0. The balance of both carbon flux and energy flux was analyzed and presented in Fig. 3.3.

It was found that less carbon flux was distributed to the biomass production by PAK-Em than wild type at each pH, which indicated more carbon fluxed to the pyruvate in the PAK-Em. The acetyl-CoA and butyryl-CoA nodes, which are the key metabolites related to the metabolic flux from the C2 to C4, were influenced by the downregulation of the acetate pathway and the culture pH levels. Compared to wild type, the PAK-Em directed a lower metabolic flux to acetyl-CoA (<

0.2 mol/mol-glucose) and higher flux to the butyryl-CoA (> 0.8 mol/mol-glucose). As fermentation pH increased, more butyryl-CoA (from 0.83 to 0.91 mol/mol-glucose) was produced in the PAK-Em, which was consistent with the higher concentration of butyrate.

In addition to providing the information of carbon flux distribution, FBA allowed for the calculation of net ATP accumulation, defined as the amount of ATP produced by glycolysis, acetate biosynthesis, and butyrate biosynthesis minus the ATP required for cell growth, by each strain at various pHs. The net ATP produced by the PAK-Em at pH 6.0-7.0 was significantly greater than that produced by the wild type in the same pH range. Furthermore, the net ATP produced by both strains appeared to be largely independent of fermentation pH, excepting the jump in net ATP production by PAK-Em from 1.45 mol-ATP/mol-glucose at pH 5.5 to 2.63 mol-ATP/mol-glucose at pH 6.0. The increase of net ATP production observed in PAK-Em can be attributed to a redirection of carbon flux from biomass formation to acids synthesis. The decrease of carbon flux to biomass formation not only decreased the amount of ATP consumption by PAK-Em, it also increased the carbon flux participation in glycolysis that produced ATP, as well as increased the carbon flux to acetate and butyrate biosynthesis that produced ATP.

3.4. Conclusion

Taken together, the *C. tyrobutyricum* mutant PAK-Em obtained from integrational mutagenesis to selectively downregulate the acetate pathway was used to produce a high level of butyric acid with fermentation parameter optimization. This study demonstrated the feasibility and advantage of combining genetic engineering techniques with process optimization (i.e. environmental adaptation in FBB bioreactor and pH optimization). The butyrate production was improved significantly to 63.02 g/L in the immobilized-cell fermentation at pH 6.5 by the PAK-Em. The

high butyric acid concentration could reduce the production cost of bio-based butyric acid and allow its bioproduction to compete more favorably in the marketplace.

3.5. References

[1] D. Wei, X. Liu, S.T. Yang. "Butyric acid production from sugarcane bagasse hydrolysate by *Clostridium tyrobutyricum* immobilized in a fibrous-bed bioreactor". Bioresour. Technol., vol. 129, pp. 553-60, 2013.

[2] M. Dwidar, J.Y. Park, R.J. Mitchell, B.I. Sang. "The future of butyric acid in industry". Scientific World Journal, pp. 471417, 2012.

[3] G.F. Atweh, J. DeSimone, Y. Sauntharajah, H. Fathallah, R.S. Weinberg, R.L. Nagel, M.E. Fabry, R.J. Adams. "Hemoglobinopathies". Hematology Am. Soc. Hematol. Educ. Program, pp. 14-39, 2003.

[4] R.B. Canani, M.D. Costanzo, L. Leone, M. Pedata, R. Meli, A. "Calignano. Potential beneficial effects of butyrate in intestinal and extraintestinal diseases". World J. Gastroenterol, vol. 17, pp. 1519-28, 2011.

[5] D.L. Lazarova, C. Chiaro, M. Bordonaro. "Butyrate induced changes in Wnt-signaling specific gene expression in colorectal cancer cells". BMC Res. Notes, vol. 7, pp. 226, 2014.

[6] J. Huang, J. Cai, J. Wang, X. Zhu, L. Huang, S.T. Yang, Z. Xua. "Efficient production of butyric acid from Jerusalem artichoke by immobilized *Clostridium tyrobutyricum* in a fibrous-bed bioreactor". Bioresour. Tech., vol. 102, pp. 3923–3926, 2011.

[7] Q. Kong, G.Q. He, F. Chen, H. Ruan. "Studies on a kinetic model for butyric acid bioproduction by *Clostridium butyricum*". Lett. Appl. Microbiol., vol. 43, pp. 71–77, 2006.

[8] C. Zhang, H. Yang, F. Yang, Y. Ma. "Current progress on butyric acid production by fermentation". Current Microbiology, vol. 59, pp. 656–663. 2009.

[9] F. Canganella, J. Wiegel. "Continuous cultivation of Clostridium thermobutyricum in a rotary fermentor system". J. Ind. Microbiol. Biotechnol., vol. 24, pp. 7–13, 2000.

[10] C. Ma, K. Kojima, N. Xu, J. Mobley, L. Zhou, S.T. Yang, X.M. Liu. "Comparative proteomics analysis of high n-butanol producing metabolically engineered *Clostridium tyrobutyricum*". J. Biotechnol., vol. 193, pp. 108-119, 2015.

[11] G.B. Patel, B.J. Agnew. 'Growth and butyric acid production by *Clostridium populeti*". Arch. Microbiol., vol. 150, pp. 267–271, 1988.

[12] G.Q. He, Q. Kong, Q.H. Chen, H. Ruan. "Batch and fed-batch production of butyric acid by *Clostridium butyricum* ZJUCB". Journal of Zhejiang University, vol. 6, pp. 1076–1080, 2005.

[13] R. Cascone. "Biobutanol—A replacement for bioethanol". Chem. Eng. Prog., vol. 104, pp. 4–9, 2008.

[14] S. Alam, D. Stevens, R. Bajpai. "Production of butyric acid by batch fermentation of cheese whey with *Clostridium beijerinckii*". J. Ind. Microbiol., vol. 2, pp. 359–364, 1988.

[15] F. Canganella, S.U. Kuk, H. Morgan, J. Wiegel. "*Clostridium thermobutyricum*: Growth studies and stimulation of butyrate formation by acetate supplementation". Microbiol. Res., vol. 157, pp. 149–156, 2002.

[16] J.H. Jo, D.S. Lee, J.M. Park. “The effects of pH on carbon material and energy balances in hydrogen-producing *Clostridium tyrobutyricum* JM1”. Bioresour. Technol., vol. 99, pp. 8485–8491, 2008.

[17] Y.L. Huang, Z. Wu, L. Zhang, C.M. Cheung, S.T. Yang. “Production of carboxylic acids from hydrolyzed corn meal by immobilized cell ermentation in a fibrous-bed bioreactor”. Bioresour. Technol., vol. 82, pp. 51–59, 2002.

[18] D. Michel-Savin, R. Marchal, J.P. Vandecasteele. “Butyric fermentation: Metabolic behavior and production performance of Clostridium tyrobutyricum in a continuous culture with cell recycle”. Appl. Microbiol. Biotechnol., vol. 34, pp. 172–177, 1990.

[19] X. Liu, S.T. Yang. “Kinetics of butyric acid fermentation of glucose and xylose by *Clostridium tyrobutyricum* wild type and mutant”. Process Biochem., vol. 41, pp. 801-808. 2006.

[20] L. Jiang, J. Wang, S. Liang, J. Cai, Z. Xu, P. Cen, S.T. Yang, S. Li. “Enhanced butyric acid tolerance and bioproduction by *Clostridium tyrobutyricum* immobilized in a fibrous bed bioreactor”. Biotechnol. Bioeng., vol. 108, 31–40, 2009.

[21] M. Saini, Z.W. Wang, C.J. Chiang, Y.P. Chao. “Metabolic engineering of *Escherichia coli* for production of butyric acid”. J. Agric. Food. Chem., vol. 62, pp. 4342–4348, 2014.

[22] X. Liu, Y. Zhu, S.T. Yang. “Butyric acid and hydrogen production by *Clostridium tyrobutyricum* ATCC 25755 and mutants”. Enzyme Microb. Technol., vol. 38, pp. 521-528. 2006.

[23] V.P. Lewis, S.T. Yang. “Continuous propionic acid fermentation by immobilized Propionibacterium acidipropionici in a novel packed-bed bioreactor”. Biotechnol. Bioeng., vol. 40, pp. 465-474, 1992.

[24] Y. Huang, S.T. Yang. “Acetate production from whey lactose using co-immobilized cells of homolactic and homoacetic bacteria in a fibrous-bed bioreactor”. Biotechnol. Bioeng., vol. 60, pp. 499-507, 1998.

[25] E.M. Silva, S.T. Yang. “Kinetics and stability of a fibrous bed bioreactor for continuous production of lactic from unsupplemented acid whey”. J. Biotechnol., vol. 41, pp. 59-70, 1995.

[26] X. Liu, Y. Zhu, S. Yang. “Butyric acid and hydrogen production by *Clostridium tyrobutyricum* ATCC 25755 and mutants”. Enzyme Microb. Technol., vol. 383, pp. 521-528, 2006.

[27] S.T.Yang. “Extractive fermentation using convoluted fibrous bed bioreactor”. U. S. Patent, 5563069, 1996.

[28] Y. Zhu. “Enhanced butyric acid fermentation by *Clostridium tyrobutyricum* immobilized in a fibrous-bed bioreactor”. Dissertation for the Doctoral Degree, Columbus: The Ohio State University, USA, 99-100. 2003.

[29] Y. Zhu, S.T. Yang. “Effect of pH on metabolic pathway shift in fermentation of xylose by *Clostridium tyrobutyricum*.” J. Biotechnol., vol. 110, pp. 143-157, 2004.

[30] Y. Zhu, X. Liu, S.T. Yang. “Construction and characterization of pta gene deleted mutant of *Clostridium tyrobutyricm* for enhanced butyric acid fermentation”. Biotechnol. Bioeng., vol. 90, pp. 154-166, 2005.

[31] Y. Du , W. Jiang, M. Yu, I. Tang, S.T. Yang. “Metabolic process engineering of *Clostridium tyrobutyricum* Δack–adhE2 for enhanced n-butanol production from glucose: Effects of methyl viologen on NADH availability, flux distribution, and fermentation kinetics”. Biotechnol. Bioeng., vol. 112, pp. 705-715, 2014.

Table 3.1 Recent progresses of butyric acid production from sugar

Strain	Fermentation mode	Sugar	Concentration/ (g/L)	Ref
C. populeti	Batch, free-cell	Glucose	6.30	[11]
C. butyricum ZJUCB	Batch, free-cell	Glucose	12.25	[12]
	Fed-batch, free-cell	Glucose	16.74	
C. butyricum S21	Batch, free-cell	Lactose	18.60	[13]
C. beijerinckii	Batch, free-cell	Lactose	12.00	[14]
C. thermobutyricum	Fed-batch, free-cell	Glucose	19.40	[15]
*C. tyrobutyricu*m JM1	Batch, free-cell	Glucose	13.76	[16]
C. tyrobutyricum, wild type	Fed-batch, free-cell	Glucose	24.88	[17]
	Continuous, free-cell	Glucose	33.00	[18]
C. tyrobutyricum, mutant	Fed-batch, immobilized-cell	Glucose	49.90	[19]
	Repeated fed-batch, immobilized-cell	Glucose	86.9	[20]
E. coli	Batch, free-cell	Glucose	10.00	[21]

Table 3.2 Stoichiometric equations used in the FBA modeling of *C. tyrobutyricum.*

Reaction No.	Biological Function	Stoichiometric Equation [a,b]
(1)	Biomass formation	2 Glucose + 1.75 NADH + 1.75 H^+ + 29.7 ATP → 3 $C_4H_{6.4}O_{1.72}N$ + 1.75 NAD^+ + 29.7 ADP + 29.7 Pi
(2)	Formation of pyruvate (glycolysis)	Glucose + 2 NAD^+ + 2 ADP + 2 Pi → 2 Pyruvate + 2 NADH + 2 H^+ + 2 ATP
(3)	Formation of AcCoA and CO_2	Pyruvate + CoA + Fd_{ox} → AcCoA + Fd_{red} + CO_2
(4)	Formation of H_2	Fd_{red} + 2 H^+ → H_2 + Fd_{ox}
(5)	Formation of NADH	Fd_{red} + NAD^+ ⇔ NADH + H^+ + Fd_{ox}
(6)	Formation of acetate	AcCoA + ADP + Pi ⇔ Acetate + CoA + ATP
(7)	Formation of BuCoA and water	2 AcCoA + 2 NADH + 2H^+ → BuCoA + 2 NAD^+ + CoA + H_2O
(8)	Formation of butyrate or acetate	BuCoA + Acetate ⇔ Butyrate + AcCoA
(9)	Formation of butyrate	BuCoA + ADP + Pi ⇔ Butyrate + CoA + ATP

a) Reversible reactions are indicated by '⇔' while irreversible reactions are indicated by '→'.

b) Pi = inorganic phosphate; Fd_{ox} = oxidized ferredoxin; Fd_{red} = reduced ferredoxin; BuCoA = butyryl-CoA; AcCoA = acetyl-CoA.

Table 3.3 Comparison of fermentation products by wild type (control) and PAK-Em.

Products		**Wild type (Control)**	**PAK-Em**
Cell growth	Growth rate μ (h^{-1})	0.21±0.01	0.14±0.01
	Biomass yield (g/g)	0.06±0.01	0.04±0.01
Butyric acid	Concentration (g/L)	19.24±0.05	38.44±0.03
	Yield (g/g)	0.34±0.02	0.42±0.01
Acetic acid	Concentration (g/L)	4.22±0.002	7.16±0.002
	Yield (g/g)	0.07±0.001	0.07±0.01
C4/C2	B/A ratio (g/g)	4.56±0.85	5.36±0.61

Notes:

a) These free-cell fermentations were performed at pH 6.0.

b) The data were presented as the average of duplicated fermentations with standard deviation.

c) The biomass yield was calculated using 1 OD_{600} = 0.38 g/L [10].

Table 3.4 Effect of pH on acids production in immobilized-cell fermentations by PAK-Em.

Products	pH	5.0	5.5	6.0	6.5	7.0
Butyrate	Conc. (g/L)	14.79±0.99	23.18±0.78	50.11±2.42	63.02±1.54	61.01±0.78
	Yield (g/g)	0.37±0.03	0.38±0.01	0.45±0.02	0.45±0.01	0.42±0.01
Acetate	Conc. (g/L)	2.11±0.02	3.13±0.02	7.03±0.01	7.26±0.03	7.09±0.02
	Yield (g/g)	0.03±0.004	0.03±0.006	0.08±0.01	0.05±0.01	0.04±0.01
C4/C2	Ratio (g/g)	6.53	6.77	7.12	8.60	8.60

Table 3.5 Effect of pH on acids production in immobilized-cell fermentations by wild type.

Products / pH		5.0	5.5	6.0	6.5	7.0
Butyrate	Conc. (g/L)	11.02±0.04	17.18±0.04	18.01±0.05	15.03±0.15	16.03±0.25
Acetate	Conc. (g/L)	3.68±0.01	2.71±0.01	2.01±0.02	3.04±0.01	4.52±0.01
Biomass	Conc. (g/L)	1.8±0.001	3.1±0.002	3.4±0.002	3.4±0.001	2.7±0.003

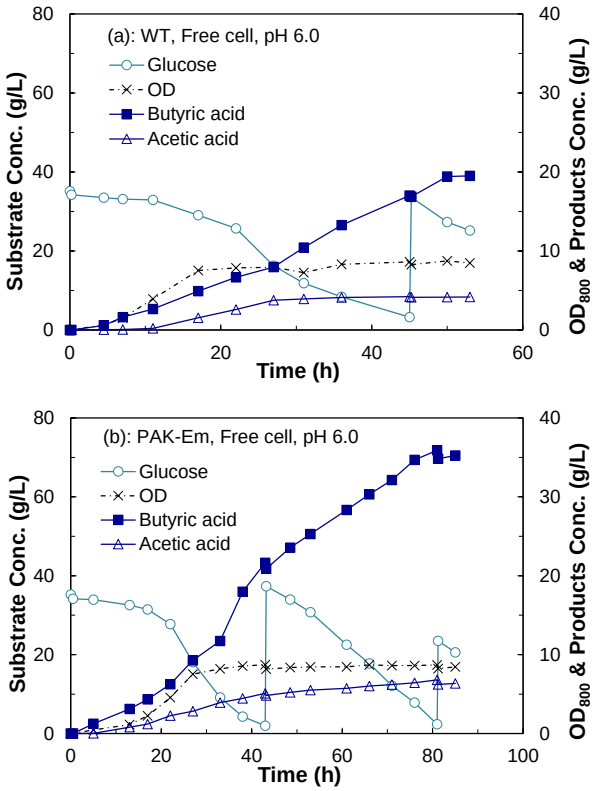

Fig 3.1. Kinetics of free-cell fermentations by *C. tyrobutyricum* ATCC 25755 wild type (a) and PAK-Em mutant (b) at pH 6.0 and Temp 37 ºC. ○: Glucose, □: Butyric acid, ▲: Acetic acid, ×: OD.

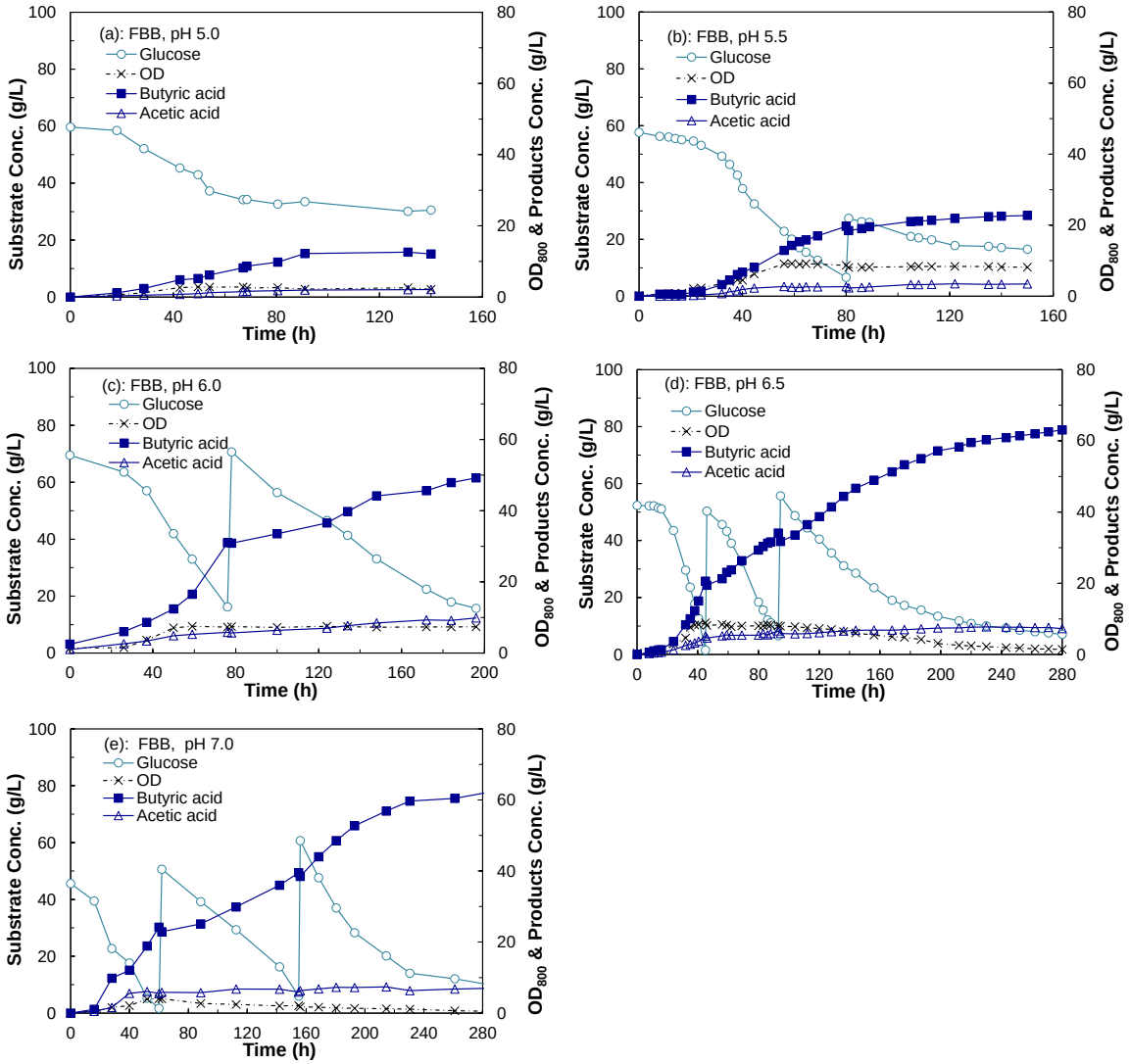

Fig 3.2. Kinetics of immobilized-cell fermentations by PAK-Em at pH 5.5 (a), 5.5 (b), 6.0 (c), 6.5 (d), and 7.0 (e) and Temp 37 ºC. ○: Glucose, □: Butyric acid, ▲: Acetic acid, ×: OD.

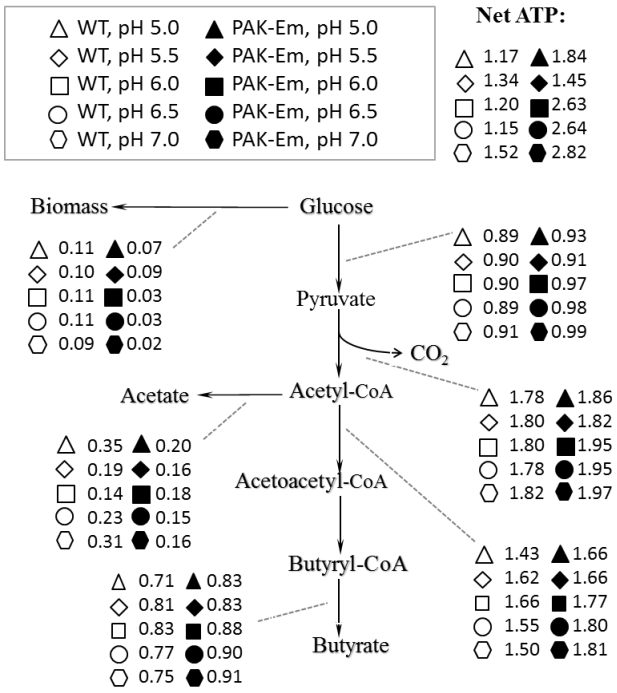

Fig. 3.3. *C. tyrobutyricum* metabolic flux distribution on a basis of 1 mole glucose consumed by wild type and PAK-Em at 37 ℃ and pH's ranging from 5.0 to 7.0.

CHAPTER 4

CHARACTERIZATION OF EVOLUTIONARILY ENGINEERED MUTANTS

Abstract

In this study, it is applied evolutionary engineering to further engineer metabolically engineered mutant of *Clostridium tyrobutyricum* ATCC 25755, PAK-Em. An evolutionarily engineered strain, Hyd-Em, was obtained after a long-term adaptation in a fibrous-bed bioreactor (FBB). The new mutant strain was first evaluated in butyrate fermentation, showing that the cell growth rate was increased by 61-100% and butyrate productivity was improved by 44-102% compared to PAK-Em. To understand these new phenotypes in butyrate fermentation, genomics analysis was performed to investigate the genome mutations in Hyd-Em. Several mutations correlating with cell growth (*gerB3/KC*), host protein expression (*upp*), and nutrient metabolism and transport (*e.g.*, *moeA* and *phoU*) were identified. The mutant characterization by butyrate fermentation and genome analysis could provide a guideline for further genetic engineering. This study also demonstrated that the integration of gene manipulation and cell adaptation could efficiently engineer *C. tyrobutyricum* to improve butyric acid production.

4.1 Introduction

Clostridium tyrobutyricum ATCC 25755 is a Gram-positive, rod-shaped, spore-forming, obligate anaerobic bacterium. It is capable of producing butyrate, acetate, hydrogen and carbon dioxide from various sugars (e.g. glucose, xylose, cellobiose and arabinose) present in the hydrolysates of lignocellulosic biomass [1,2,3]. Compared to other bacteria, *C. tyrobutyricum* produces butyrate as the main product with a relatively high productivity, final titer and yield, and thus has great potential for industrial application.

The draft genome sequences of *C. tyrobutyricum* strains were reported recently [4,5,6,7], which provided the genome information for genetic engineering. Moreover, the proteomics study was performed to create the global intracellular map of *C. tyrobutyricum*, and the host cell regulators involved in carbohydrate metabolism, energy and redox metabolism, and cellular response to stress were also identified [8]. In addition, various molecular biology tools, including gene knockout (ClosTron), gene integration (ACE), and unique methylation, were developed to genetically engineer clostridia [9,10,11,12]. The comprehensive functional genomics studies and the advanced molecular biology could accelerate the metabolic engineering of *C. tyrobutyricum*.

Extensive metabolic engineering research was performed to construct high butyrate or hydrogen producing *C. tyrobutyricum*. For instance, phosphotransbutyrylase (*ptb*) or phosphotransacetylase (*pta*) was knocked out using homologous recombination [13,14], and butyrate production was significantly enhanced. The overexpression of [FeFe]-hydrogenase resulted in 1.5-fold increase in hydrogen yield [15]. The engineered *C. tyrobutyricum*, PAK-Em, with down-regulated acetate pathway showed improved butyrate production, but this mutant suffered from low cell growth rate [16,17]. Recent metabolic engineering of *C. acetobutylicum* also produced high concentration of butyrate, comparable to *C. tyrobutyricum*, by deleting *pta*,

butyrate kinase (*buk*), acetate/butyrate CoA transferase B (*ctfB*), bifunctional acetaldehyde/alcohol dehydrogenase (*adhE1*) and hydrogenase A (*hydA*) [18].

In addition to metabolic engineering, the evolution of *C. tyrobutyricum* can also improve butyrate production. As described by Olson-Manning et al., "Adaptive evolution is shaped by the interaction of population genetics, natural selection and underlying network and biochemical constraints" [19]. Over the past two decades, the fibrous-bed bioreactor (FBB) has been developed and applied to produce various chemicals and biofuels [20,21,22]. The FBB can be used to immobilize cells, gradually adapt cells, and increase cell growth, bioreactor productivity and product concentration via evolutionary engineering. For example, this technology was used to evolve *C. tyrobutyricum* and improved butyrate volumetric productivity [23].

The main objective of this study was to develop and characterize a novel *C. tyrobutyricum* mutant to reach both high butyrate production and fast cell growth. An evolutionarily and metabolically engineered strain was developed via a long-term adaptation of the metabolically engineered mutant in a FBB. The kinetics of cell growth and butyrate production (i.e., concentration, yield and productivity) of the new mutant, Hyd-Em, was characterized in both free- and immobilized-cell butyrate fermentations. The comparative genomics study was also performed to further characterize Hyd-Em by analyzing the possible genome regulators responsible for the new phenotypes.

4.2 Materials and Methods

4.2.1 Strains, Cultures and Media

The metabolically engineered mutant of *C. tyrobutyricum* ATCC 25755, PAK-Em developed in a previous study [16], was used as the parental strain for evolutionary engineering. The

evolutionarily and metabolically engineered mutant developed in this study was named as Hyd-Em [24]. The seed culture of these strains was cultivated in Reinforced Clostridium Medium (RCM; Difco, Kansas City, MO). The PAK-Em and Hyd-Em were maintained with 40 μg/mL of erythromycin (Em, Alfa Aesar, Ward Hill, MA). In butyrate fermentation, the clostridial cells were grown in Clostridium Growth Medium (CGM) with glucose as the carbon source. The CGM contained (g/L): 50 glucose, 5 trypticase, 5 yeast extract, 6 $NaHCO_3$, 0.31 $K_2HPO_4 \cdot 3H_2O$, 0.24 KH_2PO_4, 0.24 $(NH_4)_2SO_4$, 0.48 NaCl, 0.1 $MgSO_4 \cdot 7H_2O$, 0.0064 $CaCl_2 \cdot 2H_2O$ [16,25]. All chemical reagents were purchased from Sigma-Aldrich (St. Louis, MO), unless otherwise specified.

4.2.2 Butyrate Fermentation

The free-cell fermentations of PAK-Em was carried out in 5-L stirred-tank fermentor (Marubishi MD-300) containing 2-L CGM without antibiotics. After autoclaving at 121 ^oC for 60 mins, the fermentor was brought to anaerobiosis by sparging the medium with nitrogen for about 1 h, and then inoculated with 50-mL seed culture grown overnight in RCM. The fermentation was operated in a fed-batch mode at 37 ^oC, agitation of 150 rpm, and pH controlled at 6.0 with 5 N NaOH.

In immobilized-cell fermentations, the two strains were immobilized in the FBB with a working volume of 500 mL, which was connected to a stirred-tank fermentor with 2-L medium recirculation. Both stirred-tank fermentor and FBB bioreactor were sparged with nitrogen to achieve anaerobiosis before inoculation. The concentrated glucose solution was fed when sugar level was close to zero. The fed-batch fermentation was continued until the glucose consumption ceased or butyrate production stopped. All the fermentations were run in duplicate. Fermentation samples were taken at regular intervals (twice a day) from the stirred tank to monitor cell growth and titrate glucose, butyrate, and acetate.

4.2.3 Comparative Genomics Analysis

The genome DNA sequencing of *C. tyrobutyricum* strains was performed on the Illumina HiSeq2000. Briefly, the genomic DNA was quantitated using the Qubit assay and tested for quality by agarose gel electrophoresis. DNA with very high molecular weight and little to no smearing was used for library construction. The DNAs were subjected to the Illumina TruSeq library generation protocol as per the manufacturer's instructions (Illumina, San Diego, CA). Library construction consisted of shearing the genomic DNA in the Covaris S2 sonicator to an average size of 200-400bp. The ends of the fragmented DNA were repaired to generate blunt ends, and an A-tailing reaction was performed to provide an A-overhang for the efficient ligation of the adaptors. The adaptors had sequences for flowcell attachment, sequencing and indexing. The genomic DNA libraries were quantitated using qPCR in a Roche LightCycler 480 with the Kapa Biosystems kit for library quantitation (Kapa Biosystems, Woburn, MA) prior to cluster generation. The Illumina sequencing raw data of *C. tyrobutyricum* ATCC 25755 mutants, i.e. PAK-Em and Hyd-Em, were deposited to NCBI Sequence Read Archive database as a BioProject (accession no. SRP051738).

To call the genome variants between PAK-Em and Hyd-Em, the raw fastq reads were aligned to the reference genome using BWA [26] Then, the variants were identified using Broad's Genome Analysis Toolkit (GATK) and following their Best Practices for Variant Detection protocol [27]. Briefly, the aligned file from BWA was realigned and recalibrated using GATK. Following recalibration, GATKs UnifiedGenotyper was used to call the variants. These raw variants were then recalibrated to produce an analysis ready variant file for further filtering and effect annotations.

4.2.4 Analytical Methods

The cell growth of *C. tyrobutyricum* was analyzed by measuring the optical density of suspended cells at 600 nm (OD_{600}) using a spectrophotometer (Biomate3; Thermo Fisher Scientific,

Waltham, MA). High performance liquid chromatography (HPLC, Shimadzu, Columbia, MD) was used to analyze the concentration of glucose, butyrate, and acetate. The HPLC system consisted of an automatic injector (Shimadzu SIL-10Ai), a pump (Shimadzu LC-10A), an organic acid analysis column (Bio-Rad HPX-87H), a column oven at 45 ^{o}C (Shimadzu RID-10A), and a refractive index detector (Shimadzu RID-10A). The 0.005 N H_2SO_4 with flow rate of 0.6 mL/min was used as eluent solution.

4.3 Results

4.3.1 Fermentation with PAK-Em

The parental PAK-Em was immobilized in the FBB to perform eight cycles of cell adaptation, i.e. evolutionary engineering. During cell adaptation, the butyrate production was also improved by optimizing fermentation conditions. Specifically, various fermentation pHs, including 6.0, 5.0, 7.0, and 6.3, were evaluated and each pH was applied to two cycles of fed-batch fermentations. As shown in Fig. 4.1, the first cycle was performed at pH 6.0 and stopped at butyrate concentration of 50.1 g/L (Fig. 4.1a), while the eighth cycle reached a final butyrate concentration of 80.2 g/L (Fig. 4.1b). Compared to the first cycle, the butyrate concentration in the end of adaptation was improved by 60%, which was one of the highest butyrate productions ever achieved. Previous studies produced butyrate 62.8 g/L from sucrose [28], 57.9 g/L from xylose [29], and 42.5 g/L from glucose [30].

The high-level butyrate in the FBB provided the cells a selection pressure to drive the evolution towards better cell growth. The survivability of the cells immobilized in the fibrous bed matrix was increased because the dead cells killed by butyrate or the fragile cells with slow cell growth were washed out from the FBB by the circulating fermentation broth. At the end of the adaptation, a mutant strain Hyd-Em was screened from the cell pools harvested from the FBB [24].

As discussed in the following sections, the metabolically and evolutionarily engineered Hyd-Em was first characterized by butyrate production in both free-cell and immobilized-cell fermentations. Then the genome analysis was performed to further investigate the possible genotypes underlying the new Hyd-Em.

4.3.2 Characterization of Hyd-Em by Genomics Analysis

As observed in butyrate fermentation, Hyd-Em had significantly higher growth rate and butyrate productivity than PAK-Em (Table 4.1 and Table 4.2), and these desired phenotypes were achieved in the evolutionary engineering. To understand how the genotypes possibly correlate with these phenotypes, the genome differences between PAK-Em and Hyd-Em were analyzed.

It was sequenced the genomes of PAK-Em (control) and Hyd-Em to identify the genome mutations introduced during evolutionary engineering. In the comparative genomics analysis, a total of 10 mutations were identified and annotated using the clostridial genome databases deposited to GenBank. The gene ID, encoded protein, protein function, gene mutation and amino acid change of the representative mutated genes are summarized in Table 4.3. These genes can be classified in the following two categories, including the host protein expression regulators that could change key enzymes expression and cellular metabolism, and the nutrient binding and transporters that could affect nutrient uptake and metabolic activity.

First, the sequences of three genes encoding the proteins involved in transcription and translation were changed during evolutionary engineering (Table 4.3). Specifically, the uracil phosphoribosyltransferase (*upp*) had a 72-bp fragment deletion at position of 138 in PAK-Em, and this mutation was cured in Hyd-Em. This protein catalyzes the production of UMP from uracil and phosphoribosylpyrophosphate. UMP is a nucleotide used for mRNA synthesis, so the 72-bp deletion in *upp* (24 missing amino acids) could reduce the overall expression level of host cell

proteins and thus the cellular metabolism. The cured mutation in *upp* by evolutionary engineering could improve the efficiency of the metabolism. Other two point-mutations were also observed in Hyd-Em, including tTt/tGt (F94C) in the ribosomal protein L22 (*rplV*) and Ttt/Gtt (F35V) in the ribosomal protein S11 (*rpsK*). Previous studies showed that RplV is important to form an early folding intermediate of the 23S rRNA, response to the binding of antibiotics erythromycin and impair peptide-mediated translation arrest, and RpsK plays an essential role in selecting the correct tRNA in protein biosynthesis [31,32,33].

Second, mutations were observed in the enzymes involved in the metabolism and transport of nutrient components. The stop codon gain/lost mutations in three proteins of PAK-Em, including phosphate transport regulator (*phoU*, Gaa/Taa, E171*), molybdate-binding protein (taG/taT, *320Y), and molybdopterin biosynthesis protein (*moeA*, Gaa/Taa, E303*), were cured in Hyd-Em by evolutionary engineering. These three proteins play important roles in the transport and metabolism of molybdate and the transport of phosphate, which could further affect cellular metabolism of end product formation.

In addition to cell growth and butyrate productivity, the acetate pathway "acetyl-CoA → acetyl-P → acetate" catalyzed by phosphotransacetylase (*pta*) and acetate kinase (*ack*) was also analyzed. The genome analysis showed that the *ack* gene (GenBank ID 516360615) had no mutation in PAK-Em and Hyd-Em. Further analysis revealed that the promoter area, site of -103 upstream of *pta-ack* operon, had a point mutation (T/TA), and the ribosomal protein L32 (*rpmF*) in the downstream of *ack* gene had a 21-bp fragment insertion. These genomics data indicated that the transcription and translation of *ack* gene was down regulated. Our previous proteomics study also confirmed that the expression of this *ack* gene decreased 33% in PAK-Em [8]. In addition, previous study demonstrated that the acetate production was not completely eliminated and the

enzyme activity of acetate kinase was reduced [16]. Taken together, both Omics studies and butyrate fermentation demonstrated that the acetate pathway was not inactivated but down regulated, thus a certain amount of acetate was still produced in the fermentation by PAK-Em and Hyd-Em.

4.4 Discussion

4.4.1 Engineering of *C. tyrobutyricum*

C. tyrobutyricum ATCC 25755 has been metabolically engineered by modifying a specific pathway or gene to improve the production of butyrate. For example, the down-regulation of acetate improved butyrate concentration by 100% in PAK-Em, but the cell growth rate decreased by 33% and the maximum productivity reduced by 50% compared to wild type. The carbon redistribution in metabolic engineering caused the imbalance of energy metabolism, low cell growth rate, and reduced productivity. Therefore, it was very important to rationally design the strategy of cell engineering by considering the metabolic shift at the systems level. However, the rational cell engineering requires a deep understanding of cellular metabolism, which is hard to achieve in one study.

The previous proteomics study in *C. tyrobutyricum* demonstrated that the expression of most enzymes in glycolysis, core metabolic pathway, and end-product formation was reduced in PAK-Em [8]. This comparative genomics analysis also revealed that metabolic engineering caused multiple genome mutations (Table 4.3 and NCBI BioProject SRP051738), which could explain the inhibited overall cellular metabolism in PAK-Em. Very interestingly, Hyd-Em showed fast cell growth and high level of butyrate production (i.e. concentration and productivity) with a short fermentation timeline (shown in Table 4.1 and Table 4.2). It is usually difficult to achieve both desired phenotypes using traditional metabolic engineering.

For the first time this study demonstrated the feasibility to obtain novel engineered mutants with desired phenotypes, such as high product concentration, yield, and productivity by combining gene modification and cell adaptation. While metabolic engineering largely relies on the available molecular or functional knowledge, evolutionary engineering does not need extensive genetic and physiological information. Therefore, the integration of these two cell-engineering approaches provides an effective method to construct new mutant strain for industrial production of biochemicals.

4.4.2 Genomics of *C. tyrobutyricum*

The genome of wild type *C. tyrobutyricum* ATCC 25755 was completed by a couple of labs or institute, and the databases were deposited to GenBank with accession numbers of ANOE00000000.1, AUCO00000000.1, APMH00000000.1, ARYO00000000.1, and CBXI000000000.1. The genome consists of 3.01 Mb with an average G+C content of 30.48 % and a total of 3,040 open reading frames (ORFs) [5]. We sequenced both PAK-Em and Hyd-Em mutants and annotated the genes using the published genome database. The genome background of the interested phenotypes achieved in evolutionary engineering was analyzed using comparative genomics. It was found that the evolutionary engineering caused some mutations and cured the mutations (genotypes). Although further multiple genetic engineering studies are needed to confirm the function of the identified genes with each mutation, the results from comparative genomics could provide some hints of the possible correlation between the increased butyrate productivity and cell growth (phenotypes) and the genotypes.

In addition, it was found that a certain number of mutated genes detected in this study could not be defined due to the incomplete genome database. Several key enzymes in the carbohydrate core pathway, such as phosphotransbutyrylase (*ptb*) and acetate/butyrate CoA transferase (*ctf*),

could not be identified or annotated. These results indicated that the genomics of *C. tyrobutyricum* might have gap, or some key enzymes in this strain could be very different from other clostridia. Further genomics study is highly needed to develop a complete genome background in *C. tyrobutyricum* ATCC 25755.

4.4.3 Advantages of Immobilized-cell Butyrate Fermentation

In addition to evolutionary engineering, the immobilized-cell fermentation greatly improved butyrate concentration by PAK-Em and Hyd-Em compared to free-cell fermentation. A high butyrate concentration of 80 g/L was achieved from immobilized-cell fermentation in this study. This high butyrate production was benefited from the high density of cells attached or entrapped inside the FBB that had highly porous fibrous matrix with large surface area and void volume. The adapted culture in FBB could also reduce the butyrate inhibition on phosphotransbutyrylase and ATPase [34], so the immobilized-cell fermentation increased the reactor productivity and titer of butyrate. In addition to high butyrate production, the immobilized *C. tyrobutyricum* can be used to ferment the hydrolysate of low-value biomasses, such as sugarcane bagasse and cane molasses, without detoxification, which will be applied to further characterize the Hyd-Em mutant.

4.5 Conclusions

In summary, a novel mutant strain of *C. tyrobutyricum* was developed by integrating metabolic engineering through gene manipulation and evolutionary engineering through adaptation in a fibrous-bed bioreactor. The mutant produced a high level of butyric acid while maintained fast cell growth. The mutated genes that possibly correlate protein expression, cell growth, butyrate tolerance, and nutrient metabolism and transport were identified by comparative genomics. This study demonstrated that it is feasible to genetically engineer bacteria and combine the desired phenotypes using both gene manipulation and strain adaptation.

4.6 References

[1] S. Liu, K.M. Bischoff, T.D. Leathers, N. Qureshi, J.O. Rich, S.R. Hughes. "Butyric acid from anaerobic fermentation of lignocellulosic biomass hydrolysates by *Clostridium tyrobutyricum* strain RPT-4213". Bioresour. Technol., vol. 143, pp. 322-329, 2013.

[2] D. Wei, S.T. Yang, X. Liu. "Butyric acid production from sugarcane bagasse hydrolysate by *Clostridium tyrobutyricum* immobilized in a fibrous-bed bioreactor". Bioresour. Technol., vol. 129, pp. 553-560, 2013.

[3] G. Yang, G. Liu, C. Yang. "Engineering and metabolic characteristics of a *Clostridium tyrobutyricum* strain". Sheng wu gong cheng xue bao = Chinese journal of biotechnology., vol. 26, pp. 170-176, 2010.

[4] Y. Zhang. "Metabolic Engineering of *Clostridium Tyrobutyricum* for Production of Biofuels and Bio-based Chemicals". The Ohio State University, 2009.

[5] L. Jiang, L. Zhu, X. Xu, Y. Li, S. Li, H. Huang. "Genome Sequence of *Clostridium tyrobutyricum* ATCC 25755, a Butyric Acid-Overproducing Strain". Genome announcements, vol. 1, 2013.

[6] D. Bassi, C. Fontana, S. Gazzola. "Draft Genome Sequence of *Clostridium tyrobutyricum* Strain UC7086, Isolated from Grana Padano Cheese with Late-Blowing Defect". Genome announcements, vol. 1(4), 2013.

[7] M.J. Mayer, J. Payne, M.J. Gasson, A. Narbad. "Genomic sequence and characterization of the virulent bacteriophage phiCTP1 from Clostridium tyrobutyricum and heterologous expression of Its Endolysin". Appl. Environ. Microbiol., vol. 76, pp. 5415-5422, 2010.

[8] C. Ma, K. Kojima, N. Xu. "Comparative proteomics analysis of high n-butanol producing metabolically engineered *Clostridium tyrobutyricum*". J. Biotechnol., vol. 193, pp. 108-119, 2015.

[9] J.T. Heap, S.A. Kuehne, M. Ehsaan. "The ClosTron: Mutagenesis in Clostridium refined and streamlined". J. Microbiol. Methods, vol. 80, pp. 49-55, 2010.

[10] S.W. Jones, B.P. Tracy, S.M. Gaida, E.T. Papoutsakis. "Inactivation of sigmaF in *Clostridium acetobutylicum* ATCC 824 blocks sporulation prior to asymmetric division and abolishes sigmaE and sigmaG protein expression but does not block solvent formation". J. Bacteriol., vol. 193, pp. 2429-2440, 2011.

[11] T. Lutke-Eversloh. "Application of new metabolic engineering tools for *Clostridium acetobutylicum*". Appl. Microbiol. Biotechnol., vol. 98, pp. 5823-5837, 2014.

[12] M. Yu, Y. Du, W. Jiang, W.L. Chang, S.T. Yang, I.C. Tang. "Effects of different replicons in conjugative plasmids on transformation efficiency, plasmid stability, gene expression and n-butanol biosynthesis in *Clostridium tyrobutyricum*". Appl. Microbiol. Biotechnol., vol. 93, pp. 881-889, 2012.

[13] Y. Zhang, M. Yu, S.T. Yang. "Effects of ptb knockout on butyric acid fermentation by *Clostridium tyrobutyricum*". Biotechnol. Progr., vol. 28, pp. 52-59, 2012.

[14] Y. Zhu, X. Liu, S.T. Yang. "Construction and characterization of pta gene-deleted mutant of *Clostridium tyrobutyricum* for enhanced butyric acid fermentation". Biotechnol. Bioeng., vol. 90, pp. 154-166, 2005.

[15] J.H. Jo, CO Jeon, S.Y. Lee, D.S. Lee, J.M. Park. "Molecular characterization and homologous overexpression of [FeFe]-hydrogenase in Clostridium tyrobutyricum JM1". Int. J. Hydrogen. Energ., vol. 35, pp. 1065-1073, 2010.

[16] X. Liu, Y. Zhu, S.T. Yang. "Construction and characterization of ack deleted mutant of *Clostridium tyrobutyricum* for enhanced butyric acid and hydrogen production". Biotechnol. Progr., vol. 22, pp. 1265-1275, 2006.

[17] L. Jiang, J. Wang, S. Liang. "Enhanced butyric acid tolerance and bioproduction by Clostridium tyrobutyricum immobilized in a fibrous bed bioreactor". Biotechnol. Bioeng., vol. 108, pp. 31-40, 2011.

[18] Y.S. Jang, J.A. Im, S.Y. Choi, J.I. Lee, S.Y. Lee. "Metabolic engineering of *Clostridium acetobutylicum* for butyric acid production with high butyric acid selectivity". Metab. Eng., vol. 23, pp. 165-174, 2014.

[19] C.F. Olson-Manning, M.R. Wagner, T. Mitchell-Olds. "Adaptive evolution: evaluating empirical support for theoretical predictions". Nature reviews. Genetics, vol. 13, pp. 67-877, 2012.

[20] Y. Du, W. Jiang, M. Yu, I.C. Tang, S.T. Yang. "Metabolic process engineering of *Clostridium tyrobutyricum* Deltaack-adhE2 for enhanced n-butanol production from glucose: Effects of methyl viologen on NADH availability, flux distribution and fermentation kinetics". Biotechnol. Bioeng., vol. 112, pp. 705-715, 2014.

[21] X. Liu, Y. Zhu, S.T. Yang. "Kinetics of butyric acid fermentation of glucose and xylose by *Clostridium tyrobutyricum* wild type and mutant". Process Biochem., vol. 41, pp. 801-808, 2006.

[22] S.T. Yang, Y. Huang, G. Hong. "A novel recycle batch immobilized cell bioreactor for propionate production from whey lactose". Biotechnol. Bioeng., vol. 45, pp. 379-386, 1995.

[23] L. Jiang, S. Li, Y. Hu, Q. Xu, H. Huang. "Adaptive evolution for fast growth on glucose and the effects on the regulation of glucose transport system in *Clostridium tyrobutyricum*". Biotechnol. Bioeng., vol. 109, pp. 708-718, 2012.

[24] S.T. Yang. "Methods and processes for producing organic acids." U.S. Patent Application 12/999,196, filed June 19, 2008.

[25] M. Yu, Y. Zhang, I.C. Tang, S.T. Yang. "Metabolic engineering of *Clostridium tyrobutyricum* for n-butanol production". Metab. Eng., vol. 13, pp. 373-382, 2011.

[26] H. Li, R. Durbin. "ast and accurate short read alignment with Burrows-Wheeler transform". Bioinformatics, vol. 25, pp. 1754-1760, 2009.

[27] A. McKenna, M. Hanna, E. Banks. "The Genome Analysis Toolkit: a MapReduce framework for analyzing next-generation DNA sequencing data". Genome research, vol. 20, pp. 1297-1303, 2010.

[28] F. Fayolle, R. Marchal, D. Ballerini. "Effect of controlled substrate feeding on butyric acid production by *Clostridium tyrobutyricum*". J. Ind. Microbiol., vol. 6, pp. 179-183, 1990.

[29] Y. Zhu, S.T. Yang. "Effect of pH on metabolic pathway shift in fermentation of xylose by *Clostridium tyrobutyricum*". J. Biotechnol., vol. 110, pp. 143-157, 2004.

[30] D. Michel-Savin, R. Marchal, J.P. Vandecasteele. "Butyrate production in continuous culture of *Clostridium tyrobutyricum*: effect of end-product inhibition". Appl. Microbiol. Biotechnol., vol. 33, pp. 127-131, 1990.

[31] S.K. Wilcox, G.S. Cavey, J.D. Pearson. "Single ribosomal protein mutations in antibiotic-resistant bacteria analyzed by mass spectrometry". Antimicrob. Agents Chemother., vol. 45, pp. 3046-3055, 2001.

[32] M.N. Yap, H.D. Bernstein. "Mutations in the *Escherichia coli* ribosomal protein L22 selectively suppress the expression of a secreted bacterial virulence factor". J. Bacteriol., vol. 195, pp. 2991-2999,2013.

[33] J. Unge, A. berg, S. Al-Kharadaghi. "The crystal structure of ribosomal protein L22 from Thermus thermophilus: insights into the mechanism of erythromycin resistance". Structure., vol. 6, pp. 1577-1586, 1998.

[34] L. Jiang, J. Wang, S. Liang, X. Wang, P. Cen, Z. Xu. "Butyric acid fermentation in a fibrous bed bioreactor with immobilized *Clostridium tyrobutyricum* from cane molasses". Bioresour. Technol., vol. 100, 3403-3409, 2009.

Table 4.1 Kinetics of *C. tyrobutyricum* wild type and mutants in free cell fermentation

Strains	**PAK-Em**	**Hyd-Em [24]**
Cell growth		
Specific growth rate (h^{-1})	0.13 ± 0.005	0.21 ± 0.02
Biomass yield (g/g)	0.07 ± 0.004	0.14 ± 0.07
Acid production		
Butyrate conc. (g/L)	38.72 ± 0.20	41.38 ± 0.24
Acetate conc. (g/L)	7.16 ± 0.53	6.19± 0.97
Butyrate yield (g/g)	0.44 ± 0.01	0.40 ± 0.03
Acetate yield (g/g)	0.08 ± 0.003	0.07 ± 0.03
B/A ratio (g/g)	5.40 ± 0.77	6.68 ± 1.92

[1] All fermentations were duplicated and the average values with standard errors (after ±) are reported.

[2] Yields are presented as g product/g sugar.

Table 4.2 Kinetics of *C. tyrobutyricum* wild type and mutants in immobilized-cell fermentations

Strains	**PAK-Em**	**Hyd-Em [24]**
Cell Growth		
Specific growth rate (h^{-1})	0.10 ± 0.01	0.20 ± 0.02
Biomass yield (g/g)	0.05 ± 0.005	0.22± 0.04
Acid production		
Butyrate conc. (g/L)	48.5 ± 0.5	54.92 ± 0.89
Acetate conc. (g/L)	8.23 ± 0.1	7.03 ± 0.70
Butyrate yield (g/g)	0.45 ± 0.01	0.40 ± 0.00
Acetate yield (g/g)	0.07 ± 0.01	0.05 ± 0.00
B/A ratio (g/g)	5.91 ± 0.22	7.81 ± 1.26

Cell growth was based on the cell density in the suspension in the FBB and did not consider changes in the cells immobilized in the fibrous matrix.

Table 4.3 Gene variations between PAK-Em and Hyd-Em

Category	Gene			PAK-Em		Hyd-Em		Effect
	Gene ID[1]	Protein/gene name	Function	Codon	AA[2]	Codon	AA	Mutation[3]
Protein expression	516360752	Uracil phosphoribosyltransferase (*upp*)	Produce UMP from uracil and phosphoribosylpyrophosphate (PRPP)	72-bp frag /ggt	24AA 138G	No	No	D/No
	516362949	60S ribosomal protein L22 (*rplV*)	Relate to rRNA binding and response to erythromycin antibiotics	No	No	tTt/tGt	F94C	No/NSC
	516362970	40S ribosomal protein S11 (*rpsK*)	Recognize the right tRNA in protein synthesis	No	No	Ttt/Gtt	F35V	No/NSC
Nutrients metabolism and transport	587649370	Molybdopterin biosynthesis protein (*moeA*)	Involve in the molybdopterin guanine dinucleotide generation	Gaa/Taa	E303*	gCa/gAa	A102E	SG/NSC
	587651456	Phosphate transport regulator (*phoU*)	Regulate orthophosphate transport	Gaa/Taa	E171*	No	No	SG/No
	15023088	Molybdate-binding protein	Facilitate molybdate uptake	taG/taT	*320Y	No	No	SL/No

[1] The coding gene is described with GenBank accession number at National Center for Biotechnology Information (NCBI). The gene ID was searched from GenBank nucleotide.

[2] *: Translation stopped due to the stop codon gained.

[3] D: Codon deletion, I: Codon insertion, NSC: Non-synonymous coding, SG: Stop gained, SL: Stop lost, FS: Frame shift, No: no mutation as compared to wild type.

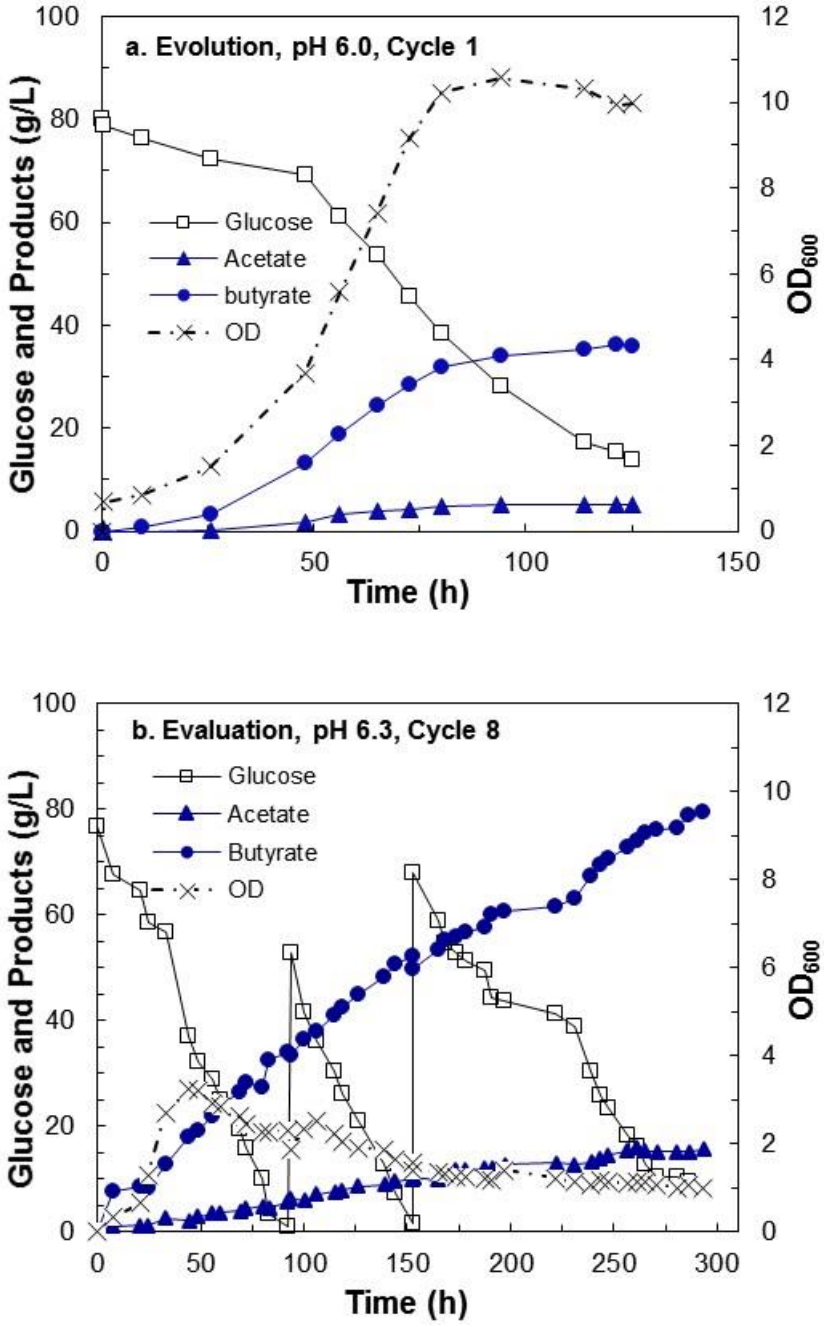

Fig. 4.1 Butyric acid production improvement by cell adaptation of the metabolically engineered mutant PAK-Em in the FBB at 37 ^{o}C and pH 6.0. a). Evolution cycle #1 and b). Evolution cycle #8. OD_{600} (×), sugar (□), acetate (▲), and butyrate (●).

CHAPTER 5

REBALANCING REDOX TO IMPROVE BIOBUTANOL PRODUCTION

Abstract

Biobutanol is a sustainable green biofuel that can substitute for gasoline. Carbon flux had been redistributed in *Clostridium tyrobutyricum* via metabolic cell engineering to produce biobutanol. However, the lack of reducing power hampered the further improvement of butanol production. The objective of this study was to improve butanol production by rebalancing redox. Firstly, a metabolically engineered mutant CTC-*fdh-adhE2* was constructed by introducing heterologous formate dehydrogenase (*fdh*) and bifunctional aldehyde/alcohol dehydrogenase (*adhE2*) simultaneously into wild type *C. tyrobutyricum*. The mutant evaluation indicated that Fdh catalyzed NADH-producing pathway improved butanol titer by 2.15 fold in serum bottle and 2.72 fold in bioreactor. Secondly, the medium supplements that could shift metabolic flux to improve the production of butyrate or butanol were identified, including vanadate, acetamide, sodium formate, vitamin B12, and methyl viologen hydrate. Finally, the free-cell fermentation produced 12.34 g/L of butanol from glucose using CTC-*fdh-adhE2*, which was 3.88-fold higher than that produced by the control CTC-*adhE2*. This study demonstrated that the redox engineering in *C. tyrobutyricum* could increase butanol production greatly.

5.1 Introduction

n-Butanol is a potential substitute for gasoline, a raw material to generate bio-jet fuel, and an important industrial chemical. Biobutanol has been produced by solventogenic Clostridia, such as *C. acetobutylicum* and *C. beijerinckii*, in acetone-butanol-ethanol (ABE) fermentation [1, 2]. Extensive metabolic engineering and fermentation development was performed to improve butanol production [3-6]. However, ABE fermentation still suffered from the relatively low butanol yield, titer and productivity due to the butanol inhibition and the complicated metabolic pathway involved in acidogenesis, solventogenesis, and sporulation.

One alternative strategy for biobutanol production is to synthesize the heterologous butanol biosynthesis pathway from solventogenic Clostridia in other microbes, including *Escherichia coli*, *Saccharomyces cerevisiae*, *Pseudomonas putida*, *Bacillus subtilis*, and *Lactobacillus brevis* [7-12]. For instance, integrated synthetic biology, carbon engineering and redox engineering have been performed in *E. coli*, which produced 14 g/L of n-butanol [13]. Despite these achievements, the inability to ferment low-cost feedstock, low efficiency to catabolize the hydrolysate of biomass, low butanol tolerance, or low butanol productivity by these mutants limited their industrial applications in biobutanol production.

C. tyrobutyricum, an anaerobic acidogenic strain naturally producing butyrate, acetate, CO_2 and H_2 [14, 15], is a promising bacterium for biobutanol production due to its advantages of high butanol tolerance, relatively simple metabolic pathway, and high conversion rate of butyryl-CoA from sugars [16-18]. Recently, the butanol-producing CTC-*adhE2* and ACKKO-*adhE2* were developed by expressing a bifunctional aldehyde/alcohol dehydrogenase (*adhE2*) from *C. acetobutylicum* ATCC 824 in wild type and high butyrate producing strain of *C. tyrobutyricum*, respectively. The free-cell fermentation produced 2.5-6.5 g/L of butanol by CTC-*adhE2* and 14.5-

16 g/L of butanol by ACKKO-*adhE2* from glucose [16, 17]. An advanced fermentation process, such as using mannitol as substrate or immobilizing mutant cells in a fibrous-bed bioreactor supplemented with methyl viologen hydrate, was also developed to further improve biobutanol titer to 20 g/L [16, 18].

Although rebalancing carbon in microorganism resulted in high butanol production by *C. tyrobutyricum*, the lack of reducing power was still a challenge to further improve biobutanol production [17, 19]. Redox engineering has been applied to improve the NADH accumulation in *E. coli*, *S. cerevisiae* and *Klebsiella pneumonia* [10, 13, 20-22]. For example, the overexpression of formate dehydrogenase (*fdh*) improved biobutanol titer from 0.2 g/L to 0.52 g/L by *E. coli* and from ~0.6 g/L to 0.9 g/L by *K. pneumonia* [10, 22]. The redox engineering via introducing Fdh into *C. tyrobutyricum* has not been evaluated so far [19].

The objective of this study was to improve biobutanol production via rebalancing redox in *C. tyrobutyricum* (Fig. 5.1). Redox engineering was performed to construct a new mutant CTC-*fdh-adhE2* and the components that boosted butanol production were also identified. The free-cell butanol fermentation indicated that redox rebalance is an efficient approach to significantly improve butanol production in addition to carbon rebalance.

5.2 Materials and Methods

5.2.1 Strains and Media

As listed in Table 5.1, wild type, mutant CTC-*adhE2* and mutant CTC-*fdh-adhE2* of *C. tyrobutyricum* ATCC 25755 were used. The wild type strain was purchased from ATCC (ATCC, Manassas, VA, USA). The control mutant (CTC-*adhE2*) was obtained from Yang's Lab [23]. In this study, the mutant CTC-*fdh-adhE2* was constructed by simultaneously expressing the

heterologous formate dehydrogenase gene (*fdh*) and bifunctional aldehyde/alcohol dehydrogenase (*adhE2*) in wild type *C. tyrobutyricum*.

The seed culture of *C. tyrobutyricum* was maintained anaerobically in the Reinforced Clostridial Medium (RCM; Difco, Kansas City, MO, USA). The 30 μg/mL of thiamphenicol (Tm, Alfa Aesar, Ward Hill, MA, USA) was used to select and maintain mutants. In serum bottle and bioreactor fermentations, the modified Clostridial Growth Medium (CGM) containing 40 g/L of glucose was used [24]. Antibiotics were added to the baseline study in serum bottle but not added to media study and bioreactor fermentation. *E. coli* was grown aerobically in Luria-Bertani (LB) media supplemented with 30 μg/mL of chloramphenicol (Cm, Alfa Aesar) or 50 μg/mL of kanamycin (Kan, Alfa Aesar). The chemical reagents were purchased from Sigma-Aldrich (St. Louis, MO, USA), unless otherwise specified.

5.2.2 Plasmid Construction

The flowchart of plasmid construction is described in Fig. 5.2. Specifically, the pMTL007 plasmid obtained from Minton's Lab [25] was used as an expression vector. The *fdh* gene was amplified from *Moorella thermoacetica* ATCC 39073 (ATCC, Manassas, VA, USA) using Q5 High-Fidelity DNA Polymerase (NEB, Ipswich, MA, USA). The plasmid pMTL-*adhE2* was constructed following previous publication [23]. The promoter of the homologous *thl* gene (Pthl) cloned from *C. tyrobutyricum*, *fdh* gene and pMTL-*adhE2* backbone were assembled to generate plasmid pMTL-*fdh-adhE2* using Gibson Assembly kit (NEB) following the manufacture's instruction.

5.2.3 Mutant Construction

The transformation of plasmid pMTL-*fdh-adhE2* into the wild type *C. tyrobutyricum* was performed *via* conjugation in an anaerobic chamber according to previous publication [23, 26] with the following modifications. The *E. coli CA434* was transformed with pMTL-*fdh-adhE2* and cultivated in LB medium containing 30 μg/mL of Cm and 50 μg/mL of Kan. The *E. coli CA434*/pMTL-*fdh-adhE2* was harvested as donor cells when the optical density at 600 nm (OD_{600}) reached ~1.5. The wild type cells were grown in RCM medium and collected as recipient cells when OD_{600} reached 1.5-3.0. The transformed clostridial cells were spread on RCM selection plates that contained 30 μg/mL of Tm and 250 μg/mL of D-cycloserine (Cy, Alfa Aesar). The selection plates were incubated at 37 ^{o}C for 72-96 h or until colonies appeared. Twenty colonies were picked and evaluated in 50-mL serum bottle culture to screen the clone with the highest butanol production, which was named as CTC-*fdh-adhE2*.

To engineer the butanol fermentation process, medium optimization was performed in the small-scale fermentations of CTC-*fdh-adhE2* in serum bottles. In this study, ten components at two levels (i.e. concentrations) were analyzed using the new mutant CTC-*fdh-adhE2*. Only the representative conditions that enhanced the production of butyrate or butanol are summarized in Table 5.2. Fresh seed culture with OD_{600} of ~1.5 was used to inoculate the 50-mL CGM medium containing 40 g/L of glucose and different medium supplements. The cultures with inoculation OD_{600} of ~0.04 were anaerobically incubated at 37 ^{o}C without pH adjustment. The samples were taken daily to monitor cell growth, glucose consumption, and products formation. All conditions were carried out in duplicate and data were reported as the average with standard deviation.

5.2.4 Butanol Fermentation

The kinetics studies of the fed-batch fermentation by CTC-*adhE2* (control) and CTC-*fdh-adhE2* mutants were performed in a stirred-tank bioreactor (FS-01-A; Major science, Saratoga, CA, USA). Fermentation setup, operation and sampling were performed as reported previously [17]. Fermentations were run in duplicate and the mean and standard deviation were calculated and presented.

5.2.5 Activity Assay of Formate Dehydrogenase

The preparation of cell extract and the measurement of formate dehydrogenase activity were performed as reported with modification [27, 28]. The cells of CTC-*adhE2* and CTC-*fdh-adhE2* were collected when the OD_{600} reached ~2.0, centrifuged, washed, and cooled in an anaerobic chamber. The suspended cells on ice were sonicated for 15 min using the sonifier (Models 250; Branson Ultrasonics, Danbury, CT, USA) with 40 % power and 30 s of interval for cooling each minute. The concentration of total protein in cell extract was titrated using Bradford's kit (Bio-Rad, Hercules, CA, USA) with bovine serum albumin as a standard.

The activity assay of formate dehydrogenase was performed at 37 ^{o}C in an anaerobic chamber. Specifically, the 0.1 mL of cell extract was added to 1 mL of pre-mixed potassium phosphate buffer containing 1.67 mM of NAD^+ and 167 mM of sodium formate. The kinetics of NADH generation was monitored by measuring the absorbance at 340 nm at reaction times of 10, 20, 30, 60, 90, and 120 s using a spectrophotometer (Biomate3; Thermo Fisher Scientific, Hudson, NH, USA). The concentration of NADH was calculated using a specific absorbance coefficient of 6220 $M^{-1}cm^{-1}$. One unit of the activity of formate dehydrogenase was defined as 1 μmol of NADH produced per minute at pH 7.5 and 37 ^{o}C. The specific activity of Fdh was calculated from the measured activity divided by total protein in the cell extract.

5.2.6 Butanol Tolerance

The wild type, CTC-*adhE2* and CTC-*fdh-adhE2* were cultivated in serum bottles with seeding OD_{600} of 0.3 to evaluate the effect of redox engineering on butanol tolerance. Butanol at final concentrations of 0, 5, 10, 15, and 20 g/L was added to the basal CGM medium. The cell growth was analyzed by sampling serum bottles every 3 h. The butanol inhibition was modeled by the equation of $\mu = \mu_{max}Kp/(Kp+P)$ where μ is the specific growth rate (h^{-1}), Kp is the inhibition rate constant (g/L), and P is butanol concentration (g/L).

5.2.7 NADH Assay

A NAD/NADH quantitation colorimetric kit (BioVision, San Francisco, CA, USA) was used to measure the intracellular concentration of NADH and NAD^+ in the CTC, CTC-*adhE2* and CTC-*fdh-adhE2*. The cells were cultivated in 50-mL CGM medium containing 1 g/L of sodium formate in serum bottles with duplication. The cultures were sampled in mid-log phase and 1-mL samples were centrifuged at 10,000 rpm for 10 min. The cell pellets were re-suspended in 400 μL of NADH/NAD extraction buffer provided in the kit. The NADH and NAD^+ were extracted by freeze/thaw for two cycles (20 min on dry-ice followed by 10 min at room temperature in each cycle). To titrate NADH, NAD^+ was decomposed by heating the cell lysate at 60 ^oC for 30 min. After cooling on ice for 10 min, the NADH samples were centrifuged at 4,000 rpm for 2 min. The 50-μL supernatant was mixed with 100 μL of NAD^+ cycling enzyme provided in the kit. The reaction mixture was incubated at the room temperature for 4 h before the value of OD_{450} was read. To measure the concentration of the mixture of NAD^+ and NADH, 4 μL of cell lysate was straightly mixed with 46 μL of NADH/NAD extraction buffer and 100 μL of NAD cycling enzyme. The NADH concentration was calculated using the equation "$Concentration_{NADH}$ (mM)

$= Mole_{NADH} / Volume_{wet\ cell} = Mole_{NADH} / (OD_{600}/mL \times 0.38\ g\text{-dry cell/L} \times 10^{-3}\ L/mL \times 4.27\ mL/g\text{-wet cell} \times 10^{-3}\ g/mg)$".

5.2.8 Analytical Methods

The cell density was analyzed by measuring the OD_{600} of the cell suspension. The concentrations of fermentation substrate and products, including glucose, butanol, butyrate, acetate and ethanol, were analyzed using the high performance liquid chromatography (HPLC, Shimadzu, Columbia, MD, USA) following previous production [17]. The glucose concentration was also daily analyzed using YSI 2700 Select Biochemistry Analyzer (YSI Life Sciences, Yellow Springs, OH, USA) to determine feeding strategy.

5.3 Results

5.3.1 Construction and Evaluation of Redox Engineered Mutant

In this study, the heterologous formate dehydrogenase gene (*fdh*) was overexpressed together with *adhE2* in wild type *C. tyrobutyricum* to generate the new mutant CTC-*fdh-adhE2*. The enzyme AdhE2 catalyzed the formation of butanol from butyryl-CoA, which had been demonstrated in the previous study [23]. The enzyme Fdh was expressed to rebalance redox by generating more reducing power, i.e. NADH, in this study.

The mutant CTC-*fdh-adhE2* was characterized using PCR, enzyme activity assay and NADH assay. The heterologous *fdh* gene was successfully amplified from CTC-*fdh-adhE2* in PCR reaction, indicating that the pMTL-*fdh-adhE2* plasmid was transformed into *C. tyrobutyricum*. The enzyme assay showed that the specific enzymatic activity of the NAD^+-dependent Fdh was 990 U/g in CTC-*fdh-adhE2* and zero in CTC-*adhE2*. These results confirmed that the heterologous fdh was expressed properly in the CTC-*fdh-adhE2*. In addition, the NADH assay demonstrated that

the intracellular NADH concentration was increased from 0.11 mM in CTC-*adhE2* to 0.28 mM in CTC-*fdh-adhE2*. The mole ratio between NADH and NAD^+ was also enhanced in CTC-*fdh-adhE2* (shown in Fig. 5.3). These results confirmed that the synthesized Fdh enzyme boosted the intracellular accumulation of NADH.

The baselines of butanol production of wild type (control 1), CTC-*adhE2* (control 2), and CTC-*fdh-adhE2* were created using 100-mL culture in serum bottles. The modified CGM medium was used without the addition of formate. As presented in the kinetics profiles in Fig. 5.4, all the three strains grew immediately after inoculation and reached a similar maximum OD_{600}. The fermentation data showed that the wild type produced 9.02 g/L of butyrate and butanol was not produced as expected. The CTC-*adhE2* produced 8.78 g/L of butyrate and 2.51 g/L of butanol, and the CTC-*fdh-adhE2* produced 6.40 g/L of butyrate and 5.41 g/L of butanol. The CTC-*fdh-adhE2* also produced 2.15-fold higher butanol than CTC-*adhE2*. These results indicated that the overexpression of the heterologous gene *fdh* in CTC-*fdh-adhE2* shifted carbon flux from butyrate to butanol.

The butanol production consumes reducing power NAD(P)H in *C. tyrobutyricum*, and it is important to evaluate the feasibility of improving butanol production via rebalancing redox. In this study, it was introduced a NADH-producing pathway by overexpressing a NAD^+-dependent enzyme Fdh in CTC-*adhE2*. The NADH can be produced from formate through the synthesized reaction "Formate + $NAD^+ \rightleftharpoons$ NADH + CO_2 + H^+". The increase of butanol production by CTC-*fdh-adhE2* indicated that the expression of Fdh generated more NADH and thus benefited butanol production.

In addition, it was noted that the butanol production was improved by CTC-*fdh-adhE2* even no additional formate was added to medium. Our proteomics study showed that pyruvate-formate

lyase (*pfl*) was expressed in *C. tyrobutyricum*. The enzyme Pfl catalyzes the reversible reaction "pyruvate + CoA ⇌ formate + acetyl-CoA". Because pyruvate was produced from glucose through the glycolysis pathway, formate could be intracellularly produced from pyruvate. The generated formate could be consumed by Fdh to boost the NADH and improve butanol production.

5.3.2 Evaluation of Medium Supplements

Medium optimization, an important process engineering strategy, was carried out to screen the components that could increase the formation of butanol. The average data of the final titers of acetate, butyrate, ethanol and butanol by CTC-*fdh-adhE2* are described in Fig. 5.5. The control culture without any medium supplement produced 5.35 g/L of butanol. Some components increased butanol up to 8.00 g/L, but some components increased butyrate up to 9.00 g/L. The ten experimental conditions were classified into two groups (Table 5.2 and Fig. 5.5), including one group that improved butanol production and another group that enhanced butyrate production.

In the first group, either sodium formate (SF, 1 g/L, condition 1) or methyl viologen hydrate (MVH, 0.1 g/L, condition 3) could obviously improve the butanol production. As discussed above, formate increased butanol production because of the Fdh enzyme synthesized more NADH. MVH is an artificial electron carrier that can boost electron supply from ferredoxin, so it increased butanol production by providing more reducing power. MVH was also used to improve butanol production by immobilized *C. tyrobutyricum* in a recent study [18]. It was reported that B12 improved the cell growth of *C. acetobutylicum* [29], but the effect of B12 on butanol production was not investigated. This study showed that vitamin B12 (B12, 0.001 g/L) did not change butanol production (condition 2) although it improved the maximum OD by 36% compared to the control.

The combination of formate, B12 and MVH (condition 6) improved the butanol titer to 8.00 g/L and reduced the butyrate titer to 5.05 g/L compared to the control condition. The selectivity of

butanol was also improved from 0.39 g/g (control) to 0.60 g/g. Interestingly, the supplement of these three components significantly reduced the acetate production to 0.01 g/L and improved C4 (butyrate and butanol) selectivity to 0.97 g/g, while the control culture produced acetate with titer of 1.70 g/L and C4 (butyrate and butanol) with selectivity of 0.87 g/g. Taken together, the addition of formate, B12 and MVH to CGM medium not only shifted more carbon flux from butyrate to butanol, but also redirected carbon from C2 to C4. It was also observed that the addition of any of these three components (conditions 1-3) did not reduce the acetate formation, but the combination of formate and MVH (conditions 5 and 6) blocked the production of acetate. It was hypothesized that a synergistic effect between formate and MVH shifted carbon flux from C2 to C4.

In the second group, the addition of vanadate and acetamide increased the production of butyrate and acetate. Acetamide could provide an extra nitrogen source and vanadate could affect the metabolism of sugar phosphate. Both components shifted carbon from butanol to butyrate. Other key findings that are not described in Table 5.2 and Fig. 5.5 include: 1) sodium pyruvate (1 g/L) did not increase the production of solvents and acids, and 2) manganese sulphate (0.1 g/L) increased acetate production (2.55 vs 1.70 g/L by control) because the high activity of acetate kinase needs manganese [30].

Very interestingly, both butanol and ethanol formation pathways consumed NADH, but neither the expression of Fdh nor the medium supplements improved the production of ethanol, i.e. 0.28 g/L in condition 6 supplemented with formate, B12 and MVH vs. 0.14 g/L in control. Our previous proteomics study of *C. tyrobutyricum* showed that the expression of alcohol dehydrogenase (*adh*) was very low while the expression of butanol dehydrogenase (*bdh*) was pretty high [17]. Therefore, the redox engineering increased the production of butanol but not ethanol due to the low expression of Adh and the low metabolic flux distributed to ethanol.

5.3.3 Butanol Fermentation

Both CTC-*adhE2* and CTC-*fdh-adhE2* were evaluated in 2-L fed-batch fermentations in stirred-tank bioreactor at 37 ^{o}C and pH 6.0 using CGM medium supplemented with the identified components. As shown in Fig. 5.6, four conditions were investigated, including CTC-*adhE2* supplemented with SF (Fig. 5.6A), CTC-*adhE2* with sodium formate (SF), vitamin B12 (B12) and methyl viologen hydrate (MVH) (Fig. 5.6B), CTC-*fdh-adhE2* with SF (Fig 5.6C), and CTC-*fdh-adhE2* with SF, B12 and MVH (Fig. 5.6D). The kinetics profiles in Fig. 5.5 showed that there was no obvious lag phase in all fermentations. As presented in Table 5.3, all four conditions had similar specific growth rate of 0.15-0.18 h^{-1} and maximum OD_{600} of 7.5-9.0.

As summarized in Table 5.3, the butanol concentrations were 3.18 g/L, 6.14 g/L, 8.83 g/L and 12.34 g/L by CTC-*adhE2* with SF, CTC-*adhE2* with SF, B12 and MVH, CTC-*fdh-adhE2* with SF, and CTC-*fdh-adhE2* with SF, B12 and MVH, respectively. It is obvious that the integration of metabolic cell engineering (Fdh synthesis) and process engineering (medium optimization) significantly increased the butanol production from 3.18 g/L to 12.34 g/L, with 3.88-fold improvement. The yield of butanol through integrated cell-process engineering (0.23 g/g) was also much higher than other conditions (0.05-0.16 g/g). The butanol production by redox engineering was slightly higher than that by medium supplement addition, *i.e.* titer of 8.83 g/L and yield of 0.16 g/g (Fig. 5.5C) vs. titer of 6.14 g/L and yield of 0.11 g/g (Fig. 5.5B). However, butanol productivity was 0.26 g/L/h by CTC-*fdh-adhE2* with medium supplements, which was much higher than other conditions (0.12-0.17 g/L/h). These results confirmed that the rebalance of redox directed more carbon to the production of butanol that consumed reducing power. In addition, the ethanol concentrations in these four fermentations were pretty low, 0.11 g/L to 0.28 g/L due to the low expression of alcohol dehydrogenase (*adh*).

To better understand the effect of carbon and redox rebalance on butanol production; the selectivity of fermentation products were compared (Fig. 5.7). The selectivity of butanol was 0 g/g; 0.15 g/g; 0.51 g/g; 0.41 g/g; and 0.69 g/g at the conditions of control; CTC-*adhE2* (C); CTC-*fdh-adhE2* (C-R1); CTC-*adhE2* with medium supplement (C-R2); and CTC-*fdh-adhE2* with medium supplement (C-R1-R2); respectively. It is clear that the rebalances of carbon and redox via integrating metabolic cell and process engineering could effectively boost the selectivity of butanol and improve the production of butanol. In addition; the conditions of C; C-R1; C-R2 and C-R1-R2 produced butyrate with concentrations of 13.22 g/L; 7.72 g/L; 9.32 g/L and 5.05 g/L; and the acetate with concentrations of 4.15 g/L; 0.69 g/L; 1.42 g/L and 0.26 g/L; respectively. These results revealed that the rebalance of redox not only redistributed carbon between C4; but also redirected the carbon flux from C2 to C4.

5.3.4 Butanol Tolerance

Butanol is a toxic solvent that could change the cell membrane fluidity and inhibit cell growth, so butanol tolerance is an important factor to evaluate the new mutant. In this study, the effect of butanol on the cell growth of wild type CTC, mutant CTC-*adhE2* and mutant CTC-*fdh-adhE2* was investigated (Fig. 5.8). At 0 g/L of butanol, both mutants and wild type showed the highest specific growth rate, while the higher butanol concentration inhibited cell growth. At 20 g/L of butanol, less than 20% of their maximum growth rate was retained. The growth inhibition by butanol followed the noncompetitive inhibition kinetics with K_P (inhibition rate constant) of 3.32 g/L. 2.70 g/L and 3.37 g/L for CTC, CTC-*adhE2* and CTC-*fdh-adhE2*, respectively. This tolerance study showed that metabolic engineering in the new mutant did not reduce butanol tolerance and cell growth.

5.4 Discussion

5.4.1 Improvement of Butanol Production by Rebalancing Redox

In previous studies, it was found that the production of solvents involved a global remodeling of metabolism in *C. acetobutylicum* [31], and different NADH/NAD^+ ratio could redistribute the metabolic flux in *E. coli* and *C. acetobutylicum* [20, 32]. The previous Omics study also showed a strong correlation between the expression level of NAD(P)H-dependent enzymes and the production of butanol in *C. tyrobutyricum*, indicating that high butanol production required more reducing power [17]. Another study showed that the addition of methyl viologen hydrate increased the butanol production in fermentation [18]. Therefore, it is hypothesized that the integration of redox rebalance in the engineered mutant of *C. tyrobutyricum* with carbon rebalance could greatly improve the butanol production.

To examine the above hypothesis, it was performed redox engineering using both cell engineering and process engineering in this study. The control mutant is CTC-*adhE2*, i.e. the wild type *C. tyrobutyricum* containing synthesized *adhE2* [23]. Compared with CTC-*adhE2*, the redox engineering by cell engineering or process engineering (i.e. medium optimization in this study) doubled the butanol production, while the integration of cell-process engineering quadrupled the butanol production (12.34 g/L vs. 3.18 g/L). It was indicated that the integration of these two engineering methods effectively improved reducing power supply and rebalanced redox. These results also demonstrated that redox engineering was essential to achieve high butanol production in addition to carbon engineering in *C. tyrobutyricum*.

Another interesting observation in this study is that the redox rebalance significantly reduced the production of acids (butyrate and acetate) by *C. tyrobutyricum*. Because butanol formation consumed NAD(P)H, the synthesis of NADH producing pathway and the medium supplements

resulted in carbon redistribution from acetate and butyrate to butanol. Therefore, the selectivity of butanol was significantly increased in the fermentation of CTC-*fdh-adhE2* with medium supplements. Moreover, ethanol production was still low even the butanol production was increased by redox balance. The high selectivity of butanol and low production of byproducts could benefit the separation of biobutanol and reduce the production cost of biofuel from bacterial fermentation.

5.4.2 Comparison with Previous Studies

As a promising host cell in butanol production, *C. tyrobutyricum* has the desired features such as unassociated sporulation and cell autolysis, high butanol tolerance, and ability to convert low-value lignocellulosic biomass feedstock. Recently, a couple of studies have been performed to improve biobutanol production by *C. tyrobutyricum* through metabolic engineering or process engineering. As summarized in Table 5.4, the mutant CTC-*adhE2* with overexpressed *adhE2* and pCB12 replicon in wild type *C. tyrobutyricum* produced butanol with titer of 2.5 g/L from glucose in serum bottle in a previous study [23], and a similar result was obtained in this study. The pBP1 replicon improved butanol titer to 6.5 g/L from glucose in serum bottle and further improved butanol titer to 20.0 g/L from mannitol in bioreactor [16]. These results elucidated that replicon optimization and substrate are very important for biobutanol production. Replicon optimization can be performed in our future metabolic engineering study. However, mannitol is an expensive raw material for butanol production, with price of ~2000 US dollars per ton, which impedes an economically competitive biobutanol in the fuel market. In this study, the redox was rebalanced by synthesizing a NADH-producing pathway in addition to carbon redistribution, resulting in doubled butanol titer. The reducing power supplement further improved butanol production by

quadrupling the titer to reach 12.3 g/L. Therefore, it is conclude that the redox rebalance is an effective approach to improve the biobutanol production by *C. tyrobutyricum*.

The recent butyrate fermentation using *C. tyrobutyricum* showed that the pH of fermentation significantly affected the production of butyrate and cell growth [33]. Specifically, the immobilized-cell fermentations at pH 6.0, 6.5 and 7.0 produced butyrate with concentrations of 50.11 g/L, 63.02 g/L and 61.01 g/L. The metabolic flux analysis demonstrated that carbon flux from acetyl-CoA to acetoacetyl-CoA and the carbon flux from butyryl-CoA to butyrate were increased at pHs of 6.5 and 7.0 as compared to pH 6.0. In addition, the biomass yield of *C. tyrobutyricum* was also decreased at a higher pH. The pH values of the butanol fermentations in bioreactors were maintained at 6.0 in this study. Because butanol is produced from butyryl-CoA directly, the improved carbon flux from C2 to C4 at higher pH could benefit the formation of butanol. In future study, the butanol fermentation by the constructed mutant CTC-*fdh-adhE2* will be optimized to further improve butanol production.

Other metabolic engineering strategies were used to increase butanol production by redistributing the metabolic flux from C2 to C4. For example, the ACKKO-*adhE2* achieved the highest concentration of butanol (14.5 g/L) in free-cell fermentation and process engineering in immobilized-cell fermentation generated > 20 g/L of butanol [18]. To achieve a higher butanol production, redox engineering could be applied in a high butanol producing mutant, e.g. ACKKO-*adhE2*, in the future. To effectively integrate cell engineering and process engineering, metabolomics should be developed and applied to *C. tyrobutyricum*. Metabolic flux analysis modeling is also an effective tool to guide the design of metabolic engineering [33, 34]. In addition, the medium components can be rationally designed to assist butanol production post cell engineering.

5.5 Conclusions

In this study, we demonstrated that redox engineering was essential to improve butanol production in *C. tyrobutyrium*. Both the titer and selectivity of butanol were significantly improved by rebalancing redox in addition to rebalancing carbon. It was also found that the integration of metabolic cell and process engineering was an efficient strategy to improve biofuel production.

5.6 Reference

[1] Y.N. Zheng, L.Z. Li, M. Xian, Y.J. Ma, J.M. Yang, X. Xu, D.Z. He. "Problems with the microbial production of butanol". J. Ind. Microbiol. Biotechnol., vol. 36, pp. 1127-1138, 2009.

[2] C.B. Milne, J.A. Eddy, R. Raju, S. Ardekani, P.J. Kim, R.S. Senger, Y.S. Jin, H.P. Blaschek, N.D. Price "Metabolic network reconstruction and genomescale model of butanol-producing strain Clostridium beijerinckii NCIMB 8052". BMC Syst. Biol., vol. 5, pp. 130-144, 2011.

[3] S.Y.Lee, J.H. Park, S.H. Jang, L.K. Nielsen, J. Kim, K.S Jung. "Fermentative butanol production by Clostridia". Biotechnol. Bioeng. vol. 101, pp. 209-228, 2008.

[4] S.A.Nicolaou, S.M. Gaida, E.T. Papoutsakis. "A comparative view of metabolite and substrate stress and tolerance in microbial bioprocessing: From biofuels and chemicals, to biocatalysis and bioremediation". Metab. Eng., vol. 12, pp. 307-331, 2010,

[5] E.T.Papoutsakis. "Engineering solventogenic clostridia'. Curr. Opin. Biotechnol., vol. 19, pp. 420-429, 2008.

[6] M.A.Al-Hinai, A.G. Fast, E.T. Papoutsakis. "Novel system for efficient isolation of Clostridium double-crossover allelic exchange mutants enabling markerless chromosomal gene deletions and DNA integration". Appl. Environ. Microbiol., vol. 78, pp. 8112-8121, 2012.

[7] S.Atsumi, A.F. Cann, M.R. Connor, C.R. Shen, K.M. Smith, M.P. Brynildsen, K.J. Chou, T. Hanai, J.C. Liao. "Metabolic engineering of Escherichia coli for 1-butanol production". Metab. Eng., vol. 10, pp. 305-311, 2008.

[8] O.V. Berezina, N.V. Zakharova, A. Brandt, S.V. Yarotsky, W.H. Schwarz, V.V. Zverlov. "Reconstructing the clostridial n-butanol metabolic pathway in Lactobacillus brevis". Appl. Microbiol. Biotechnol., vol. 87, pp. 635-646, 2010.

[9] B. Blombach, B.J. Eikmanns. "Current knowledge on isobutanol production with Escherichia coli, Bacillus subtilis and Corynebacterium glutamicum". Bioeng. Bugs., vol. 2, pp. 346-350, 2011.

[10] D.R. Nielsen, E. Leonard, S.H. Yoon, H.C. Tseng, C. Yuan, K.L. Prather. "Engineering alternative butanol production platforms in heterologous bacteria". Metab. Eng., vol. 11, pp. 262-273, 2009.

[11] C.R. Shen, J.C. Liao. "Metabolic engineering of Escherichia coli for 1-butanol and 1-propanol production via the keto-acid pathways". Metab. Eng., vol. 10, pp. 312-320, 2008.

[12] E.J. Steen, R. Chan, N. Prasad, S. Myers, C.J. Petzold, A. Redding, M. Ouellet, J.D. Keasling. "Metabolic engineering of Saccharomyces cerevisiae for the production of n-butanol". Microb. Cell. Fact., vol. 7, pp. 36, 2008.

[13] C.R. Shen, E.I. Lan, Y. Dekishima, A. Baez, K.M. Cho, J.C. Liao. "Driving forces enable high-titer anaerobic 1-butanol synthesis in Escherichia coli". Appl. Environ. Microbiol., vol. 77, pp. 2905-2915, 2011.

[14] L. Jiang, J. Wang, S. Liang, X. Wang, P. Cen, Z. Xu. "Production of butyric acid from glucose and xylose with immobilized cells of Clostridium tyrobutyricum in a fibrous-bed bioreactor". Appl. Biochem. Biotechnol., vol. 160, pp. 350-359, 2010.

[15] X. Liu, S.T. Yang. "Butyric acid and hydrogen production by Clostridium tyrobutyricum ATCC 25755 and mutants". Enzyme Microb. Technol., vol. 38, pp. 521-528, 2006.

[16] M. Yu, Y. Du, W. Jiang, W.L. Chang, S.T. Yang, I.C. Tang "Effects of different replicons in conjugative plasmids on transformation efficiency, plasmid stability, gene expression and n-butanol biosynthesis in Clostridium tyrobutyricum". Appl. Microbiol. Biotechnol., vol. 93, pp. 881-889, 2012.

[17] C. Ma, K. Kojima, N. Xu, J. Mobley, L. Zhou, S.T. Yang, X.M. Liu. "Comparative proteomics analysis of high n-butanol producing metabolically engineered Clostridium tyrobutyricum". J. Biotechnol., vol. 193, pp. 108-119, 2015.

[18] Y. Du, W. Jiang, M. Yu, I.C. Tang, S.T. Yang. "Metabolic process engineering of Clostridium tyrobutyricum Deltaack-adhE2 for enhanced n-butanol production from glucose: Effects of methyl viologen on NADH availability, flux distribution and fermentation kinetics". Biotechnol. Bioeng., vol. 112, pp. 705-715, 2015.

[19] J. Ou, C. Ma, N. Xu, Y. Du, X.M. Liu. "High Butanol Production by Regulating Carbon, Redox and Energy in Clostridia". Front. Chem. Sci. Eng., 2015.

[20] S.J. Berrios-Rivera, G.N. Bennett, K.Y. San. "Metabolic engineering of Escherichia coli: increase of NADH availability by overexpressing an NAD(+)-dependent formate dehydrogenase". Metab. Eng., vol. 4, pp. 217-229, 2002.

[21] J.M. Geertman, J.P. van Dijken, J.T. Pronk. "Engineering NADH metabolism in Saccharomyces cerevisiae: formate as an electron donor for glycerol production by anaerobic, glucose-limited chemostat cultures". FEMS. Yeast. Res., vol. 6, pp. 1193-1203, 2006,

[22] M. Wang, L. Hu, L. Fan, T. Tan. "Enhanced 1-Butanol Production in Engineered Klebsiella pneumoniae by NADH Regeneration". Energy. Fuels., vol. 29, pp. 1823-1829, 2015.

[23] M. Yu, Y. Zhang, I.C. Tang, S.T. Yang. "Metabolic engineering of Clostridium tyrobutyricum for n-butanol production". Metab. Eng., vol. 13, pp. 373-382, 2011.

[24] H. Dong, W. Tao, Y. Zhang, Y. Li. "Development of an anhydrotetracycline-inducible gene expression system for solvent-producing Clostridium acetobutylicum: A useful tool for strain engineering". Metab. Eng., vol. 14, pp. 59-67, 2012.

[25] J.T. Heap, S.A. Kuehne, M. Ehsaan, S.T. Cartman, C.M. Cooksley, J.C. Scott, N.P. Minton. "The ClosTron: Mutagenesis in Clostridium refined and streamlined". J. Microbiol. Methods., vol. 80, pp. 49-55, 2010.

[26] D. Purdy, T.A. O'Keeffe, M. Elmore, M. Herbert, A. McLeod, M. Bokori-Brown, A. Ostrowski, N.P. Minton. "Conjugative transfer of clostridial shuttle vectors from Escherichia coli to Clostridium difficile through circumvention of the restriction barrier". Mol. Microbiol., vol. 46, pp. 439-452, 2002.

[27] A. Alissandratos, H.K. Kim, H. Matthews, J.E. Hennessy, A. Philbrook, C.J. Easton. "Clostridium carboxidivorans strain P7T recombinant formate dehydrogenase catalyzes reduction of CO(2) to formate". Appl. Environ. Microbiol., vol. 79, pp. 741-744, 2013.

[28] I. Yamamoto, T. Saiki, S.M. Liu, L.G. Ljungdahl. "Purification and properties of NADP-dependent formate dehydrogenase from Clostridium thermoaceticum, a tungsten-selenium-iron protein". J. Biol. Chem., vol. 258, pp. 1826-1832, 1983.

[29] H. Heluane, M.R. Evans, S.F. Dagher, J.M. Bruno-Barcena. "Meta-analysis and functional validation of nutritional requirements of solventogenic Clostridia growing under butanol stress conditions and coutilization of D-glucose and D-xylose". Appl. Environ. Microbiol., vol. 77, 2011.

[30] R. Gheshlaghi, J.M. Scharer, M. Moo-Young, C.P. Chou. "Metabolic pathways of clostridia for producing butanol." Biotechnol. Adv., vol. 27, pp. 764-781, 2009.

[31] D. Amador-Noguez, I.A. Brasg, X.J. Feng, N. Roquet, J.D. Rabinowitz. "Metabolome remodeling during the acidogenic-solventogenic transition in Clostridium acetobutylicum". Appl. Environ. Microbiol., vol. 77, pp. 7984-7997, 2011.

[32] S. Nakayama, T. Kosaka, H. Hirakawa, K. Matsuura, S. Yoshino, K. Furukawa. "Metabolic engineering for solvent productivity by downregulation of the hydrogenase gene cluster hupCBA in Clostridium saccharoperbutylacetonicum strain N1-4. Appl". Microbiol. Biotechnol., vol. 78, pp. 483-493, 2008.

[33] C. Ma, J. Ou, S. McFann, M. Miller, X.M. Liu. "High production of butyric acid by Clostridium tyrobutyricum mutant". Front. Chem. Sci. Eng., 2015.

[34] C. Liao, S.O. Seo, V. Celik, H. Liu, W. Kong, Y. Wang, H. Blaschek, Y. Jin, T. Lu. "Integrated, systems metabolic picture of acetone-butanol-ethanol fermentation by Clostridium acetobutylicum". Proc. Natl. Acad. Sci., vol. 112, pp. 8505-8510, 2015.

Table 5.1. Strains and plasmids used in this study.

Plasmid/strain	Relevant characteristics	Reference/source
Plasmids		
*p*MTL-adhE2	*adhE2* overexpression with *thl* promoter	This study
*p*MTL-fdh-adhE2	*fdh* and *adhE2* overexpression with *thl* promoter	This study
Strains		
C. tyrobutyricum	Clostridium, ATCC 25755, wild type	ATCC
CTC-*adhE2*	Clostridium with *adhE2* overexpression, thiamphenicol resistant	Yu et al. (2011)
CTC-*fdh-adhE2*	Clostridium with *fdh* and *adhE2* overexpression, thiamphenicol resistant	This study
E. coli CA434	*E. coli* HB101 with plasmid R702, kanamycin resistant	Williams et al. (1990)

Table 5.2. Medium components screening to rebalance redox and carbon.

No.	**Sodium Formate** (1 g/L)	**Vitamin B12** (0.001 g/L)	**Methyl Viologen Hydrate** (0.1 g/L)	**Vanadate** (1 g/L)	**Acetamide** (1 g/L)
C	-	-	-	-	-
1	+	-	-	-	-
2	-	+	-	-	-
3	-	-	+	-	-
4	+	+	-	-	-
5	+	-	+	-	-
6	+	+	+	-	-
7	+	-	-	+	-
8	+	-	-	-	+
9	+	+	-	+	-
10	+	+	-	-	+

Table 5.3. Butanol fermentations using metabolically engineered *C. tyrobutyricum* by rebalancing redox.

Products		CTC-*adhE2* (control)		CTC-*fdh-adhE2*	
		SF	SF, B12 & MVH	SF	SF, B12 & MVH
Cell growth (h^{-1})		0.18±0.01	0.16±0.0004	0.15±0.001	0.15±0.001
Biomass yield (g/g)		0.10±0.01	0.09±0.003	0.09±0.001	0.08±0.002
Concentration (g/L)	Butanol	3.18±0.09	6.14±0.05	8.83±0.02	12.34±0.02
	Butyrate	13.22±0.73	9.32±0.03	7.72±0.05	5.05±0.04
	Acetate	4.15±0.25	1.42±0.07	0.69±0.01	0.26±0.03
	Ethanol	0.11±0.04	0.25±0.02	0.24±0.01	0.28±0.07
Yield (g/g-glucose)	Butanol	0.05±0.01	0.11±0.003	0.16±0.002	0.23±0.002
	Butyrate	0.27±0.02	0.20±0.004	0.19±0.01	0.10±0.001
	Acetate	0.06±0.01	0.02±0.002	0.02±0.001	0.003±0.0001
	Ethanol	0.001±0.0005	0.003±0.0004	0.004±0.0002	0.004±0.0003
Productivity (g/L/h)	Butanol	0.12±0.01	0.14±0.01	0.17±0.002	0.26±0.01
	Butyrate	0.33±0.01	0.26±0.003	0.22±0.004	0.15±0.004
	Acetate	0.14±0.01	0.07±0.004	0.05±0.01	0.01±0.002
	Ethanol	0.006±0.001	0.008±0.0001	0.010±0.0003	0.011±0.0004

Notes: The average data in this table were calculated from the duplicated fermentations. Yield = g-product/g-glucose consumed, and selectivity = g-product/g-total products. SF: sodium formate, B12: vitamin B12, and MVH: methyl viologen hydrate.

Table 5.4. Recent progresses of butanol production with *C. tyrobutyricum.*

Strain	Characteristics	Mode	Carbon	Titer (g/L)	Yield (g/g)	Productivity (g/L/h)	Reference
CTC-*adhE2*	+*adhE2*, pCB102 replicon	Bottle	Glucose	2.5	0.15*	0.04*	Yu et al. (2012)
		Bottle	Glucose	2.6	0.14	0.03	This study
CTpM2	+*adhE2*, pBP1 replicon	Bottle	Glucose	6.5	0.24	0.20*	Yu et al. (2012)
		Bioreactor	Mannitol#	20.0#	0.33#	0.32#	Yu et al. (2012)
CTC-*fdh-adhE2*	+*fdh*+*adhE2*, pCB102 replicon	Bottle	Glucose	6.9	0.21	0.20	This study
		Bioreactor	Glucose	12.3	0.23	0.26	This study

Notes: *: These data were estimated from fermentation kinetic profile. #: Mannitol is an expensive substrate that significantly increases the production cost of biobutanol.

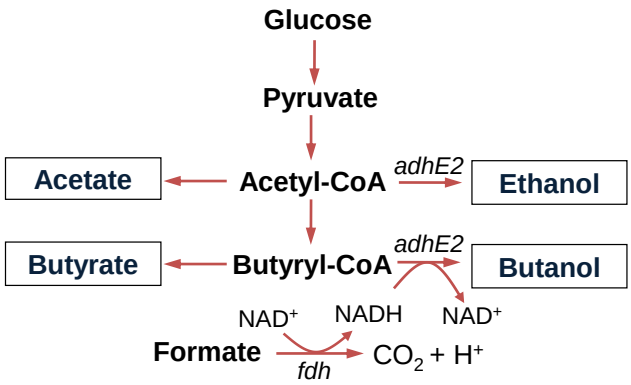

Figure 5.1. Butanol producing metabolic pathway in *C. tyrobutyricum*. The wild type CTC produces butyrate and acetate; mutant CTC-*adhE2* produces butanol and ethanol with carbon rebalance by overexpressing *adhE2* gene [16]; and mutant CTC-*fdh-adhE2* constructed in this study shows improved butanol production with redox rebalance by overexpressing *fdh* gene.

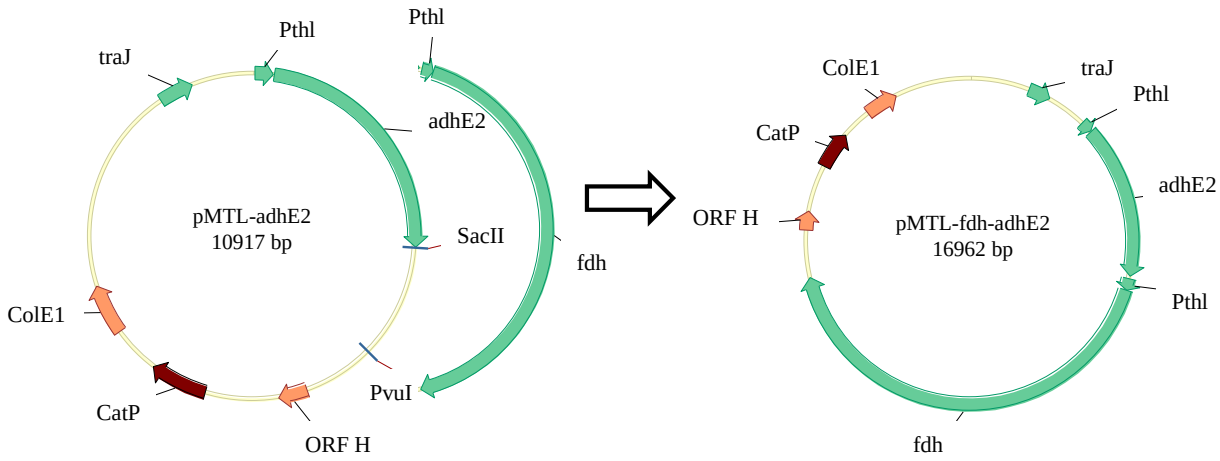

Figure 5.2. Plasmid construction. *ORF H*: *pCB102* replicon from *Clostridium butyricum*; *CatP*: chloramphenicol and thiamphenicol resistant gene; *ColE1*: *E. coli* replicon; *fdh*: formate dehydrogenase from *Moorella thermoacetica*; *Pthl*: promoter of thiolase from *Clostridium tyrobutyricum*; *traJ*: regulator of the F plasmid transfer operon; *adhE2*: bifunctional aldehyde/alcohol dehydrogenase (*adhE2*) from *Clostridium acetobutylicum*.

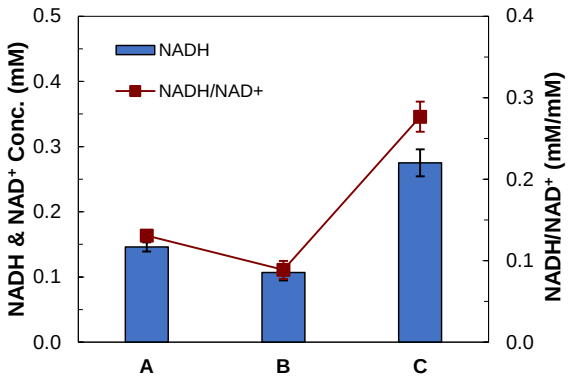

Figure 5.3. NADH assay. A: CTC wild type; B: CTC-*adhE2*; and C: CTC-*fdh-adhE2*. ■: mole ratio between NADH and NAD^+.

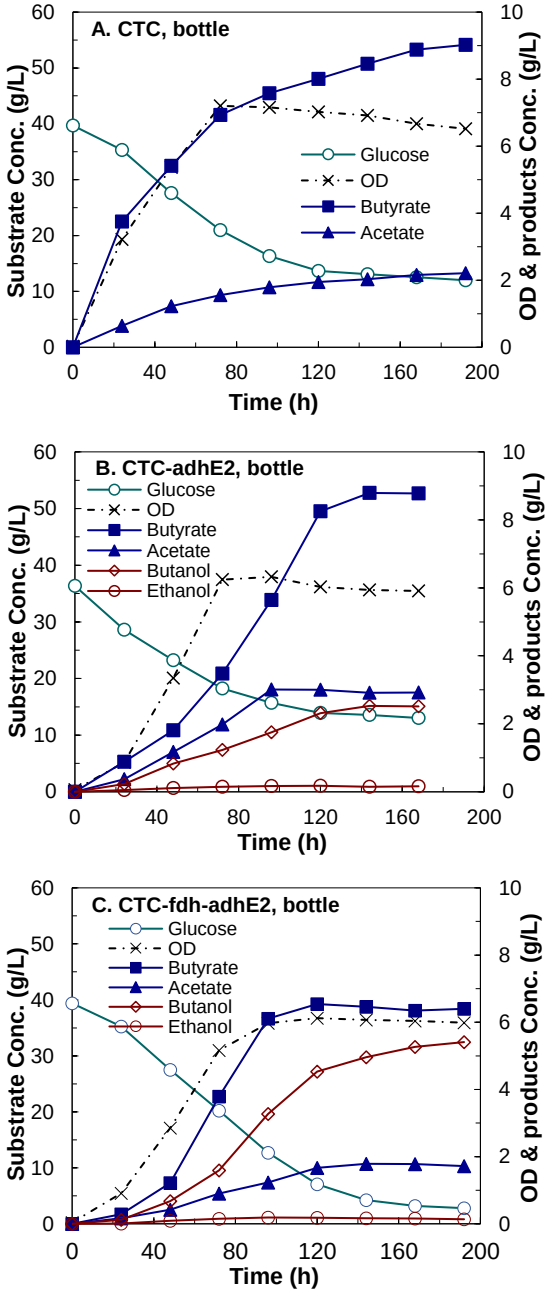

Figure 5.4. Kinetics of butanol fermentation by *C. tyrobutyricum* in serum bottles. A: CTC wild type; B: CTC-*adhE2*; and C: CTC-*fdh-adhE2*. ○: Glucose, ×: OD, ■: Butyrate, ▲: Acetate, ◊: Butanol, and ○: Ethanol.

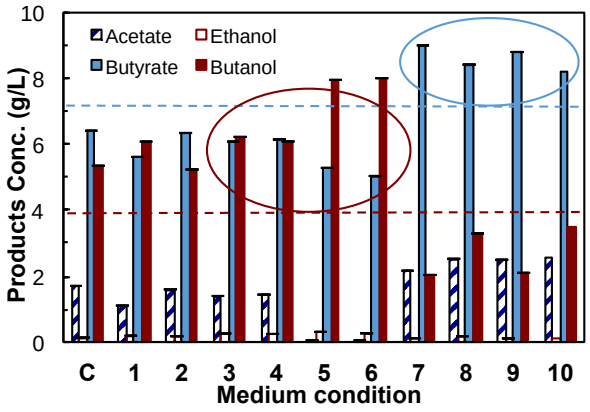

Figure 5.5. Medium components screening to rebalance carbon and redox flux of CTC-*fdh-adhE2*. C: control without medium supplement; 1: + sodium formate (formate); 2: + vitamin B12 (B12); 3: + methyl viologen hydrate (MVH); 4: + formate + B12; 5: + formate + MVH; 6: + formate + B12 + MVH; 7: + formate + vanadate; 8: + formate + acetamide; 9: + formate + B12 + vanadate; and 10: + formate + B12 + acetamide. □: Acetate, □: Ethanol, ■: Butyrate, and ■: Butanol. The data are the average of the duplicated fermentations in serum bottles.

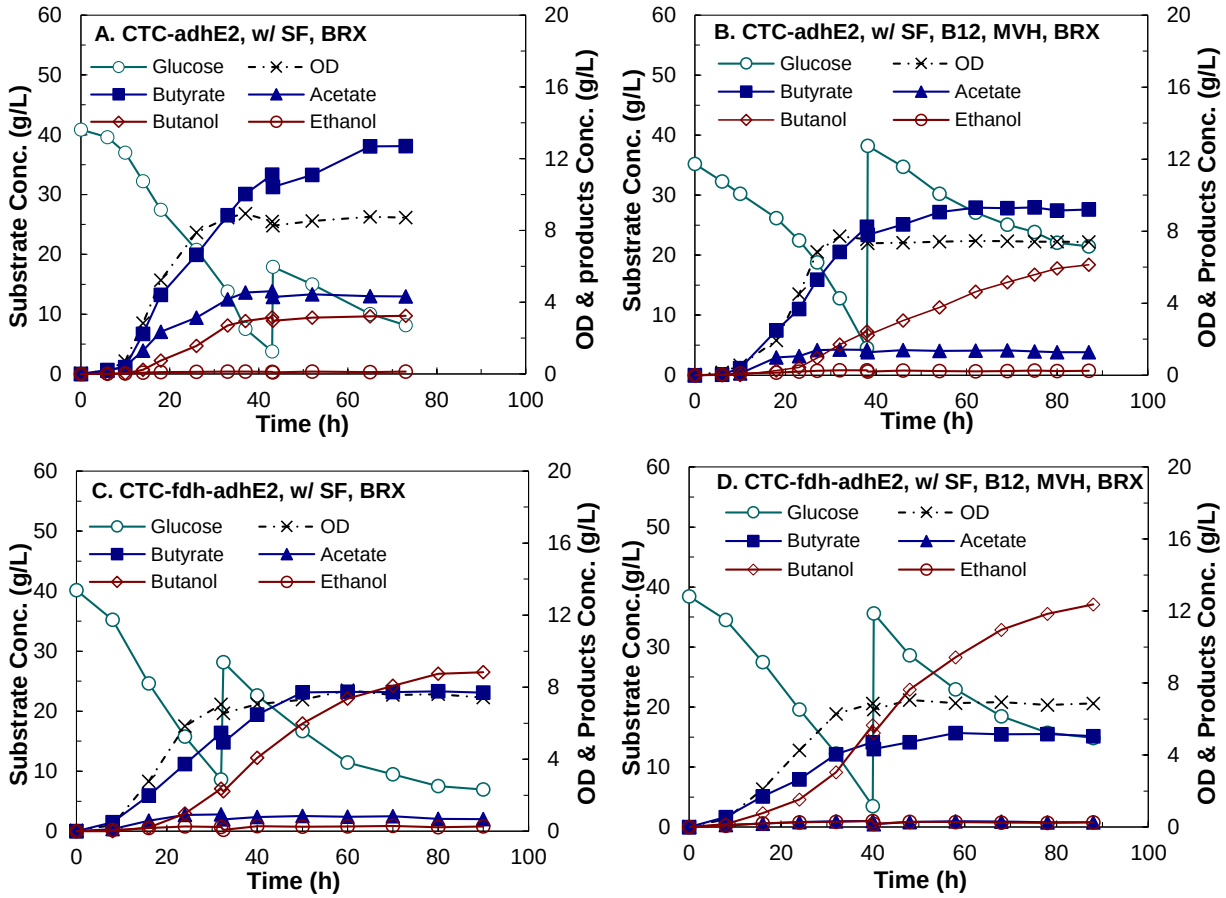

Figure 5.6. Kinetics of butanol fermentation by *C. tyrobutyricum* in 2-L bioreactors at pH 6.0, 37ºC, and 100 rpm. A: CTC-*adhE2* with sodium formate (SF); B: CTC-*adhE2* with sodium formate, vitamin B12 (B12) and methyl viologen hydrate (MVH); C: CTC-*fdh-adhE2* with SF; and D: CTC-*fdh-adhE2* with SF, B12 and MVH. ○: Glucose, ×: OD, ■: Butyric acid, ▲: Acetic acid, ◊: Butanol, and ○: Ethanol.

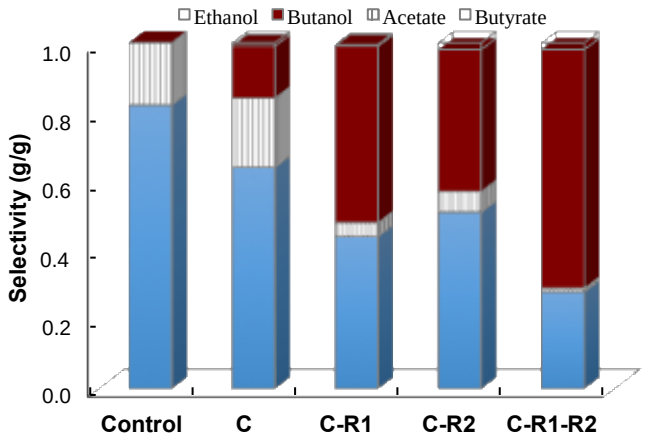

Figure 5.7. Improvement of n-butanol selectivity by rebalancing carbon and redox flux. Control: wild type CTC without sodium formate; C: CTC-*adhE2* without sodium formate; C-R1: CTC-*adhE2* with sodium formate, vitamin B12 and methyl viologen hydrate; C-R2: CTC-*fdh-adhE2* with sodium formate; and C-R1-R2: CTC-*fdh-adhE2* with sodium formate, vitamin B12 and methyl viologen hydrate.

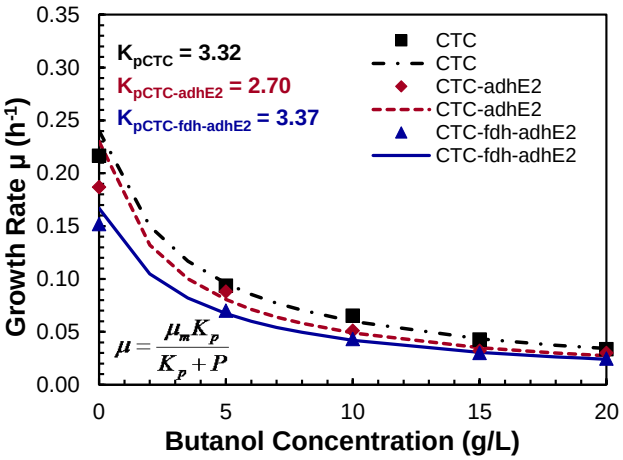

Figure 5.8. Butanol tolerance study of *C. tyrobutyricum* in serum bottles. ■: WT; -.-.-.-: WT; ♦: CTC-*adhE2*, ------: CTC-adhE2; ▲: CTC-*fdh-adhE2*, ——: CTC-*fdh-adhE2*.

CHAPTER 6

METABOLIC-PROCESS ENGINEERING

Abstract

Biobutanol is a sustainable and environmentally friendly fuel that has great potential to substitute for fossil fuel. To achieve high n-butanol production, the acidogenic *Clostridium tyrobutyricum* has been metabolically engineered though rebalancing carbon and redox. However, the effect of nitrogen source on butanol production by *C. tyrobutyricum* has not been evaluated. In this study, the metabolism of various amino acids by the butanol-producing mutant of *C. tyrobutyricum* was investigated. Firstly, the extracellular amino acids were titrated, showing that most amino acids in basal medium were depleted during butanol fermentation. Secondly, the comparative proteomics study indicated that the amino acid metabolism regulated butanol production via a TCA cycle and central carbohydrate pathway. Thirdly, both yeast extract and casamino acids were fed to free-cell fermentation, which increased butanol titer to 18.97 g/L from 14.32 g/L without nitrogen supplement. This study demonstrated that nitrogen supplement could be an effective factor to improve biobutanol production via manipulating amino acids metabolism in *C. tyrobutyricum*.

6.1 Introduction

Since the 1950s, significant attention has been drawn to biobutanol production using *Clostridia*, such as *C. acetobutylicum* and *C. beijerinckii*, [1,2,3]. Recently *C. tyrobutyricum* has widely been studied as a promising host cell for biobutanol production through advanced metabolic engineering and process development technology [4,5] due to its advantages of high butanol tolerance and high ratio of C4 to C2 produced from sugar [6,7]. Our previous study demonstrated that overexpression of formate dehydrogenase (*fdh*) from *Moorella thermoacetica* in *C. tyrobutyricum* significantly improved the butanol production from 3.18 to 12.34 g/L through increasing NADH accumulation [8]. Immobilized-cell fermentation with a fibrous-bed bioreactor (FBB) was performed to increase butanol production to 20 g/L via adaptation of the *C. tyrobutyricum* to be more tolerant to butanol [9].

It has been reported that the addition of amino acids increased the solvent ratio to higher butanol and ethanol production in *C. acetobutylicum* [10]. Another study showed that single addition of tryptophan, glutamine, asparagine, cysteine, and histidine increased cell growth of *C. beijerinckii* [11]. Extra feeding of yeast extract helped the shift to the solventogenic phase from the acidogenic phase by *C. acetobutylicum* using cassava as a substrate [12]. However, most recent butanol production research in *C. tyrobutyricum* has only focused on the carbohydrate metabolic pathway.

Multiple proteomics studies of *Clostridia* have also been performed recently and made it possible to have a comprehensive understanding of amino acid metabolism in butanol production. High butanol tolerance and butanol yield mutant of *C. acetobutylicum* was reported to develop a mechanism to slow down amino acid metabolism and protein synthesis to adapt to butanol challenge, compared to the wild type [13]. A metabolically engineered butanol producing mutant

of *E.coli* also had a downregulation of the enzymes in an amino acid mechanism [14]. However, effect of butanol stress on amino acid mechanisms has not been investigated in *C. tyrobutyricum*.

The objective of this study was to investigate the relationship between amino acids and butanol synthesis metabolism in *C. tyrobutyricum* and to improve biobutanol production via extra amino acids feeding in the metabolically engineered *C. tyrobutyricum* butanol producing strain. The expression levels of key enzymes used in amino acid metabolism and transportation were analyzed and compared in *C. tyrobutyricum*. Process development was conducted to supply extra nitrogen source (yeast extract or casamino acid) during the fermentation.

6.2 Materials and Methods

6.2.1 Strain, culture and Media

Two *C. tyrobutyricum* ATCC 25755 strains, wild type and butanol-producing mutant, were investigated in this research. The wild type strain was purchased from ATCC, and the butanol producing mutant was obtained from the Yang lab [7]. The seed cultures of these microorganisms were stocked anaerobically at –80 ^{o}C in Reinforced Clostridial Medium (RCM; Difco, Kansas City, MO, USA) supplemented with 30 μg/mL of erythromycin (Em, Alfa Aesar, Ward Hill, MA, USA) and 30 μg/mL of thiamphenicol (Tm, Alfa Aesar) for the butanol producing mutant. The cells were cultivated in the modified Clostridial Growth Medium (CGM) for fermentation in the bioreactor and serum bottle, [11, 15]. All chemicals were purchased from Sigma-Aldrich (St. Louis, MO, USA), unless noted otherwise.

6.2.2 Fermentation Kinetics

Kinetics studies of the fed-batch fermentation by butanol producing mutant with different types of amino acid sources additions were performed in a stirred-tank bioreactor (FS-01-A; Major science, Saratoga, CA, USA). Concentrated yeast extract or casamino acid (200 g/L) stock

solutions were fed into the bioreactor to a final concentration of 5 g/L yeast extract or casamino acid, when the 80% amino acids were consumed. Fermentation setup, operation, and sampling were performed as reported previously [8]. Fermentations were duplicated and the means and standard deviations were calculated and presented.

6.2.3 Fermentation Products Titration

The cell density was analyzed by measuring the optical density of cell suspension at 600 nm using a spectrophotometer (Biomate3; Thermo Fisher Scientific Inc, Hudson, NH, USA). High performance liquid chromatography (HPLC, Shimadzu, Columbia, MD, USA) was used to analyze the concentrations of fermentation substrates and products, including glucose, butanol, butyrate, acetate and ethanol in Section 2.2 [8]. The glucose concentration was monitored daily using a YSI 2700 Select Biochemistry Analyzer (YSI Life Sciences, Yellow Springs, OH, USA) and used to determine the feeding strategy and to maintain the glucose concentration higher than 10 g/L.

6.2.4 Amino Acid Analysis

Amino acid samples collected from the supernatant were prepared in 0.2 N borate buffer (pH 10.0), 15 mM 9-fluorenylmethyl-chloroformate solution, and acetonitrile with the ratio of 1:2:1:1. It took about 5 minutes to finish the derivatization reaction. The concentrations of free amino acid in fermentation broth, including arginine, serine, aspartic acid, glutamic acid, threonine, glycine, alanine, proline, methionine, valine, cysteine, histidine, lysine, and tyrosine, were analyzed using high performance liquid chromatography (HPLC, Shimadzu, Columbia, MD) with an amino acid analysis column (Restek, Raptor™ C18 LC Columns, Bellefonte, PA) and a UV detector (Shimadzu SPD-20A). The amino acid concentrations were measured under the following conditions: reverse column Raptor™ C18 3.0 x 100 mm; temperature 30 ^{o}C; flow rate 0.8 mL/min; Eluent A 0.1% formic acid and 20 mM ammonium formate in distilled deionized (dd) water; Eluent

B 0.1% formic acid and 10 mM ammonium formate in 90:10 acetonitrile: dd water; UV/Vis 265 nm.

6.2.5 Proteomics: GeLC-MS/MS

The cells of wild type and butanol producing mutant were collected at 30 mins post inoculation for baseline evaluation. To prepare proteomics samples, the fermentations were sampled in mid-log phase and early-stationary phase, i.e. 11.0 h (wild type) and 29 h (butanol producing mutant without amino acid feeding). At sampling points, the values of OD600 were 3.94 (wild type) and 4.51 (butanol producing mutant without amino acid feeding). Protein extraction, 1-D SDS-PAGE (sodium dodecyl sulfate-polyacrylamide gel electrophoresis) gel electrophoresis, digestion, and 1D reverse phase nLC-ESI-MS (liquid chromatography-electrospray ionization-tandem mass spectrometry) were performed as previously reported in Section 2.2 [6].

6.3 Results

6.3.1 Butanol Fermentation in Wild Type and Butanol Producing Mutant of *C. tyrobutyricum*

The free-cell fermentations of wild type and butanol producing mutant were performed using a 2-L bioreactor and the proteomics samples were taken during the middle-log phase. As shown in Fig. 6.1, wild type produced 18.27 g/L butyrate and 3.5 g/L acetate. Compared to wild type, butanol producing mutant produced significantly less butyrate (7.1 g/L) and acetate (0.87 g/L). However, after completing the solvent biosynthesis pathway through introducing bifunctional aldehyde/alcohol dehydrogenase (*adhE2*) into the *C. tyrobutyricum*, the solvent producing mutant produced butanol at a concentration of 14.03 g/L and ethanol at 1.03 g/L. In the condition that the fermentation was performed only in basal medium without extra amino acid feeding, more than 90% free amino acids were consumed by the end of the fermentation. Therefore, it is necessary to

evaluate the feasibility of improving butanol production via optimizing the extra amino acids feeding strategy during the fermentation.

6.3.2 Comparative Proteomics Related to Amino Acid Mechanism in Wild Type and butanol Producing Mutant

In order to understand the effect of butanol production on amino acid mechanism, the comparative proteomics study was performed between wild type and the butanol producing mutant. The data involved in the tricarboxylic acid cycle (TCA) (Fig. 6.2) and amino acids (AA) (Fig. 6.3) metabolism are described as the mass spectra normalized by the total proteins in the same sample and summarized in Table 6.1 (TCA) and Table 6.2 (AA). In the TCA cycle, the expression of pyruvate carboxylase in the butanol producing strain, which catalyzes the reaction from pyruvate to oxaloacetate, was decreased significantly from 108 SC to 1 SC, compared to wild type (Fig. 6.4). There was more carbon flux to butyryl-CoA from pyruvate in the butanol producing strain, but more carbon flux to oxaloacetate from pyruvate in the wild type. Similar results were obtained in malate dehydrogenase (5 SC in wild type vs 0 SC in the butanol producing strain) and fumarate hydratase (6 SC in wild type vs 0 SC in the butanol producing strain), which participated in the conversion from oxaloacetate to fumarate with malate as an intermediate. However, aconitate hydratase, which was involved in the reaction from citrate to α-ketoglutarate, had a 2.42-fold higher expression in the butanol producing strain, compared with the wild type.

The key proteins catalyzing amino acid biosynthesis and catabolization were also analyzed in our study in *C. tyrobutyricum*. The enzymes involved in the reaction between the TCA-cycle chemicals and amino acids were summarized in Table 6.1. Most enzymes had similar or lower mass spectral counts in wild type and the butanol producing strain. This result explained that more amino acids supplied carbon source to TCA cycle. As we described in Chapter 3.3, valine,

threonine, aspartate, alanine, proline, tyrosine were identified as the important enzymes in butanol production. The enzymes correlated to these six amino acids were summarized in Table 6.2. It was found that in the mid-log phase, most enzymes had significantly lower expressions in the butanol producing strain, due to the large amount of amino acid consumption and less substrates left for the reaction.

6.3.3 Extra Amino Acid Feeding in Butanol Production

In cellular metabolism, amino acids were involved in the cell growth mechanism in *Clostridia*. As demonstrated in Chapter 3.2, the amino acid mechanism was also significantly affected by butanol production in *C. tyrobutyricum*. In this study, we introduced extra yeast extract into free-cell fermentation of the butanol producing strain first. In order to avoid interference of other growth factors in yeast extract, we further evaluated the casamino acids with a high proportion of free amino acids.

As presented in Fig. 6.5 and Table 6.3, three conditions were evaluated, including no amino acid feeding, extra yeast extract feeding, and extra casamino acid feeding. Fig. 6.3 and Table 6.4 showed that the butanol producing strain grew with a similar log phase of 10~15 hours after inoculation and growth rate of 0.15~0.19 in all three conditions, whereas the butanol producing strain with extra yeast extract and casamino acid feeding strategy at the mid-log phase reached a higher maximum OD_{600} of 9.5, compared to a maximum OD_{600} of 7.0 without extra amino acid feeding conditions. It is obvious that biomass yield of the butanol producing strain increased from 0.08 to 0.12, with a 1.5-fold improvement. Another interesting phenomenon was that the cell density of the butanol producing strain decreased after early stationary phase in no extra amino acid feeding condition, which did not occur with the extra amino acid feeding strategy.

Since the same seed culture preparation and inoculation strategy were used in all three fermentation conditions, the higher maximum OD_{600} and no cell density decrease after entering the stationary phase might be attributed to an extra amino acid feeding strategy. Recently a similar phenomenon of the biomass increase through extra yeast extract feeding has been reported in *C. beijerinckii* fermentation [16].

Besides the influence on cell growth, the amino acids are important metabolic intermediates in butanol fermentation. As summarized in Table 6.3, the butanol concentrations were 14.52 g/L, 18.80 g/L, and 18.94 g/L by the butanol producing strain without extra amino acid feeding, the butanol producing strain with yeast extract feeding, and the butanol producing strain with casamino acid, respectively. The fermentation data showed that butanol producing strain with extra nitrogen source feeding produced as much as 1.30-fold of butanol, compared with the same strain without extra nitrogen source feeding. However, butyrate production decreased to 5.21-5.35 g/L with extra yeast extract or casamino acid feeding. It was noted that ethanol and acetate production did not have an obvious change in three conditions. These results revealed that the extra amino acid feeding strategy redirected more carbon flux to the production of butanol.

The yields, productivity, and butanol selectivity were also evaluated in three conditions to further investigate effects of different amino acid feeding strategies on carbon redistribution. The yields and productivity of butanol through optimizing the nitrogen source feeding strategy (~0.31 g/g-glucose & ~0.27 g/L/h) were also much higher than the control (0.20 g/g-glucose & 0.18 g/L/h without extra amino acid feeding). In addition, the selectivity of butanol (total solvent) was 0.72 g/g (0.75 g/g), 0.71 g/g (0.74 g/g), and 0.60 g/g (0.63 g/g) at the conditions of extra yeast extract feeding, extra casamino acid feeding, and control, respectively.

In this study, the extra yeast extract feeding increased the butanol production. Extra feeding of casamino acids with a high proportion of free amino acids also improved the butanol production in *C. tyrobutyricum* fermentation. These results indicated that extra amino acid feeding shifted carbon flux to butanol from butyrate in butanol producing strain fermentation.

6.3.4 Amino Acid Analysis

Nitrogen sources are related to cell growth and butanol production. It was reported previously that excess nitrogen source was necessary in production medium for butanol fermentation with *C. beijerinckii*, *C. acetobutylicum*, and *C. saccharobutylicum* [17,18,19]. Therefore, it is important to recognize the relationship between butanol production and nitrogen addition in *C. tyrobutyricum*. In our study, extra yeast extract or casamino acid feeding influenced the cell growth and butanol production significantly. That should be attributed to rebalance of carbon and redox regulated by amino acid metabolism.

We measured the major amino acid concentration accumulated in fermentation broth before and after addition of yeast extract and casamino acids, to figure out the reasonable explanation of butanol production improvement after extra amino acid feeding in the fermentation. With extra yeast extract feeding, seven types of amino acid extracellular concentration (alanine, lysine, proline, serine, threonine, tyrosine, valine, and, aspartate) were decreased by 90% in the fermentation broth, compared with total feeding amount of each amino acid. However, five types of amino acids with obvious changes (more than 90% consumed), including alanine, lysine, serine, threonine, tyrosine, and, aspartic acid were identified in the fermentation with extra casamino acids feeding.

As described before, amino acid metabolism is correlated to carbon and redox rebalance. It has been reported that certain amino acid additions are favorable for butanol generation. Other studies

suggested that threonine, lysine, and aspartate from the aspartic acid family, as well as tyrosine from aromatic family, enhance butanol synthesis [16,20]. The first metabolite in the core pathway (Fig. 6.1), pyruvate, was correlated with valine, tyrosine and alanine. These three amino acids could produce pyruvate to supply carbon source and synthesize the reducing power, as shown in equations of the complementary files.

6.4 Discussion

6.4.1 Understanding of Amino Acid Metabolism via Comparative Proteomics

It has been previously established that *C. acetobutylicum* had a bifurcated TCA cycle [21]. However, this is the first study to establish the TCA cycle enzyme file in *C. tyrobutyricum*. As described in section 2.1, most of the enzymes to suppport the TCA cycle were identified in *C. tyrobutyricum*. Similar to *C. acetobutylicum* [22], the TCA cycle of C. *tyrobutyricum* was also incomplete, because of the absence of the enzymes involved in the conversions from oxaloacetate to citrate, from α-ketoglutarate to succinyl-CoA, and from oxaloacetate to citrate. The lacing of these enzymes could be caused by no existence of relational functional enzymes or incomplete annotation of the published genome sequence of *C. tyrobutyricum*.

It was reported that the chemicals participated in the TCA cycle and served as the intermediates in the reversible reaction between the carbon sources and amino acids [23]. Therefore, it is meaningful to identify the enzymes catalyzing the reaction between them and establish the relationship between the TCA cycle and amino acid pathway. Lower expression of enzymes in the TCA cycle in the butanol producing strain were correlated to more carbon flux flowing to butanol, which demonstrated that the amino acids metabolism had a significant influence on the core metabolic pathway through regulating the TCA cycle in *C. tyrobutyricum*.

6.4.2 Effect of Amino Acid Addition on Butanol Production

In previous studies, it was reported that extra amino acid feeding promoted the shift from the acidogenic phase to the solventogenic phase and regulated the butanol production in *C. acetobutylicum* [24]. Our previous metabolite analysis study also demonstrated that a couple of amino acids had an important influence on the metabolite profiles in the *C. tyrobutyricum* fermentation [6], which indicated that the fermentation feeding strategy could be optimized through supplying amino acids during the fermentation to increase butanol production. Another study showed amino acid biosynthesis and catabolism were correlated with pyruvate, ATP and NADH consumption [25], which meant limited carbon flux, energy, and reducing power can be directed toward butanol biosynthesis. Therefore, it was assumed that addition of amino acids in *C. tyrobutyricum* improved the butanol production.

In order to confirm our assumption, cell process engineering integrating nitrogen feeding strategy, amino acid biosynthesis and catabolism related proteomics profiling establishment, and amino acid analysis were conducted in this study. The butanol producing mutant was used as the target host cell for butanol production. The control condition was no extra amino acids feeding with the same strain during the fermentation. Compared to the control condition, extra yeast extract and casamino acid feeding increased both butanol yield and productivity by more than 1.4-fold. Our results also demonstrated that extra amino acids supplying to redistribute carbon flux were important in the butanol fermentation.

Another essential phenomenon is that acetate and ethanol production did not change but butyrate production was reduced. This result suggested that the improved butanol production came from carbon rebalance from both butyrate and amino acid to butanol. It might be attributed to more ATP and NADH supplying to meet the requirement from the conversion of the butyryl-CoA to

butanol. Therefore, the selectivity of butanol increased with the amino acid feeding strategy to benefit further separation of butanol.

6.4.3 How to Improve the Butanol Production

In order to meet the requirement of industry production, the cost of the butanol production needs to be paid attention to. Extra amino acid feeding strategy increased the butanol production, but it also increased the prime investment of the butanol fermentation. Therefore, we fed the yeast extract and casamino acid instead of the single amino acids. Our results demonstrated extra amino acids feeding increased butanol titer, yield, and productivity by more than 1.35 fold. In a future study, we will also investigate how to optimize the basal medium with our amino acid study.

Our study also demonstrated that the amino acid mechanism were related to the consumption of NADH. Therefore, metabolic engineering and proecess strategies to increase the redox pool in the fermentation could also be applied to increase the butanol production. Our other study demonstrated that redox engineering can be applied to improve the butanol production by 2.72-fold through introducing heterologous formate dehydrogenase (*fdh*) into *C. tyrobutyricum* to enhance intracellular NADH pool [8].

In this study, the butanol titer was lower than 20 g/L. Our previous study showed that *C. tyrobutyricum* retained less than 20% of their maximum growth rate at 20 g/L of butanol. Therefore, it is necessary to increase the tolerance of *C. tyrobutyricum* to improve the butanol production. The fibrous-bed bioreactor (FBB) designed for immobilized-cell fermentations had a significant influence on the production of butyrate and cell growth by concentrating the cell density and adapting cell cultures with a high tolerance against the butyrate toxicity [24]. Compared with free-cell fermentation, butyrate production was improved from 20 g/L to 50 g/L with *C. tyrobutyricum* in the immobilized-cell fermentation [26]. Furthermore the immobilized-cell

fermentations study will be performed with the extra amino acid feeding strategy to improve the butanol production.

6.5 Conclusions

In this study, enzymes expression correlated to amino acids biosynthesis and catabolization have obviously changed between wild type and the butanol producing mutant. Key amino acids with significantly changes during the fermentation were identified. We demonstrated that the extra amino acid feeding strategy could improve butanol production in *C. tyrobutyricum*. Both the yield and productivity of butanol were significantly improved by supplying enough yeast extract or casamino acids.

6.6 References

[1] J. Lee, Y.S. Jang, S.J. Choi, J.A. Im, H. Song, J.H. Cho, E.T. Papoutsakis, G.N. Bennett, S.Y. Lee. "Metabolic engineering of *Clostridium acetobutylicum* ATCC 824 for isopropanol-butanol-ethanol fermentation". Appl. Environ. Microbiol., vol. 78, pp. 1416-1423, 2012.

[2] X. Kong, A. He, J. Zhao, H. Wu, J. Ma, C. Wei, W. Jin, M. Jiang. "Efficient acetone–butanol–ethanol (ABE) production by a butanol-tolerant mutant of *Clostridium beijerinckii* in a fermentation–pervaporation coupled process". Biochem. Eng. J., vol. 105, pp. 90-96, 2016.

[3] D.T. Jones, D.R. Woods. "Acetone-butanol fermentation revisited". Microbiol. Rev., vol. 50, pp. 484–524, 1986.

[4] J. Ou, C. Ma, N. Xu, Y. Du, X.M. Liu. "High butanol production by regulating carbon, redox and energy in Clostridia". Front. Chem. Sci. Eng., vol. 9, pp. 317-323, 2015.

[5] X. Liu, Y. Zhu, S.T. Yang. "Butyric acid and hydrogen production by *Clostridium tyrobutyricum* ATCC 25755 and mutants". Enzyme Microb. Technol., vol. 38, pp. 521-528, 2006.

[6] C. Ma, K. Kojima, N. Xu, J. Mobley, L. Zhou, S.T. Yang, X.M Liu. "Comparative proteomics analysis of high n-butanol producing metabolically engineered *Clostridium tyrobutyricum*". J. Biotechnol., vol. 193, pp. 108–119, 2015.

[7] M. Yu, Y. Zhang, I.C. Tang, S.T. Yang. "Metabolic engineering of *Clostridium tyrobutyricum* for n-butanol production". Metab. Eng., vol. 13, pp. 373-82, 2011.

[8] C. Ma, J. Ou, N. Xu, J.L. Fierst, S.T. Yang, X.M. Liu. "Rebalancing redox to improve biobutanol production by *Clostridium tyrobutyricum*". Bioengineering, vol. 3, 2015.

[9] M. Yu, Y. Du, W. Jiang, W.L. Chang, S.T. Yang, I.C. Tang, "Effects of different replicons in conjugative plasmids on transformation efficiency, plasmid stability, gene expression and n-butanol biosynthesis in *Clostridium tyrobutyricum*". Appl. Microbiol. Biotechnol., vol. 93, pp. 881-889, 2012.

[10] E. Masion, J. Amine, R. Marczak. "Influence of amino acid supplements on the metabolism of *Clostridium acetobutylicum*". FEMS Microbiol. Lett., vol. 43, pp. 269-274, 1987.

[11] H. Dong, W. Tao, Z. Dai, L. Yang, F. Gong, Y. Zhang, Y. Li. "Biobutanol". Adv. Biochem. Eng. Biotechnol., vol. 128, pp. 85–100, 2012.

[12] X. Li, Z. Li, J. Zheng, Z. Shi, L. Li. "Yeast extract promotes phase shift of bio-butanol fermentation by *Clostridium acetobutylicum* ATCC824 using cassava as substrate". Bioresour. Technol., vol. 125, pp. 43-51, 2012.

[13] S. Mao, Y. Luo, G. Bao, Y. Zhang, Y. Li, Y. Ma. "Comparative analysis on the membrane proteome of *Clostridium acetobutylicum* wild type strain and its butanol-tolerant mutant". Mol. Biosyst., vol. 7, pp. 1660-1677, 2011.

[14] B.J. Rutherford, R.H. Dahl, R.E. Price, H.L. Szmidt, P.I. Benke, A. Mukhopadhyay, J.D. Keasling. "Functional genomic study of exogenous n-butanol stress in *Escherichia coli*". Appl. Environ. Microb., vol. 76, pp. 1935-1945, 2010.

[15] S.W. Jones, B.P. Tracy, S.M. Gaida, E.T. Papoutsakis. “Inactivation of *sigmaF* in *Clostridium acetobutylicum* ATCC 824 blocks sporulation prior to asymmetric division and abolishes *sigmaE* and *sigmaG* protein expression but does not block solvent formation”. J. Bacteriol., vol. 193, pp. 2429–2440, 2011.

[16] H. Heluane, M.R. Evans, S.F. Dagher, J.M. Bruno-Barcena. “Meta-analysis and functional validation of nutritional requirements of solventogenic clostridia growing under butanol stress conditions and coutilization of D-glucose and D-xylose”. Appl. Environ. Microb., vol. 77, pp. 4473–4485, 2011.

[17] J.C. Gottschal, J.G. Morris. “Non-production of acetone and butanol by *C. acetobutylicum* during glucose- and ammonium-limitation in continuous culture”. Biotech. Lett., vol. 3, pp. 525-530, 1982.

[18] W. Andersch, H. Bahl, G. Gottschalk. “Acetono-butanol production by *Clostridium acetobutylicum* in an ammonium-limited chemostat at low pH values”. Biotech. Lett., vol. 4, pp. 29-32, 1982.

[19] S. Long, D.T. Jones, D.R. Woods. “Initiation of solvent production, clostridial stage and endospore formation in *Clostridium acetobutylicum* P262”. Appl. Microbiol. Biotechnol., vol. 20, pp. 256-261, 1984.

[20] E. Masion, J. Amine, R. Marczak. “Influence of amino acid supplements on the metabolism of *Clostridium acetobutylicum*”. FEMS Microbiol. Lett., vol. 43, pp. 269–274, 1987.

[21] S.B. Crown, D.C. Indurthi, W.S. Ahn, J. Choi, E.T. Papoutsakis, M.R. Antoniewicz. “Resolving the TCA cycle and pentose-phosphate pathway of *Clostridium acetobutylicum* ATCC 824: Isotopomer analysis, in vitro activities and expression analysis”. Biotechnol. J., vol. 6, pp. 300-305, 2011.

[22] D. Amador-Noguez, X.J. Feng, J. Fan, N. Roquet, H. Rabitz, J.D. Rabinowitz. “Systems-level metabolic flux profiling elucidates a complete, bifurcated tricarboxylic acid cycle in *Clostridium acetobutylicum*”. J. Bacteriol., vol. 192, pp. 4452-4461, 2010.

[23] R.S. Senger, E.T. Papoutsakis. “Genome-scale model for *Clostridium acetobutylicum*: Part II. Development of specific proton flux states and numerically determined sub-systems”. Biotechnol. Bioeng., vol. 101, pp. 1053-1071, 2008.

[24] C. Ma, J. Ou, M. Miller, S. McFann, X.M. Liu. “High production of butyric acid by *Clostridium tyrobutyricum* mutant”. Front. Chem. Sci. Eng., vol. 9, pp. 369-375, 2015.

[25] D. Amador-Noguez, I.A. Brasg, X.J. Feng, N. Roquet, J.D. Rabinowitz. “Metabolome remodeling during the acidogenic-solventogenic transition in *Clostridium acetobutylicum*”. Appl. Environ. Microbiol., vol. 77, 7984-7997, 2011.

[26] X. Liu, S.T. Yang. “Kinetics of butyric acid fermentation of glucose and xylose by *Clostridium tyrobutyricum* wild type and mutant”. Process Biochem., vol. 41, pp. 801–808, 2006.

Table 6.1. Comparison of TCA-related proteins among *C. tyrobutyricum* WT and butanol producing mutant.

Function	Protein			Spectral Count	
	UniRef ID	Name	Probability	WT	Mutant
TCA Cycle	GB000474	Pyruvate carboxylase (*pcb*)	1	108	1
	GB001253	Malate dehydrogenase (*mdh*)	0.99	5	0
	GB002348	Fumarate hydratase (*fum*)	0.99	6	0
	GB002389	Isocitrate dehydrogenase (*idh*)	1	38	6
	GB002388	Aconitate hydratase (*aco*)	1	84	204
AA to TCA	GB002440	Aromatic aminotransferase (*arat*)	1	6	10
	GB001127	Aldehyde oxidase (*aox*)	1	2	2
	GB002426	Branched-chain amino acid aminotransferase (*bct*)	1	103	111
	GB001523	Acyl-CoA dehydrogenase (*acad*)	1	64	110
	GB000459	3-hydroxyacyl-CoA dehydrogenase (*hdah*)	0.99	180	480
	GB001492	D-alanine aminotransferase (*alt*)	1	14	6
	GB000826	Aspartate aminotransferase (*ast*)	1	27	36
	GB001191	Cysteine desulfurase (*iscs*)	0.99	36	41
	GB000904	L-serine dehydratase (*sdh*)	0.99	4	5
	GB002084	Serine hydroxymethyltransferase (*shmt*)	1	115	109
	GB002494	Glutamate dehydrogenase (*gldh*)	1	72	62
	B1QVS1	Glutamine amidotransferase (*gat*)	0.98	9	1

Table 6.2. Comparison of representative amino acid mechanism proteins among *C. tyrobutyricum* WT and butanol producing mutant.

Function	Protein			Spectral Count	
	UniRef ID	Name	Probability	WT	Mutant
Valine	GB001200	Acetolactate synthase (*als*)	0.99	13	0
	GB001201	Ketol-acid reductoisomerase (*kari*)	1	87	116
	GB001199	Dihydroxy-acid dehydratase (*dhad*)	1	42	68
	GB002426	Branched-chain amino acid aminotransferase (*bct*)	1	103	111
Threonine	GB001260	Aspartokinase (*ask*)	1	44	0
	GB000338	Aspartate-semialdehyde dehydrogenase (*asd*)	0.99	75	0
	GB001700	Homoserine dehydrogenase (*hsd*)	0.99	7	3
	GB000290	Homoserine kinase (*hsk*)	0.99	1	0
	GB001885	Threonine synthase (*thrc*)	1	37	27
Aspartate	GB000474	Pyruvate carboxylase (*pcb*)	1	108	1
	GB000826	Aspartate aminotransferase (*ast*)	1	27	36
Alanine	GB001492	D-alanine aminotransferase (*alt*)	1	14	6
	GB001496	Alanine racemase (*alr*)	0.99	2	0
Proline	GB002590	Glutamate 5-kinase (*nagk*)	0.90	12	0
	GB001772	Glutamate-5-semialdehyde dehydrogenase (*gpr*)	1	24	2
	GB000264	Pyrroline-5-carboxylate reductase (*pcr*)	0.99	23	28
Tyrosine	GB002156	3-dehydroquinate synthase (*aroB*)	0.99	16	0
	GB000984	Shikimate 5-dehydrogenase (*sdh*)	0.99	10	0
	GB001243	3-phosphoshikimate 1-carboxyvinyltransferase (*epsp*)	0.99	14	0
	GB001244	Chorismate synthase (*aroC*)	1	33	34
	GB001245	Prephenate dehydratase (*pdt*)	0.99	10	0
	GB002440	Aromatic aminotransferase (*arat*)	1	6	10

Table 6.3. Comparison of cell growth, final product concentrations, and yield from *C. tyrobutyricum* butanol producing mutant by proteomics with process development.

Condition		No Feeding	YE Feeding	CA Feeding
Cell growth (h^{-1})		0.15±0.002	0.19±0.001	0.19±0.002
Biomass yield (g/g)		0.08±0.005	0.12±0.002	0.11±0.004
Concentration (g/L)	Butanol	14.32±0.41	18.80±0.20	18.94±0.18
	Butyrate	7.15±0.03	5.35±0.03	5.21±0.31
	Acetate	1.21±0.01	0.41±0.06	0.52±0.02
	Ethanol	1.03±0.01	0.88±0.01	0.73±0.04
Yield (g/g-glucose)	Butanol	0.20±0.01	0.31±0.01	0.30±0.02
	Butyrate	0.14±0.001	0.09±0.02	0.10±0.02
	Acetate	0.008±0.002	0.004±0.001	0.005±0.0001
	Ethanol	0.011±0.0004	0.008±0.0001	0.009±0.002
Productivity (g/L/h)	Butanol	0.19±0.004	0.27±0.001	0.26±0.01
	Butyrate	0.16±0.003	0.12±0.003	0.13±0.01
	Acetate	0.05±0.003	0.04±0.005	0.03±0.001
	Ethanol	0.02±0.002	0.02±0.004	0.01±0.001
Selectivity (g/g-total product)	Butanol	0.60±0.01	0.72±0.02	0.71±0.02
	Butyrate	0.31±0.03	0.24±0.01	0.25±0.01
	Acetate	0.06±0.006	0.01±0.003	0.01±0.003
	Ethanol	0.03±0.002	0.03±0.001	0.03±0.002

Note:

1) The data in this form is the average of duplicated fermentation.
2) Yield = g-product /g-glucose consumed. Selectivity = g-product /g-total products.
3) YE, yeast extract; CA, casamino acid.

Table 6.4. Comparison of amino acid consumption from *C. tyrobutyricum* butanol producing mutant with process development.

	w/o YE		w/ YE		w/ CA	
	(g/L)	**(%)**	**(g/L)**	**(%)**	**(g/L)**	**(%)**
Arginine	0.397	99.25	0.498	81.64	0.459	59.61
Serine	0.297	99.01	0.247	88.21	0.259	76.18
Aspartate	1.280	98.46	1.749	97.17	1.966	93.62
Glutamate	1.054	95.45	1.134	88.28	1.821	74.38
Threonine	0.793	99.12	1.092	99.09	1.084	90.33
Glycine	0.399	99.75	0.382	76.40	0.481	68.71
Alanine	1.975	98.65	3.067	98.94	2.833	94.33
Proline	0.049	99.38	0.059	99.33	0.0594	84.86
Methionine	0.021	70.03	0.027	67.50	0.025	0.625
Valine	0.496	99.24	0.531	98.39	0.653	76.47
Cysteine	0.098	98.03	0.042	80.77	0.087	66.92
Histidine	0.362	90.05	0.393	79.59	0.360	61.017
Lysine	0.078	98.25	0.083	92.22	0.112	91.67
Tyrosine	0.129	99.53	0.179	95.21	0.211	91.31

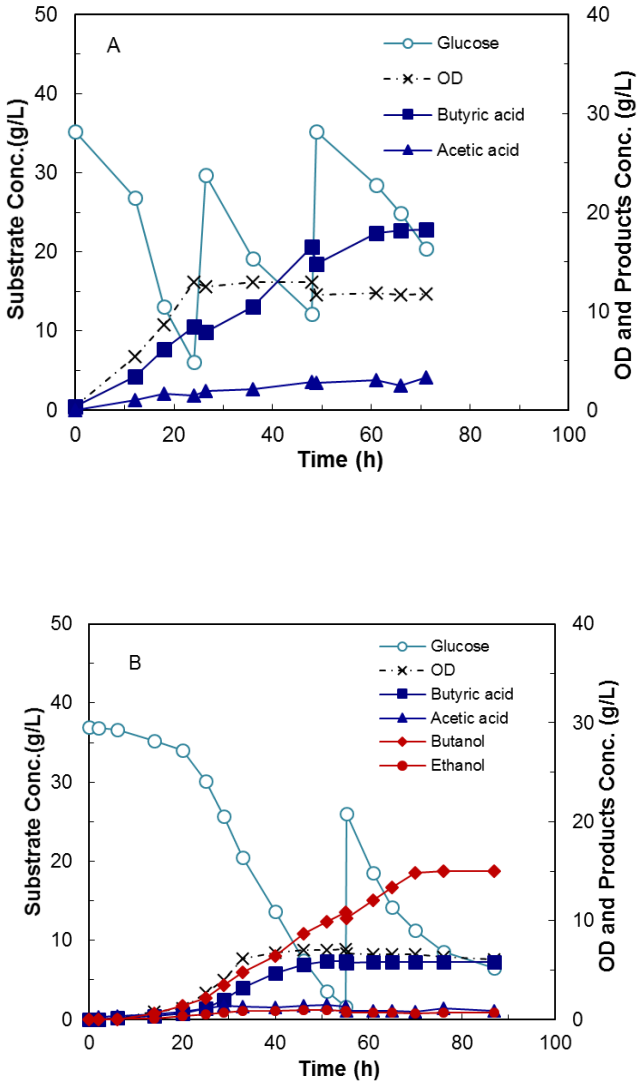

Figure 6.1. Fermentation kinetics of *C. tyrobutyricum* WT w/o amino acid feeding (A) and butanol producing mutant w/o amino acid feeding (B) in a 2 L bioreactor using glucose as substrate at pH 6.0, temperature 37 ºC, and 100rpm. ○: Glucose, ×OD, ■: Butyric acid, ▲: Acetic acid, ♦: Butanol, ●: Ethanol.

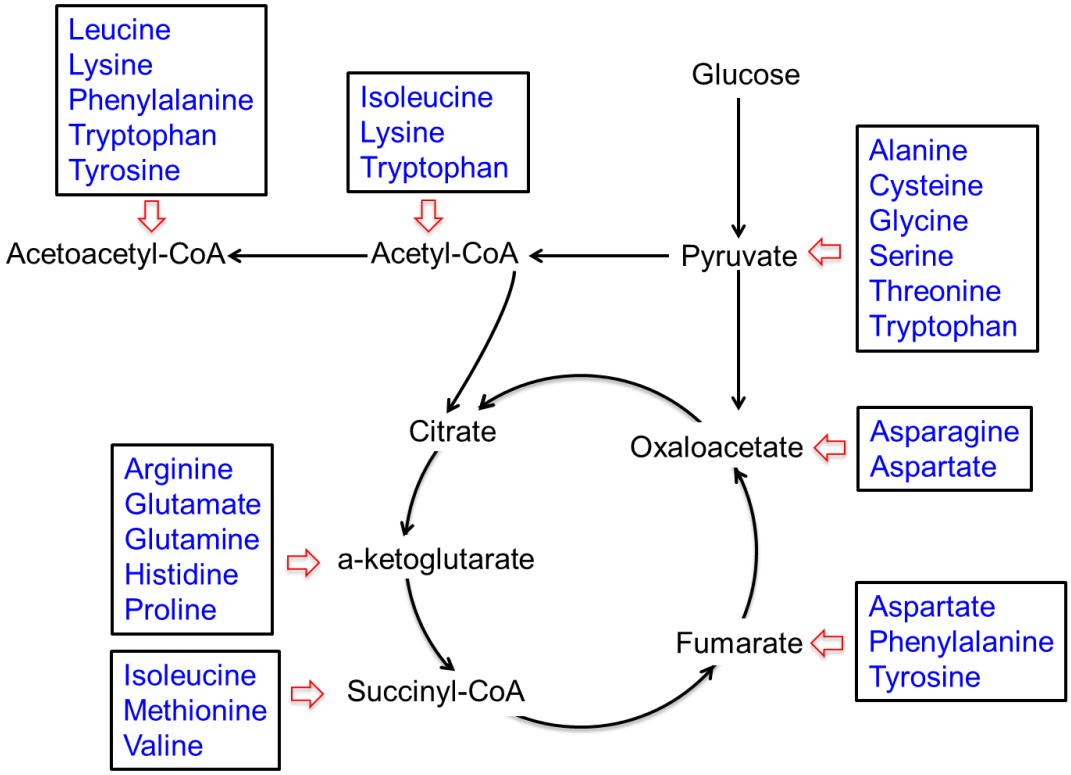

Figure 6.2. Metabolic pathway of TCA and related aa mechanism in *C. tyrobutyricum* butanol producing mutant.

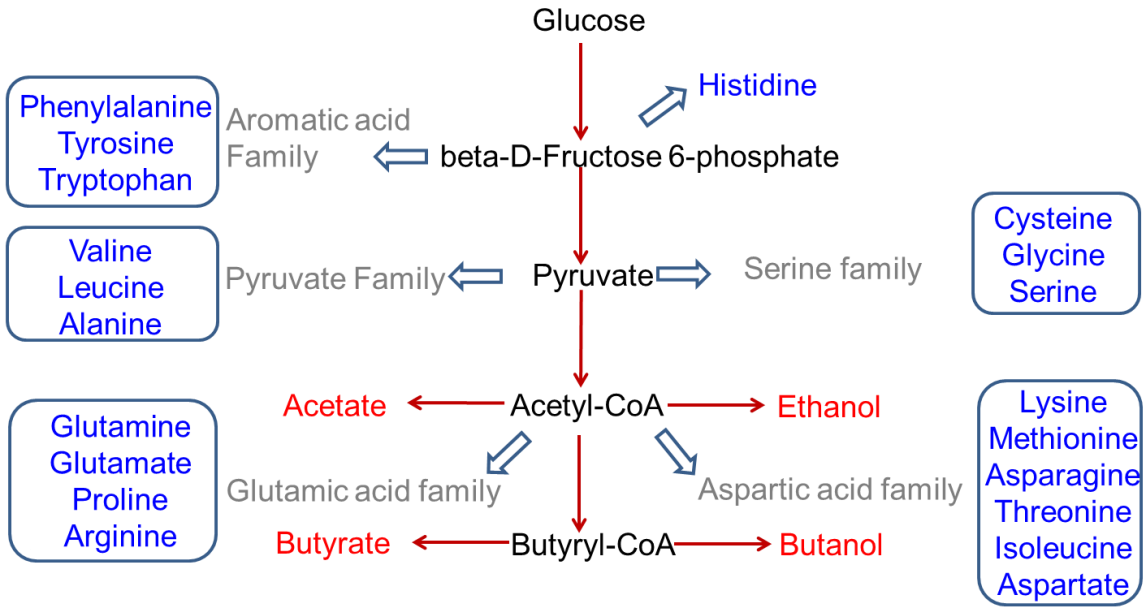

Figure 6.3. Metabolic pathway of butanol related aa mechanism in *C. tyrobutyricum* butanol producing mutant.

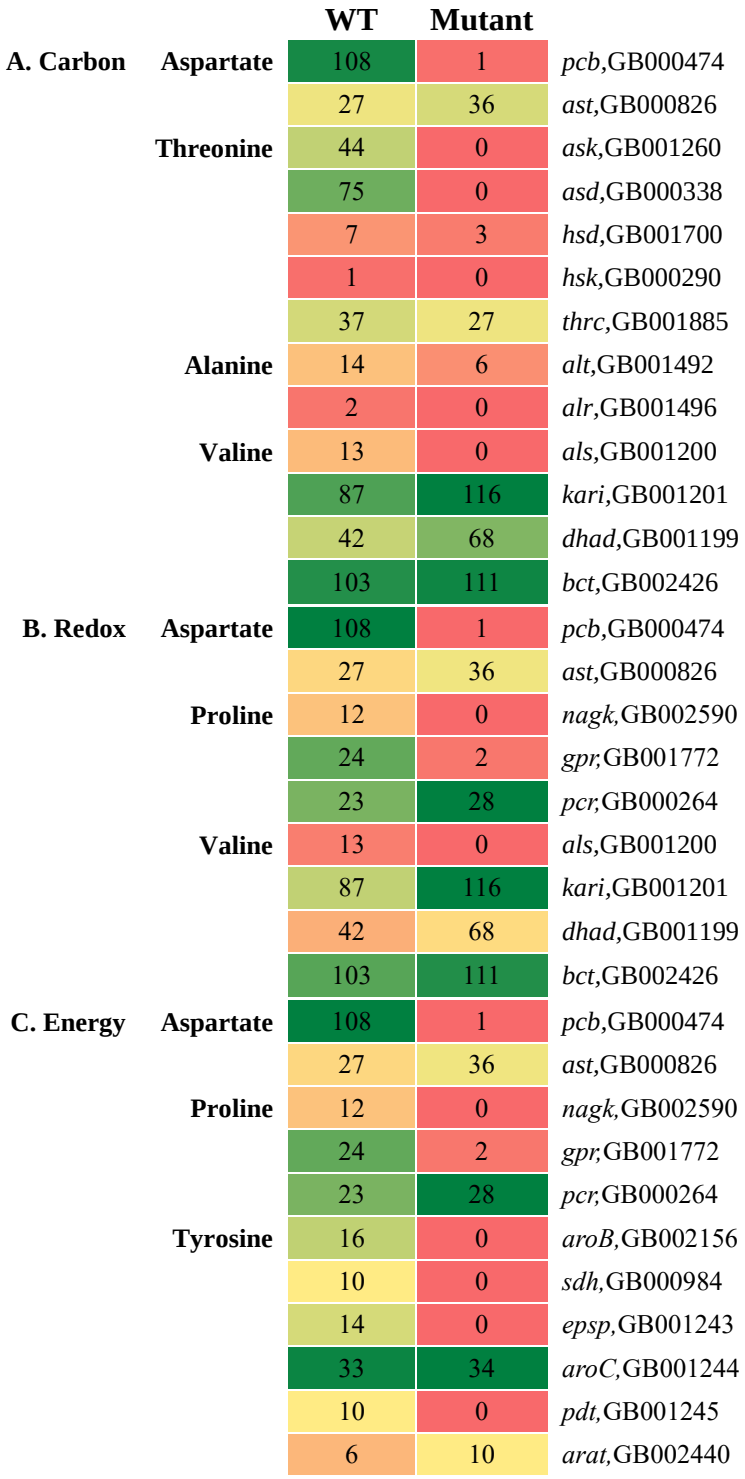

Figure 6.4. Heat map of protein expression level in *C. tyrobutyricum* WT and butanol producing mutant. Red color: low expression, Yellow color: medium expression, and Green color: high expression.

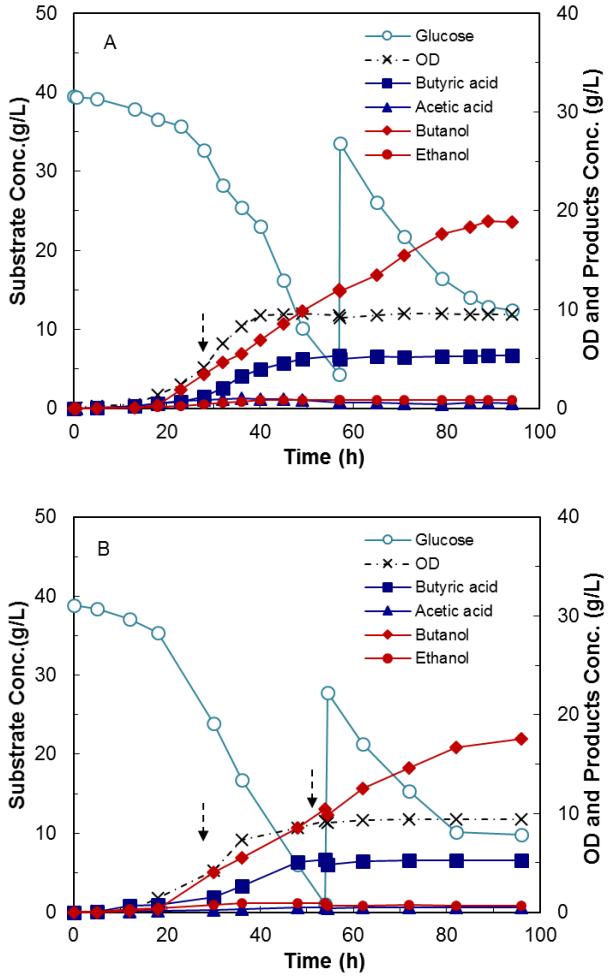

Figure 6.5. Fermentation kinetics of *C. tyrobutyricum* butanol producing mutant with yeast extract feeding (A) and butanol producing mutant with casamino acid feeding (B) in a 2 L bioreactor using glucose as substrate at pH 6.0, temperature 37 ºC, and 100rpm. ○: Glucose, ×OD, ■: Butyric acid, ▲: Acetic acid, ♦: Butanol, ●: Ethanol.

CHAPTER 7

CONCLUSIONS AND FUTURE WORK

7.1 Conclusions

A comprehensive dataset of the intracellular protein expression of *C. tyrobutyricum* was constructed using GeLC-MS/MS. The key enzymes regulating carbon, energy and redox balance in the core metabolic pathway were identified using comparative proteomics study. The addition of a butanol synthesis pathway and other consequently unregulated NADH consuming pathways caused obvious redirection of electrons. The efficiency of butyryl-CoA synthesis from crotonyl-CoA could be low due to the decreased expression of butyryl-CoA dehydrogenase (*bcd*) and electron transfer flavoproteins (*etf*). The butyrate production was low (5.06 g/L), and butanol production was high (16.68 g/L) in the butanol producing strain. Consistent with the fermentation results, there was upregulation of the enzymes that catabolized acetyl-CoA and the upregulation of the enzymes involved in butanol synthesis in butanol producing strain. The key finding suggested metabolic engineering strategies to metabolically engineer *C. tyrobutyricum* by rebalancing carbon and redox for the improvement of biobutanol production.

The results in pH optimization demonstrated that the fermentation pH is an important process parameter in order to achieve high butyrate production. To rationally optimize fermentation process, it is very important to understand how the pH correlates with the intracellular metabolic flux distribution. The *C. tyrobutyricum* mutant PAK-Em with acetate pathway downregulation produced a high concentration butyrate with pH optimization. The highest butyrate production was

63.02 g/L in FBB at pH 6.5 by the PAK-Em. The mutant strain Hyd-Em was constructed by integrating metabolic engineering through gene manipulation and evolutionary engineering through adaptation in a fibrous-bed bioreactor. Compared to PAK-Em, this mutant maintained a high level of butyrate production and had a fast cell growth. This result demonstrated that it is feasible to genetically engineer bacteria with gene manipulation and strain adaptation.

The redox engineering by cell engineering or process engineering (i.e. medium optimization in this study) doubled the butanol production, while the integration of cell-process engineering quadrupled the butanol production. The free-cell fermentation produced 12.34 g/L of butanol from glucose by rebalancing redox to redirect carbon flux, which was 3.88-fold higher than control. In the medium study, sodium formate or methyl viologen hydrate could also obviously improve the butanol production. The integration of these two engineering methods effectively improved reducing power supply and rebalanced redox. Redox engineering was essential to achieve high butanol production in addition to carbon engineering in *C. tyrobutyricum*. It was concluded that the integration of metabolic engineering and process engineering was feasible in biofuel production improvement.

Lower expression of enzymes in the TCA cycle in the butanol producing strain were correlated to more carbon flux flowing to butanol. The amino acid metabolism had a significant influence on the core metabolic pathway through regulating the TCA cycle in *C. tyrobutyricum.* Supplying enough yeast extract or casamino acids could improve butanol production in terms of titer (18.94 g/L vs 14.32 g/L in control), yield (0.30 g/g-glucose vs 0.20 g/g-glucose in control) and productivity (0.27 g/L/h vs 0.19 g/L/h in control). Compared to the control condition, extra yeast extract and casamino acid feeding increased both butanol yield and productivity by more than 1.4-fold. Extra amino acids supplying to redistribute carbon flux was important in the butanol

fermentation. This result demonstrated that amino acid biosynthesis and catabolism regulated butanol production.

7.2 Future Works

Biobutanol is a promising energy alternative in the future. Integration of carbon and redox rebalance through metabolic engineering and process development in *C. tyrobutyricum* significantly improved butanol production. However, there are still many challenges remaining for butanol to replace traditional fossil fuel and apply in the market.

7.2.1 Metabolic engineering strategy

The Metabolomics is a study to construct a complete set of small-molecule metabolites in one type of organism [1]. Metabolic modeling was been established in *Clostridium acetobutylicum* to map the metabolite changes during the acidogenic-solventogenic transition and propose a possible metabolic regulation method for further improvement [2]. However, Metabolomics has not been studied in *C. tyrobutyricum*. In order to further engineer *C. tyrobutyricum* and increase butanol production, Metabolic modeling of our mutants will be performed to identify the key intracellular and extracellular regulators.

Multiple mutants of *C. tyrobutyricum* were constructed (shown in Table 7.2 and Figure 7.1), including CTC-*thl-fdh-adhE2* (control), ACKKO-*fdh-adhE2* (control), and ACKKO-*thl-fdh-adhE2*. The butanol production by CTC-*adhE2*, CTC-*fdh*-adhE2, CTC-*thl-fdh-adhE2*, ACKKO-*adhE2*, ACKKO-*fdh-adhE2*, and ACKKO-*thl-fdh-adhE2* were evaluated in fed-batch fermentations in a 2-L stirred-tank bioreactor, produced butanol concentrations of 6.14 g/L, 12.34 g/L, 14.14 g/L, 14.32 g/L, 18.37 g/L, and 19.41 g/L, respectively (Fig. 7.2). All six mutants had no obvious lag phase (Fig. 7.2) and had similar specific growth rates of 0.15-0.16 h^{-1} (Table 7.2). This result demonstrated that the integration of carbon and redox rebalance significantly improved

the butanol production from 6.14 g/L to 19.41 g/L, with 3.16-fold improvement. The yield of butanol in ACKKO-*thl-fdh-adhE2* (0.32 g/g) was much higher than other mutants. It was also found that the butanol productivity was improved by *fdh* overexpression, from productivity of 0.28 g/L/h by ACKKO-*fdh-adhE2* to 0.20 g/L/h by ACKKO-*adhE2*. All these strains need to be characterized using PCR and enzymes assay, which shows that the heterologous genes *thl*, *fdh* and *adhE2* were introduced successfully.

7.2.2 Immobilized-cell Fermentation and Online Butanol Recovery

Biobutanol can increase *C. tyrobutyricum* cytomembranes fluidity, destroy their structures, and hamper their functions. *C. tyrobutyricum* retained less than 20% of their maximum growth rate at 20 g/L of butanol. That might be one reason that the butanol titer in free-cell fermentation could not be higher than 20 g/L. Therefore, it is necessary to increase the tolerance of *C. tyrobutyricum* to improve the butanol production.

As we discussed before, the fibrous-bed bioreactor (FBB) for immobilized-cell fermentations had a significant influence on products and cell growth [3-6]. The increased productivity in immobilized-cell fermentation offers a harsh environment for cell mutation and evolution over an extended period of time. The immobilized-cell fermentations study with our carbon, nitrogen, and redox rebalanced conditions will be performed to improve the butanol production. The *C. tyrobutyricum* mutant with overexpressing heterologous NAD^+-dependent formate dehydrogenase (*fdh*), thiolase (*thl*), and acetaldehyde/alcohol dehydrogenase (*adhE2*) will be used as host cell and adapted in the immobilized-cell fermentation. This cell-adaption process will be repeated until butanol production does not change in three successive fed-batches to kill the cells with low butanol tolerance.

Because the amino acid feeding strategy affected butanol production in the free-cell fermentation, we will also optimize the amino acid feeding strategy in our immobilized-cell fermentation. The *C. tyrobutyricum* cell growth rate will be different between free-cell and immobilized-cell fermentation, leading to a different amino acid consumption rate in a different fermentation mode. Therefore, the feeding timeline of amino acid, concentration of amino acid feeding solution, and new cheaper amino acid source to control the fermentation cost need to be considered based on cell adaptation and butanol production.

To further improve cell retaining efficiency, cell recycle technology using gas stripping and membrane recovery will be integrated with cell immobilization. This integrated technology can recycle cells and prevent cell loss that happened in the immobilized-cell bioreactors.

7.3 Reference

[1] S.G Oliver, M.K. Winson, D.B. Kell, F. Baganz. "Systematic functional analysis of the yeast genome". Trends Biotechnol., vol. 16, pp. 373–378, 1998.

[2] D. Amador-Noguez, I.A. Brasg, X.J. Feng, N. Roquet, J.D. Rabinowitz. "Metabolome remodeling during the acidogenic-solventogenic transition in *Clostridium acetobutylicum*". Appl. Environ. Microbiol., vol. 77, pp. 7984-7997, 2011.

[3] C. Ma, J. Ou, S. McFann, M. Miller, X.M. Liu. "High production of butyric acid by *Clostridium tyrobutyricum* mutant". Front. Chem. Sci. Eng., 2015.

[4] X. Liu, Y. Zhu, S. Yang. "Butyric acid and hydrogen production by *Clostridium tyrobutyricum* ATCC 25755 and mutants". Enzyme Microb. Technol., vol. 383, pp. 521-528, 2006.

[5] D. Wei, X. Liu, S.T. Yang. "Butyric acid production from sugarcane bagasse hydrolysate by *Clostridium tyrobutyricum* immobilized in a fibrous-bed bioreactor". Bioresour. Technol., vol. 129, pp. 553-60, 2013.

[6] S.T.Yang. "Extractive fermentation using convoluted fibrous bed bioreactor". U. S. Patent, 5563069, 1996.

Table 7.1. Strains and plasmids used in this study.

Plasmid/strain	Relevant characteristics	Reference/source
Plasmids		
*p*MTL-adhE2	*adhE2* overexpression with *thl* promoter	This study
*p*MTL-fdh-adhE2	*fdh* and *adhE2* overexpression with *thl* promoter	This study
*p*MTL-thl-fdh-adhE2	*thl, fdh* and *adhE2* overexpression	This study
Strains		
C. tyrobutyricum	*Clostridium*, ATCC 25755, wild type	ATCC
CTC-*adhE2*	*Clostridium tyrobutyricum* with *adhE2* overexpression, thiamphenicol resistant	[4]
CTC-*fdh-adhE2*	*Clostridium tyrobutyricum* with *fdh* and *adhE2* overexpression, thiamphenicol resistant	This study
CTC-*thl-fdh-adhE2*	*Clostridium tyrobutyricum* with *thl*, *fdh* and *adhE2* overexpression, thiamphenicol resistant	This study
ACKKO-*adhE2*	*Clostridium* ACKKO with *adhE2* overexpression, thiamphenicol resistant	[4]
ACKKO-*fdh-adhE2*	*Clostridium* ACKKO with *fdh* and *adhE2* overexpression, thiamphenicol resistant	This study
ACKKO- *thl-fdh- -adhE2*	*Clostridium* ACKKO with *fdh* and *adhE2* overexpression, thiamphenicol resistant	This study
E. coli CA434	*E. coli* HB101 with plasmid R702, kanamycin resistant	[4]

Table 7.2. Butanol fermentations using metabolically engineered *C. tyrobutyricum* by rebalancing redox and carbon.

Products		**CTC-*adhE2***	**CTC-*fdh-adhE2***	**CTC-*thl-fdh-adhE2***	**ACKKO-*adhE2***	**ACKKO-*fdh-adhE2***	**ACKKO-*thl-fdh-adhE2***
Cell growth (h^{-1})		0.16±0.0004	0.15±0.001	0.14±0.001	0.15±0.002	0.14±0.001	0.14±0.002
Biomass yield (g/g)		0.09±0.003	0.08±0.002	0.07±0.001	0.08±0.005	0.06±0.002	0.06±0.001
Concentration (g/L)	Butanol	6.14±0.05	12.34±0.02	14.14±0.001	14.32±0.41	18.37±0.22	19.41±0.13
	Butyrate	9.32±0.03	5.05±0.04	4.13±0.002	7.15±0.03	4.28±0.002	3.37±0.001
	Acetate	1.42±0.07	0.26±0.03	0.21±0.001	1.21±0.01	0.72±0.003	0.42±0.002
	Ethanol	0.25±0.02	0.28±0.07	0.22±0.002	1.03±0.01	0.94±0.03	0.80±0.03
Yield (g/g-glucose)	Butanol	0.11±0.003	0.23±0.002	0.25±0.001	0.20±0.01	0.28±0.02	0.32±0.02
	Butyrate	0.20±00.004	0.10±0.001	0.10±0.003	0.14±0.001	0.11±0.03	0.08±0.01
	Acetate	0.02±0.002	0.003±0.0001	0.002±0.0002	0.009±0.002	0.007±0.001	0.004±0.001
	Ethanol	0.003±0.0004	0.004±0.0003	0.003±0.0004	0.011±0.0004	0.006±0.0002	0.005±0.0002
Productivity (g/L/h)	Butanol	0.14±0.01	0.26±0.01	0.27±0.002	0.20±0.004	0.28±0.001	0.31±0.001
	Butyrate	0.26±0.003	0.15±0.004	0.14±0.01	0.16±0.003	0.11±0.002	0.08±0.002
	Acetate	0.07±0.004	0.01±0.002	0.008±0.001	0.05±0.003	0.04±0.004	0.03±0.004
	Ethanol	0.008±0.0001	0.011±0.0004	0.007±0.0004	0.03±0.002	0.02±0.001	0.01±0.001

Notes: The average data in this table were calculated from the duplicated fermentations. Yield = g-product/g-glucose consumed, and selectivity = g-product/g-total products.

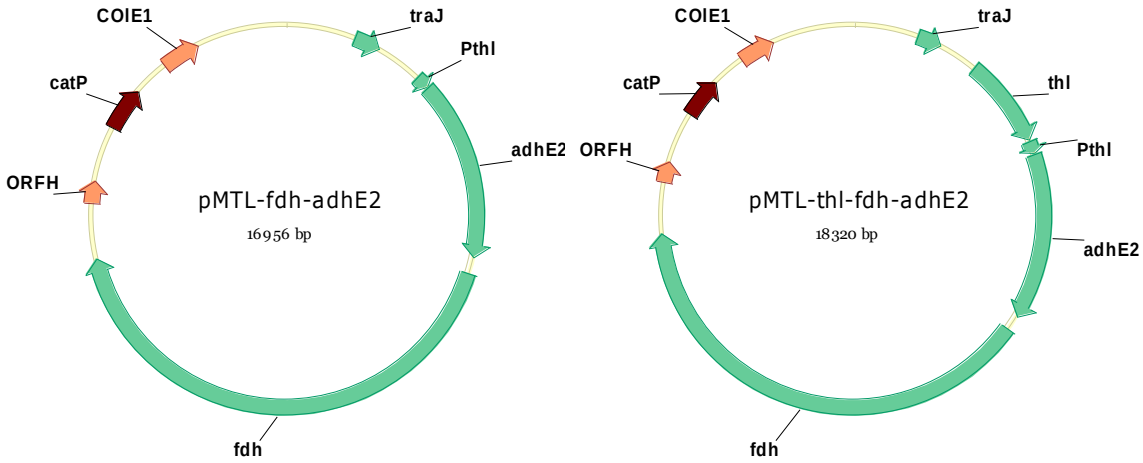

Figure 7.1. Plasmid of pMTL-fdh-adhE2 and pMTL-thl-fdh-adhE2. *ORF H*: *pCB102* replicon from *Clostridium butyricum*; *CatP*: chloramphenicol and thiamphenicol resistant gene; *ColE1*: *E. coli* replicon; *fdh*: formate dehydrogenase from *Moorella thermoacetica*; *Pthl*: promoter of thiolase from *Clostridium tyrobutyricum*; *traJ*: regulator of the F plasmid transfer operon; *adhE2*: bifunctional aldehyde/alcohol dehydrogenase (*adhE2*) from *Clostridium acetobutylicum*; *thl*: thiolase gene from *Clostridium tyrobutyricum*.

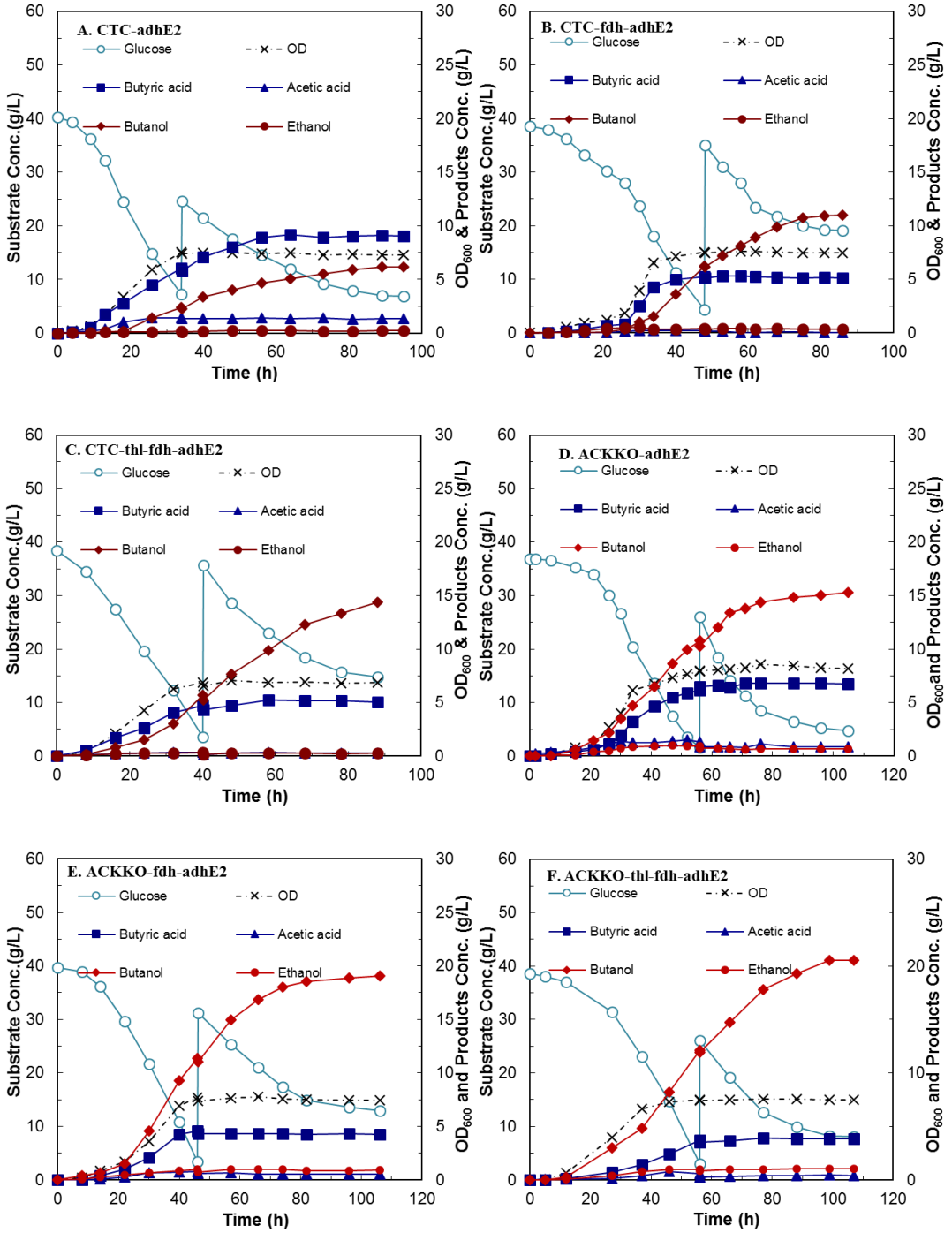

Figure 7.2. Fermentation kinetics of *C. tyrobutyricum* ACKKO-*adhE2* mutant (A) and butanol producing mutant with casamino acid feeding (B) in a 2 L bioreactor using glucose as substrate at pH 6.0, temperature 37 ºC, and 100rpm. ○: Glucose, ×OD, ■: Butyric acid, ▲: Acetic acid, ♦: Butanol, ●: Ethanol

APPENDIX IGene sequences

I.1 Gene *adhE2* sequence

atgaaagttacaaatcaaaaagaactaaaacaaaagctaaatgaattgagagaagcgcaaaagaagtttgcaacctatactcaagagcaag

ttgataaaatttttaaacaatgtgccatagccgcagctaaagaaagaataaacttagctaaattagcagtagaagaaacaggaataggtcttgt

agaagataaaattataaaaaatcattttgcagcagaatatatatacaataaatataaaaatgaaaaaacttgtggcataatagaccatgacgatt

ctttaggcataacaaaggttgctgaaccaattggaattgttgcagccatagttcctactactaatccaacttccacagcaattttcaaatcattaat

ttctttaaaaacaagaaacgcaatattcttttcaccacatccacgtgcaaaaaaatctacaattgctgcagcaaaattaattttagatgcagctgtt

aaagcaggagcacctaaaaatataataggctggatagatgagccatcaatagaactttctcaagatttgatgagtgaagctgatataatattag

caacaggaggtccttcaatggttaaagcggcctattcatctggaaaacctgcaattggtgttggagcaggaaatacaccagcaataatagat

gagagtgcagatatagatatggcagtaagctccataattttatcaaagacttatgacaatggagtaatatgcgcttctgaacaatcaatattagtt

atgaattcaatatacgaaaaagttaaagaggaatttgtaaaacgaggatcatatatactcaatcaaaatgaaatagctaaaataaaagaaacta

tgtttaaaaatggagctattaatgctgacatagttggaaaatctgcttatataattgctaaaatggcaggaattgaagttcctcaaactacaaaga

tacttataggcgaagtacaatctgttgaaaaaagcgagctgttctcacatgaaaaactatcaccagtacttgcaatgtataaagttaaggattttg

atgaagctctaaaaaaggcacaaaggctaatagaattaggtggaagtggacacacgtcatctttatatatagattcacaaaacaataaggata

aagttaaagaatttggattagcaatgaaaacttcaaggacatttattaacatgccttcttcacagggagcaagcggagatttatacaattttgcg

atagcaccatcatttactcttggatgcggcacttggggaggaaactctgtatcgcaaaatgtagagcctaaacatttattaaatattaaaagtgtt

gctgaaagaagggaaaatatgctttggtttaaagtgccacaaaaaatatattttaaatatggatgtcttagatttgcattaaaagaattaaaagat

atgaataagaaaagagcctttatagtaacagataaagatctttttaaacttggatatgttaataaaataacaaaggtactagatgagatagatatt

aaatacagtatatttacagatattaaatctgatccaactattgattcagtaaaaaaaggtgctaaagaaatgcttaactttgaacctgatactataa

tctctattggtggtggatcgccaatggatgcagcaaaggttatgcacttgttatatgaatatccagaagcagaaattgaaaatctagctataaac

tttatggatataagaaagagaatatgcaatttccctaaattaggtacaaaggcgatttcagtagctattcctacaactgctggtaccggttcaga

ggcaacacctttgcagttataactaatgatgaaacaggaatgaaataccctttaacttcttatgaattgaccccaaacatggcaataatagata

ctgaattaatgttaaatatgcctagaaaattaacagcagcaactggaatagatgcattagttcatgctatagaagcatatgtttcggttatggcta

cggattatactgatgaattagccttaagagcaataaaaatgatatttaaatatttgcctagagcctataaaaatgggactaacgacattgaagca

agagaaaaaatggcacatgcctctaatattgcggggatggcatttgcaaatgctttcttaggtgtatgccattcaatggctcataaacttgggg

caatgcatcacgttccacatggaattgcttgtgctgtattaatagaagaagttattaaatataacgctacagactgtccaacaaagcaaacagc

attccctcaatataaatctcctaatgctaagagaaaatatgctgaaattgcagagtatttgaatttaaagggtactagcgataccgaaaaggtaa

cagccttaatagaagctatttcaaagttaaagatagatttgagtattccacaaaatataagtgccgctggaataaataaaaaagatttttataata

cgctagataaaatgtcagagcttgcttttgatgaccaatgtacaacagctaatcctaggtatccacttataagtgaacttaaggatatctatataa

aatcatttta

I.2 Gene *fdh* sequence

gaattcatttatggtattggtaaatttttagggatataggagtatctcaatcgctgccgataccgaagtcataatgctcgacttgatgctgaggtc

atccgggattaaaggccgatcttggtgatttgaatcattttatgataactataaaaaaacgactgggaattaactgatggggaaacggttattgtt

atttttatcgttttctgctttatgttaactctctccggtacggggagcaggcccgagggctggcccctgacagcgccggtggtgcaggcggat

attgttgtctatggcggcggcctggccgggtgcgcggcggcctggaaagccgcggtcgcggcgccggacaagcaggtggccctggtgg

tcccctaccccggccgcgagtacggcggcctggctacggtgggcggccagaacttctgggacctgcgctactgggaccgggacgggaa

gctggcccaggggggctcatttgcccactggttgaaagcggtaggtccttttaccgcacggcagatcttgcggcgcggattgccgcggac

ctgggaaggctgccgaacctcaaaacttactgggctatggacataaccgccgtccggaaggaccggcgtggccgcctgcgcgccctggc

attgcgggaactgcaacgtgatgcgaccgggaccatcgcctggggtagcgggaaagaaatcctggcggcgccgatatttgttgacgcctc

cgaggacggcaggctcagccgcctgagccaggccggggtgacggtgggccgggcggactggccggccgaactcctgaccagagattt

tctgaatggcagcagcgacctccgcccgcgccagcaagcggctactttgatgtttaaggtgaaggggttcggccgggccgctacccgg

atatggtttttcaacgagcaaaaggggtatgggggcctacggcggtaaaaaagtttacataagcgaccggtggttaccgcttttaacgataa

atacggccccctgggctttgccctgaaacccctcaacgccgcccaggacgggccgggaagcccggagtggtgggttaatgccctccttat

ctttaacgtcgacggccgggccaacggccgcgaccgggggcatgatgcctatcccggggatatggcgccaggggccctggacacggat

acggcctggcagcgggcgcgccagttactggacgacccggagttcatccgggccttgcgccgttttcaagggttcgaagaggccgaggt

ggtgcgggatgcagcaggccggccggtgaccggcgatatcctctacctgcgggagacagtgcacacggtgatggaccccagggaaac

ccgtccggggactgagaataacaattacgccctgaacgcatcggctgcccggggcgcaggttctggcccccctgatggcgatgatctcgg

gaattatgccaaccgtatcggcctgggcttttactggcaggatatcaatgcctatcatttcagcgatcttaaagggagcgacggcagctaccg

ctggccggtgacgccctttttgcggcccgattatcctcggacaacgccgggaccagacggatggccacaaaatccggtgtatattcccttta

acgttctccttagccggacggtgcccaacctccttatccctggttatgcagccagcatctcctccctggcctgggccgagctgcgggtgctg

cccaatagttgcgtcctgggagatgcggccggggtagcggctgcctatgccgcccgtgtgggccgcgacccgggcaccttcactgacgc

cgatgtagcggctatcagggaaatactggtcaaaagtttcggcgccagggtagataagtgaggcgaaaaatccgcaagccggcgaaagt

gctggaagcagagctggaaaagatttaaaatgatgagggcctgagagtttgattatctttgttcaaattttcgtataaatatttttttctagccaata

gtcttctgctctgctataattctcatagaggctcttctattcatgatagagaaagattgtgaagagtatcgcatttatgcttataaggaggttccgg

gcttgccccgggacaggacccaaaggagggatactgccttgggagaggtggtatttagcacctggggaggaaaagttgtcgatcaccg

gggcggtccgtcgggggaggaccgtcctgggccggggaatttggcggtcggcagttaaaggcctttattggctgggatggtctcgtagt

caccgacccggccgtagacctgctggctgctttacaggcttactaccaggccgtccaggggaatcctgcggccgctgcgtaccctgccg

ggtagggaccagggttatttacaatgtcctggtacgcatcgccgggggcgaaggccttccctccgatttagaccttctccgacgggtggcct

ggattgtacgggatggttctctgtgcgagctcggccaggctggggccaaagctgttcttgatttttagattattatagcgaggccttgcgacct

ttcctggaggatagcggcagggtcgccgggggtcaacggagaccagggcctggaggccgggtgcaggttctggcttccggacgggtcc

tggtggggaacgaccgcggaaagggagcggccgccgcttccccggcagccggtttaacctataaacctttgttactgcgccctgcctcaa

gcggtgcccggcccacctggacatcccggcttatattgacgccattaaggatggccgctatgaggaatccctggccatcatccgccagcg

gaccgccctggccggtgtcctgggacgggtctgcgtccacccgtgtgaagaaaactgccgccgcggcaatgttgacgaacccctggcca

tccggggcctgaagcgcttcgtagccgattatgaggtgaaacgcggccgccggccggtcgccgtctgcgggggtaatctctttacgggac

cctggcggccggcaggacaggccggtggggaagaaacaacggccgtcacttcaggcaagaaggtagccatcatcggtgccggaccgg

cgggtctcagcgccgcctaccagctcgccggtcggggctataaagtgactattttcgaggccttgccggtggccggcggtatgctggcggt

gggtattcccagctaccggttgccacgggatatcctggctggagagatcgaggccatcaaggctctgggcgtaaccatcaacctcaacacc

cgggtcggcgtcgacgtgaccatggaccaattacagcgcgattacgacgccgtctttattgctaccggcctccatgccagctcccgcatgg

gagtagccggcgaggatgaaggctatggaggatttatccccggggtcaagttcctgcgagatttgaacctggaccggtgtccttccctgga

gggcaaggtggtggccgtcgtcggcggcggcaatgtagcgatggattgcgcccgttccgccctgcgccgggggggcccgggaggtgca

ccttatttaccggcgttcccgggcggaaatgccggcccatgcgaccgaggtcagggatgccgaggccgagggggttatttatcacttcctg

gttaatcccaccgccctggtagcggaaaaaggcaatatcaagggtatgcagtgcgtccggatgaaacttggcgagccggacgattctggc

cggcgccggcccgtacccgtgccgggaacggagtttttcctgccctgcgatattgtggtgccggctatcggccaggcggccgacctgtctt

tcctggacggccggatcgaggtgggcaaacgtggtaccatcagtgttgacccggtgaccctggctaccagtgtccccggcgtcttcgccg

gcggcgatatcgtcctgggggccaggacggtagttgaggccgtggcccagggcaaccgggcggcagtttccattgaccagtacctgcgc

caggggaccaccagtcccacggtagaggacgagctggacgcgtggctggaaaaggtcggcgtctatgacccggaagaggatgtagga

atctacggcggccggccgcggcaggcagaaagggtggcgccgttggccgagcgggtaaaggacttccgggaagttgaaggcggcttc

gatttctacgcaggcagggccgaagccgaacgctgcctgcgctgttaccgggtcgggatgatggtcctggccggagagggggagagta

atggttaacctgaccattgacggacaaagggttacggctccagagggcatgaccatcctggaggtggcccgggaaaatggtatccatatcc

ccaccctgtgccaccatccaaagttgcggcccctggggtattgccgtctgtgcctggtcgacatcgagggcgccgcaaaacccatgacgg

cctgcaatacgccggtcgccgagggtatggtgatccggaccagcacgcctgttatagaggagatgcgcaagggtattattgaaatgctttta

agcctccacccggaggactgcctgacctgcgaaaaagcaggtaactgccagctccaggattgcgcctacacttacggtgtaaagcatggc

gaactgccagtaaaacgcgaggaattgcccgttttgaaggaaaatcccttcattgtgcgggattataataaatgtatcgtttgcggccgttgcg

tccgcgcctgccaggaggtgcaggtccagagggtcgtggacctggtgggtaaaggcagcgccgcccgggtgggggcgacgaaggcc

ggagcggaagtaagcctggaagaaggggctgcgtcttttgcggtaactgtgtccaggtctgcccggtgggagctctgacggagaaggc

cggcctgggccagggccgcgagtgggagttcaaaaaagtccgcagtatttgttcttactgcggcgtgggttgtaatctcacccttatgtaaa

agatggtaaggtggtaaaagttaggggttacgaaaaccctgaggtaaacaacggctggctgtgcgtaaaaggccgctttggttttgactatat

tcacaatcctgacaggataaccaggccgttgatccgggagggagatagggaaaaaggctatttccgggaggcttcctgggaagaagcttt

agcccttgtatcccagaaattaactcagattaaaggcagctacggctctgaagctctgggctttctttgttcagctaaatgtaccaatgaagaga

attatctcttacaaaagctggcccgggggggtactgggcaccaataatgttgatcactgtgctcgcctctgacactcttctacagttgccggtctg

gcaacaacctttggcagcggtgcaatgaccaattctatcgctgacatcgccagcgcagattgtatctttgtcattggcagcaatacaaccgag

aaccatcctgttattgcccttaaagtaaaagaagctgtccgtcgtggagccaggctcattgttgctgatccccggcgtattgaactggtgaactt

cagttacttgtggttaagacaaaaacccggaacagatcttgctctgctgaatggactgcttcatgtaatcatcaaggaagagctttatgacaaa

gaatttattgcccagaggacggaaggttttgaggctctaaaacttgccgtagaggagtatacaccagcaaaggtgtcagaagttacaggtgtt

ccggcaggcgatattatcgaggcagcaaggacttatgcccggggtccgagctctactattttgtacgcaatgggaataacccagcatataac

tggtacggccaacgtgatggccctggccaacctggccatggcctgtggtcaggtcggtaaagaaggtaacggcgtaaatcccctgcggg

ggcagagcaatgtccagggtgcctgcgatatgggtggattacccaatgtattaccgggataccaaccagtaacagatccgggggttcgcca

taaatttagcgaaacctgggggggtaccggacttacccggagaacctggcctgacattaatggagatgatggcggcagcccaagaaggca

aattgaaagggatgtatattttaggagaaaaccctgtcttgactgatccagatgtctcccatgtaaaagaggcgttaaagaacctggagtttctg

gtggtacaggatatttttttgacggagacagccaggatggcggatgttgttttacctggagcttcctttgcggaaaaggaaggtacctttacca

gtacggagcgccgggtgcagcttttgcataaagccattgaacctcccggtgaagcacggccggattggcttattttaaacgatttgttgctgtt

aatgggatatccgcggaaatattcgtcgcctggggagataatgcaggagatagcagggttaactcccagctatgcgggtataacttatgagc

gcctggaagataaagggttacagtggccggtgctttccctcgaacatccgggtacacccgttctccatcgggaaaaatttagcagaggttat

gggcagttccaggtagtgcattaccggccgccggccgaagaacctgatgaagagtacccgttcttatttaccactggcaggaatttgtatca

ctatcatactgttatttcccgtaagtccaggggctggaagagatgtgtcctgctcctgtggtggagattaatgataacgatgcagcccgtttg

ggtatacgggaaggagaaatgattgagattgtttcccgacgtggtaaagtaagggttaaagcattggttacggatcgcataccccggggcc

aggtatttatgaatttccatttccatgaagcagcagccaacctgcttacaattgctgccctggatccggttgctaaaataccgattataaaacctg

tgctgtagctatcaaggttaaaaagtagctgtgggagattattttcccaccagccgcccctatccggggcggttttttattcttttaccggggag

cgaccgggaaccctgcaggagcaattgcttactgttgccggcggggtgtataatctaatt

I.3 Gene *thl* sequence

atattcagcgaaaatagtatattatataattataaattgatgaatagctagagtggtcagacctcctagctattgttttagaaaactttgtgttttttta

acaaaaatattgataaatttttaattatctagtataatgaagttgttggtaaaaaggtttgtaatcaatttaaattttaaaatataaatatttaggagga

atagtcatgagtgaagttgtaattgcaagtgccgttagaacagcaataggtaaatttggaggtagcttgaagtcagttccagcaactgatttag

gagctttggttataaaagaagcattaaaaagagctaatgttaaaccagaacttgtagatgaagttgtaatgggtaatgtattacaggcaggttta

ggtcagaatccagcaagacaagcattgataaaatcaggtatacctaatacagtccctggatttactataaataaagtttgtggttcaggacttag

agcagtaagtttagcagctcaaatgataaaagctggcgatgatgatatcgttgtagctggtggaatggaaaatatgtctgctgctccatatgta

atgcctagtgcaagatggggacaaagaatgtttgatggtaagattatagatgaaatggtaaaagacggactttgggatgcttttaataactatc

acatgggtattacggctgaaaatatagcagaaaagtggaacataacaagacaaatgcaggatgaatttgcagctgcatcacaacaaaaagc

agtagcagctataaaatctggcaagtttaaagatgaaatagttccagtagtaatcaaggatagaaaaaagggagaaatagtatttgatactgat

gaattccctagagatggtgtaactgtcgaaggaatatcaaaattaaaaccagcatttaagaaggatggtggaactgttacagctgccaatgctt

caggtataaatgatgcagctgcagcattagttataatgagtgcagacaaagcaaaagaattgggaattaaaccacttgctaaaattacttcttat

ggatcaaaaggcttggatcctagcataatgggatatggaccattccatgctacaaaactagcacttaaaaaagctaatttaactgtagatgattt

agatttaatagaagcaaacgaagcatttgctgctcagagtttagctgttgcaaaagacttgaaatttgatatgagcaaagtaaatgtaaatgga

ggagcaatagcacttggacatcctattggagcttcaggcgcaagaatacttactactttgctttatgaaatgcagaaaagagattcaaaacgtg

gtttagctacattatgtataggcggtggaatgggaactgctataatcgttgaaagataa

APPENDIX IIHPLC operation for substrate and products

The concentrations of fermentation products, including butanol, butyrate, acetate and ethanol, were analyzed using high performance liquid chromatography (HPLC, Shimadzu, Columbia, MD). The HPLC system was equipped with an automatic sampler (Shimadzu SIL-20A), a solvent delivery unit (Shimadzu LC-20AT), an organic acid and solvent analysis column (Rezex RHM-Monosaccharide H^+, Phenomenex, Torrance, CA), a column oven at 78 ^oC (CTO-20A), and a refractive index detector (Shimadzu RID-10A). The eluent was HPLC-grade H_2O at a flow rate of 0.6 mL/min.

[1] Before starting data acquisition, please set up the data acquisition conditions on "LabSolutions" software. The table below shows the basic information of the condition set up.

Column: Rezex™ RHM-Monosaccharide H+ (8%), LC Column 300 x 7.8 mm

Mobile phase: Pump A = Water, Pump B = Nothing

Flow rate: Pump A = 0.6 mL/min, Pump B = 0 mL/min

Column temperature: 78 degree C

Sample Injection volume: 10 uL

Start up

a. Check the connections. Ensure that all the units (pump, autosampler, column oven, and detector) of the instruments are connected to the system controller and optical link cables.

b. Turn the power on for each of the instruments.

c. Turn the PC on

d. Double-click the “LabSolution” on the desktop.

e. Log in.

[2] LabSolution Main Window. The analytical instruments connected to the PC are displayed as icons.

a. Instruments. Double-click “Instruments” icon to start the program where data acquisition setting are set and data is acquired. Double-click the “HPLC” to start the data acquisition.

b. Postrun. Displays the icons for the [Postrun Analysis] program (data analysis) and the [browser] program (chromatogram display and quantitative calculation of results).

c. Administration. Displays the icons of the system administration programs for setting security policies, user administration and the log browser.

d. Manual. Displays the icons for the various PDF manuals and Help menu provided with LabSolutions.

[4] Open the [Data Acquisition] window. After double-click the “HPLC” icon, there are 7 icons in main window. In normal state, [Ready] is displayed on the top of the window for the status. Follow the recommendations if [Not Connected] is displayed. The power is ON. The instrument are connected right. The system configuration settings are correct.

a. System Configuration. If the system configuration need to be changed, please click on this icons to open the sub-window.

b. System Check. Output the System Check report to ensure every instrument is right.

c. Data Acquisition. Display the icons for the [data acquisition] program.

d. Realtime Batch. Display the icons for the [Realtime Batch] program.

e. Report Format. Display the icons for the [Report format] program.

f. Calculation Curve. Display the icons for the [Calculation Curve] program.

g. Batch Editor. Display the icons for the [Batch Editor] program.

[5] Data acquisition parameters set-up.

a. Open the [Data Acquisition] window

b. Set each of the parameters on the [Simple Settings] tab. If the method already set up and download to the system, please double check the system conditions and write down the parameters in your notebook.

3. System Start up and Purge

[1] Open the [Data Acquisition] window. There are four parts in the window.

a. The first part on the top of the window include the title bar, menu bar, tool bar. The title bar displays the names of the current program, window, loaded file, and other information. Menu Bar displays the current window and menus that area available based on the operating rights of the current user, containing Files, Edit, View, Method, Instrument, Acquisition, Data, Tools, Windows, and Help. Tool bar displays icons of frequently used menu items and icons for operating analytical instruments.

b. The second part in the left of the window [Assistant Bar] displays icons for frequently used data acquisition operations, such as [Instrument Parameters], [Start Single Run], [Stop], and [Data Analysis].

c. The third part in the right of the window displays parameter details and can be changed as experiment conditions change. It includes [Data Acquisition], [LC Time Prog], [pump], [Detector A], [Detector B], [Column Oven], [Controller], [Autosampler], and [AutoPurge] sub-window.

d. Output window at the bottom of the window displays the operation history and error messages that occur.

[2] Click [file] icon in the [Assistant Bar], open method file and double-click the method. Notes: Please refer the method established already in the lab. If you want to make a new method file, please save the old one first.

[3] Click [download] in the third part of the window. Note: please make sure you download the method by confirming the parameters in the third part of the window one by one.

[4] Make sure the valve R in position 1 on the [Column Oven] sub-window, when you start up the system. Notes: In position 1, the mobile phase flows through the waste tubing not the column and detector.

[5] Let the mobile phase flow through the waste tubing for 1 hours. Notes: This step helps us not contaminate our column.

[6] Change the valve R in position 3 on the [Column Oven] sub-window. Notes: The column and tubing in the detector will be purged with this step.

[7] Purge the pump first. Step 1: Turn off the pump click the [pump] on the screen of LC-20AT Pump A. Step 2: Turn the knob 90 degrees to the left. Step 3: Click [purge] on LC-20AT Pump A.

[8] Purge the autosampler. Click on the [purge] on the Shimadzu SIL-20A autosampler. Notes: It will take 25 minutes.

[9] Baseline Check.

a. Click [zero detector A] in the tool bar.

b. Click [Balance RID detector A] in the tool bar. Wait until the baseline rebalanced. Notes: the numbers on refractive index detector (Shimadzu RID-10A) should be 0.

c. Repeat Step a and Step b by 3 times.

4. Realtime Batch.

[1] Create a Batch Table

a. Open the [Realtime Batch] window.

b. Click on [wizard] icon in the assistant bar at the left of the window.

c. Chose the parameters as follows.

Batch Table: New

Method file: Confirm the method

Injection Volume: 10 uL

Number of Sample groups: 1

Sample Type: Unknown only

Sample Name: Create the name

Sample ID: Create ID

Create file names: Save your data in the file you create

Number of Unknown Sample Vials in each Group: List the number of samples

Repetition per Run: List the number of repetition

Auto Condtioning: Click the [shutdown] icon

Shutdown Method File: Choose the right method

Cool down time: 0 min

Batch file name: Create the name of the batch file

d. Start the realtime batch run by clicking the [Queue Batch Run] icon.

5. Data Analysis

[1] Open the [Postrun Analysis] program.

[2] Open the [Data Analysis] window.

[3] Click [file] in the menu bar.

[4] Open your data file (.lcd).

6. Maintenance

[1] Follow the procedure to change the guard column cartridge if the HPLC pressure is larger than 600 psi.

[2] Use dd H_2O (Flow. Rate 0.6 mL/min, T 85 degree C) for 12 hours and 0.025 M H2SO4 (Flow. Rate 0.2 mL/min, T 85 degree C) for 4-16 hours to wash the system if the HPLC pressure is larger than 600 psi and the impure peaks happen.

[3] If the pressure of the pump not stable, double check the plunger of the pump. If needed to change, please follow the 8.3 section of LC-20 AT manual.

[4] If the En of the lamp lower than 5000 mV, use the methanol to rinse the system. Please remember to use pump A and the column position 3 at room T. If it doesn't work, please order a new lamp. Follow the instruction to change it

APPENDIX III HPLC operation for amino acids

Amino acid samples collected from the supernatant were mixed into 0.2 N borate buffer (pH 10.0), 15 mM 9-fluorenylmethyl-chloroformate solution, and acetonitrile with the ratio of 1:2:1:1. It took about 5 minutes to finish the derivatization reaction. The concentrations of free amino acid in fermentation broth, including arginine, serine, aspartic acid, glutamic acid, threonine, glycine, alanine, proline, methionine, valine, cysteine, histidine, lysine, and tyrosine, were analyzed using high performance liquid chromatography (HPLC, Shimadzu, Columbia, MD) with an amino acid analysis column (Restek, Raptor™ C18 LC Columns, Bellefonte, PA) and a UV detector (Shimadzu SPD-20A). The amino acid concentrations were measured under the following conditions: reverse column Raptor™ C18 3.0 x 100 mm; temperature 30 ^{o}C; flow rate 0.8 mL/min; Eluent A 0.1% formic acid and 20 mM ammonium formate in dd water; Eluent B 0.1% formic acid and 10 mM ammonium formate in 90:10 acetonitrile: dd water; UV/Vis 265 nm.

[1] Before starting data acquisition, please set up the data acquisition conditions on “LabSolutions” software. The table below shows the basic information of the condition set up.

Column: Restek, Raptor™ C18 LC Columns, 3.0 x 100 mm

Mobile phase: Pump A = 0.1% formic acid and 20 mM ammonium formate water solution, Pump B = 0.1% formic acid and 10 mM ammonium formate in 90:10 acetonitrile: dd water

Initial flow rate: Pump A = 0.8 mL/min, Pump B = 0 mL/min

Column temperature: 30 ^{o} C

Sample Injection volume: 10 uL

Gradient (%B): 0 min (20%), 6.25 min (40%), 9 min (60%), 10 min (60%), 13 min (100%), 13.01 min (20%), 15 min (20%)

a. Check the connections. Ensure that all the units (pump, autosampler, column oven, and detector) of the instruments are connected to the system controller and optical link cables.

b. Turn the power on for each of the instruments.

c. Turn the PC on.

d. Double-click the "LabSolution" on the desktop.

e. Log in.

[2] LabSolution Main Window. The analytical instruments connected to the PC are displayed as icons.

a. Instruments. Double-click "Instruments" icon to start the program where data acquisition setting are set and data is acquired. Double-click the "HPLC" to start the data acquisition.

b. Postrun. Displays the icons for the [Postrun Analysis] program (data analysis) and the [browser] program (chromatogram display and quantitative calculation of results).

c. Administration. Displays the icons of the system administration programs for setting security policies, user administration and the log browser.

d. Manual. Displays the icons for the various PDF manuals and Help menu provided with LabSolutions.

[3] Open the [Data Acquisition] window. After double-click the "HPLC" icon, there are 7 icons in main window. In normal state, [Ready] is displayed on the top of the window for the status. Follow the recommendations if [Not Connected] is displayed. The power is ON. The instrument are connected right. The system configuration settings are correct.

a. System Configuration. If the system configuration need to be changed, please click on this icons to open the sub-window.

b. System Check. Output the System Check report to ensure every instrument is right.

c. Data Acquisition. Display the icons for the [data acquisition] program.

d. Realtime Batch. Display the icons for the [Realtime Batch] program.

e. Report Format. Display the icons for the [Report format] program.

f. Calculation Curve. Display the icons for the [Calculation Curve] program.

g. Batch Editor. Display the icons for the [Batch Editor] program.

[4] Data acquisition parameters set-up.

a. Open the [Data Acquisition] window

b. Set each of the parameters on the [Simple Settings] tab. If the method already set up and download to the system, please double check the system conditions and write down the parameters in your notebook.

3. System Start up and Purge

[1] Open the [Data Acquisition] window. There are four parts in the window.

a. The first part on the top of the window include the title bar, menu bar, tool bar. The title bar displays the names of the current program, window, loaded file, and other information. Menu Bar displays the current window and menus that area available based on the operating rights of the current user, containing Files, Edit, View, Method, Instrument, Acquisition, Data, Tools, Windows, and Help. Tool bar displays icons of frequently used menu items and icons for operating analytical instruments.

b. The second part in the left of the window [Assistant Bar] displays icons for frequently used data acquisition operations, such as [Instrument Parameters], [Start Single Run], [Stop], and [Data Analysis].

c. The third part in the right of the window displays parameter details and can be changed as experiment conditions change. It includes [Data Acquisition], [LC Time Prog], [pump], [Detector A], [Detector B], [Column Oven], [Controller], [Autosampler], and [AutoPurge] sub-window.

d. Output window at the bottom of the window displays the operation history and error messages that occur.

[2] Click [file] icon in the [Assistant Bar], open method file and double-click the method. Notes: Please refer the method established already in the lab. If you want to make a new method file, please save the old one first.

[3] Click [download] in the third part of the window. Note: please make sure you download the method by confirming the parameters in the third part of the window one by one.

[4] Make sure the valve R in position 1 on the [Column Oven] sub-window, when you start up the system. Notes: In position 1, the mobile phase flows through the waste tubing not the column and detector.

[5] Let the mobile phase flow through the waste tubing for 1 hours. Notes: This step helps us not contaminate our column.

[6] Change the valve R in position 2 on the [Column Oven] sub-window. Notes: The column and tubing in the detector will be purged with this step.

[7] Purge the pump first. Step 1: Turn off the pump click the [pump] on the screen of LC-20AT Pump A. Step 2: Turn the knob 90 degrees to the left. Step 3: Click [purge] on LC-20AT Pump A. Use the same method to purge Pump B.

[8] Purge the autosampler. Click on the [purge] on the Shimadzu SIL-20A autosampler. Notes: It takes 25 minutes.

4. Realtime Batch. Create a Batch Table

a. Open the [Realtime Batch] window.

b. Click on [wizard] icon in the assistant bar at the left of the window.

c. Chose the parameters as follows.

Batch Table: New

Method file: Confirm the method

Injection Volume: 10 uL

Number of Sample groups: 1

Sample Type: Unknown only

Sample Name: Create the name

Sample ID: Create ID

Create file names: Save your data in the file you create

Number of Unknown Sample Vials in each Group: List the number of samples

Repetition per Run: List the number of repetition

Auto Condtioning: Click the [shutdown] icon

Shutdown Method File: Choose the right method

Cool down time: 0 min

Batch file name: Create the name of the batch file

d. Start the realtime batch run by clicking the [Queue Batch Run] icon.

5. Data Analysis

[1] Open the [Postrun Analysis] program.

[2] Open the [Data Analysis] window.

[3] Click [file] in the menu bar.

[4] Open your data file (.lcd)

APPENDIX IV*Clostridium tyrobutyricum* transformation

The transformation of plasmid into *C. tyrobutyricum* was performed *via* conjugation in an anaerobic chamber.

1. Take a single colony of *E. coli CA434* into 2 mL LB liquid medium with 50 μg/mL Kanamycin from LB plate with 50 μg/mL Kanamycin.
2. Inoculate 1 mL overnight cell culture into 100 mL LB with 50 μg/mL Kanamycin (500 mL flask).
3. Shake vigorously at 37 ^{o}C to OD_{600} ~0.25-0.3.
4. Chill the culture on ice for 15 minutes.
5. Chill the 0.1 M $CaCl_2$ solution and 0.1 M $CaCl_2$ PLYS 15% glycerol are on ice.
6. Centrifuge the cells for 10 minutes at 3300 g at 4 ^{o}C.
7. Discard the medium and resuspend the cell pellet in 20-40 mL cold 0.1 M $CaCl_2$.
8. Keep the cells on the ice for 30 minutes.
9. Centrifuge the cells as above.
10. Remove the supernatant and resuspend the cell pellet in 6 mL 0.1 M $CaCl_2$ solution plus 15% glycerol.
11. Pipet 0.2 mL of the cell suspension into the sterile 1.5 mL micro-centrifuge tubes.
12. Freeze these tubes on dry ice and then transfer them to -80 ^{o}C.
13. Transform target plasmid into *E. coli CA434* with heat shock (42 ^{o}C) method.
14. Make stocks of the *E. coli CA434* with target plasmid by 20% glycerol in -80 ^{o}C.

15. Take a colony of *C.tyrobutyricum* from RCM plate into 3 mL RCM medium.
16. Incubate *C.tyrobutyricum* to reach OD_{600} 1.5 and inoculate cell into 3 mL RCM medium.
17. Take a colony of *E. coli CA434* with target plasmid from LB plate with 50 μg/mL Kanamycin and 30 μg/mL Chloramphenicol into 3 mL LB liquid medium with with 50 μg/mL Kanamycin and 30 μg/mL Chloramphenicol.
18. Incubate *E. coli CA434* with target plasmid overnight at 37 ºC and inoculate 0.1 mL cell into 100 mL LB medium with 50 μg/mL Kanamycin and 30 μg/mL Chloramphenicol.
19. Inoculate 0.5 mL *C.tyrobutyricum* into 50 mL RCM medium and incubate overnight at 37 ºC to reach OD_{600} 2.0-3.0.
20. Incubate *E. coli CA434* with target plasmid overnight at 37 ºC to reach OD_{600} 1.5–2.0.
21. Centrifuge 3 mL *E. coli CA434* with target plasmid at 4000 g for 2 minutes. Discard the supernatant.
22. Re-suspend the *E. coli CA434* with target plasmid by 3 mL sterile PBS buffer and centrifuge the mixture at 4000 g for 2 minutes. Discard the supernatant.
23. Re-suspend the *E. coli CA434* with target plasmid by 0.4 mL *C.tyrobutyricum*.
24. Gently pipette all of the cell mixture drop by drop onto a RCM plate.
25. Incubate the conjugation plate for 8 hours at 37 ºC under anaerobic condition.
26. Recover the all the cells from the conjugation plate with 1 mL RCM medium.
27. Inoculate the cells into 50 mL RCM medium with 30 μg/mL of Thimaphenicol and 250 μg/mL of D-cycloserine.
28. Incubate cells for 72-96 hours to reach OD_{600} ~ 2.0 and centrifuge the cells at 10000 g for 10 minutes.

29. Re-suspend the cells into 50 mL RCM medium with 30 μg/mL of Thimaphenicol and 250 μg/mL of D-cycloserine.
30. Incubate cells overnight to reach OD_{600} ~ 2.0 and centrifuge 25 mL cells at 10000 g for 10 minutes.
31. Re-suspend the cells into 50 mL RCM medium with 30 μg/mL of Thimaphenicol and 250 μg/mL of D-cycloserine.
32. Incubate cells overnight to reach OD_{600} ~ 2.0 and centrifuge 10 mL cells at 10000 g for 10 minutes.
33. Re-suspend the cells into 50 mL RCM medium with 30 μg/mL of Thimaphenicol and 250 μg/mL of D-cycloserine.
34. Incubate cells overnight to reach OD_{600} ~ 2.0 and centrifuge 5 mL cells at 10000 g for 10 minutes.
35. Re-suspend the cells into 50 mL RCM medium with 30 μg/mL of Thimaphenicol and 250 μg/mL of D-cycloserine.
36. Incubate cells overnight to reach OD_{600} ~ 2.0 and centrifuge 2 mL cells at 10000 g for 10 minutes.
37. Re-suspend the cells into 50 mL RCM medium with 30 μg/mL of Thimaphenicol and 250 μg/mL of D-cycloserine.
38. Incubate cells overnight to reach OD_{600} ~ 2.0 and centrifuge 1 mL cells at 10000 g for 10 minutes.
39. Re-suspend the cells into 50 mL RCM medium with 30 μg/mL of Thimaphenicol and 250 μg/mL of D-cycloserine.
40. Incubate cells overnight to reach OD_{600} ~ 2.0.

41. Spread cells on RCM selection plates that contained 30 μg/mL of Tm and 250 μg/mL of D-cycloserine.
42. Incubate cells to reach OD_{600} ~ 2.0.
43. Pick up twenty colonies and evaluate in 50-mL serum bottle culture to screen the clone with the highest butanol production.

APPENDIX VProteomics sample preparation

The cells of all strains at 30 min post inoculation to evaluate the baseline and the fermentations were sampled in mid-log phase to prepare the proteomics samples. The protein content in the lag phase samples was minimal and ignored in the proteomics study. At sampling point of mid-log phase, the OD_{600} were monitored and recorded.

1. Collect 2 mL cells from fermenters

2. Centrifuge the cells at 14,000 rpm for 10 mins at 4 ^{o}C.

3. Discard the supernatant.

4. Re-suspend the cell pellets using 2mL PBS buffer.

5. Centrifuge the mixture at 14,000 rpm for 10 mins at 4 ^{o}C.

6. Discard the PBS buffer.

7. Wash the cell pellets three times as step 4-6.

8. Store the washed cell pellets at -80 ^{o}C.

APPENDIX VIHigh performance liquid chromatography (HPLC) diagrams

VII.1 HPLC standard diagram for substrate and products

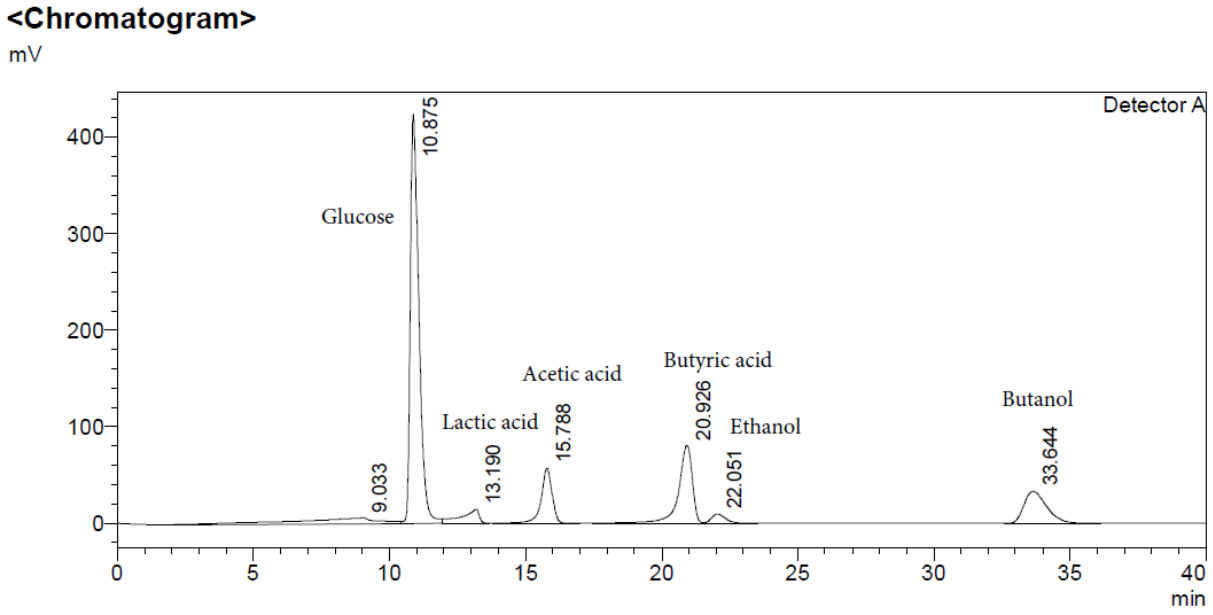

Figure II.1 HPLC standard diagram for analysis of Glucose, Lactic acid, acetic acid, butyric acid ethanol, and butanol, using external standard method (Glucose 60 g/L, lactic acid 12 g/L, acetic acid 24 g/L, butyric acid 30 g/L, ethanol 6 g/L, butanol 20 g/L).

VII.2 HPLC standard diagram for amino acids

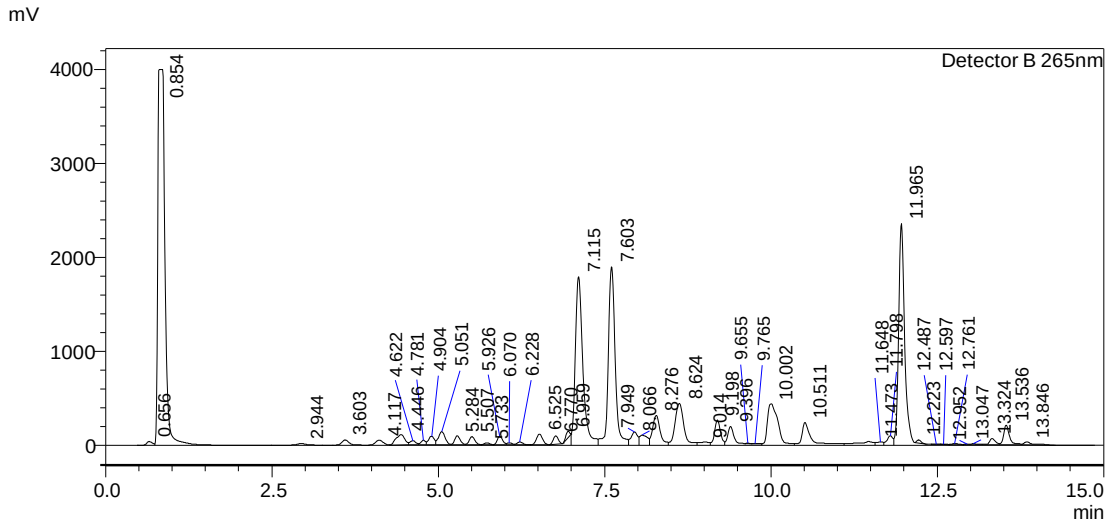

Figure II.2 HPLC standard diagram for analysis of amino acids, using external standard method (Arginine 5.051 min, serine 5.926 min, aspartic acid 6.228 min, glutamic acid 6.510 min, threonine 6.770 min, glycine 7.115 min, alanine 8.276 min, proline 8.624 min, methionine 9.655 min, valine 9.765 min, Cysteine 10.511 min, histidine 11.965 min, lysine 12.223, tyrosine 12.761. Each amino acid is 0.5 μmole/mL).

APPENDIX VII CGM medium formula

Comp.	Con.
KH_2PO_4	0.75 g/L
K_2HPO_4	0.982 g/L
$(NH4)_2SO_4$	2 g/L
NaCl	1 g/L
$FeSO_4$	0.01 g/L
$MnSO_4$	0.01 g/L
$MgSO_4$	0.348 g/L
Asparagine	2 g/L
Yeast extract	5 g/L
Tryptone	4 g/L
Sodium Acetate	2.46 g/L
Sodium Butyrate	3.6 g/L
PABA（After autoclave）	0.004 g/L

APPENDIX VIII Diagram of free-cell fermentation

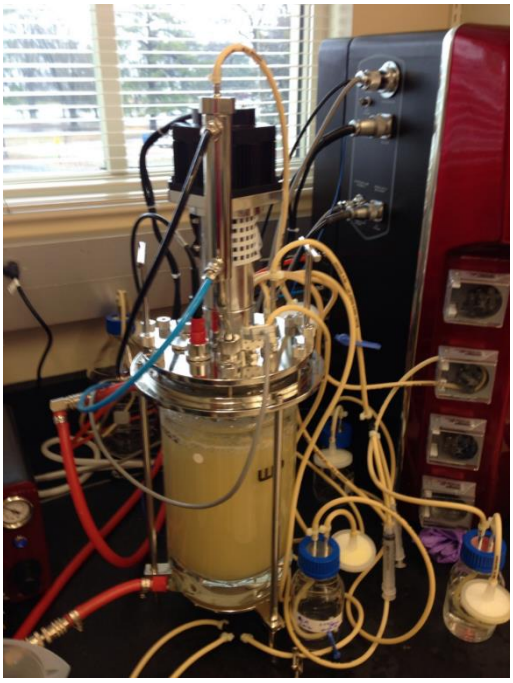

1. Free-cell fermentation set up

[1] Make 1 L 2x concentrated CGM medium.

[2] Make 1 L 80g/L glucose solution.

[3] Make 1 L 5 N NaOH solution.

[4] Connect the fermenter with CGM, glucose solution and NaOH solution.

[5] Autoclaving the fermenter at 121 ^{o}C for 60 mins.

[6] Sparge the fermenter with nitrogen gas at a flow rate of 10 mL/min for 3 hrs to reach anaerobiosis.

[7] Inoculate fresh seed culture with optical density at 600 nm (OD_{600}) of 1.5.

[8] Make sure seeding density of OD_{600} to reach ~0.04.

[9] Control Temp 37 ^{o}C, agitation 100 rpm, and pH controlled at 6.0±0.1.

[10] Feed concentrated glucose stock (400 g/L) to fermentation broth when the sugar level decreases below 10 g/L.

[11] Take sample twice a day to monitor cell growth and titrate substrate and products.

2. Sampling

[1] Collect 2x2 mL cells from fermenters

[2] Centrifuge the cells at 14,000 rpm for 10 mins at 4 ^{o}C.

[3] Add the supernatant into a new 2 mL tube.

[4] Centrifuge the supernatant at 14,000 rpm for 10 mins at 4 ^{o}C.

[5] Add the supernatant into a new 2 mL tube.

[6] Test glucose, products, and amino acid with 2 mL supernatant using HPLC.

[7] Store the other 2 mL supernatant at -80 ^{o}C

APPENDIX IX Flow chat of FBB

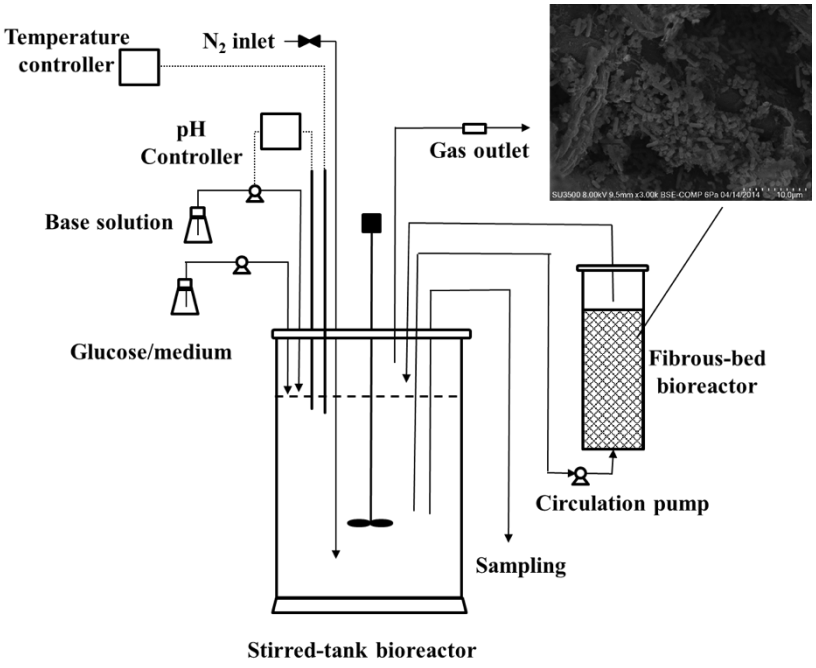

3. Immobilized-cell fermentation set up

[1] Make 1.5 L 2x concentrated CGM medium.

[2] Make 1.5 L 160g/L glucose solution.

[3] Make 1 L 5 N NaOH solution.

[4] Connect the fermenter with CGM, glucose solution and NaOH solution.

[5] Autoclaving the fermenter at 121 ^{o}C for 60 mins.

[6] Sparge the fermenter with nitrogen gas at a flow rate of 10 mL/min for 3 hrs to reach anaerobiosis.

[7] Inoculate fresh seed culture with optical density at 600 nm (OD_{600}) of 1.5.

[8] Make sure seeding density of OD_{600} to reach ~0.04.

[9] Control Temp 37 ^{o}C, agitation 100 rpm, and pH controlled at 6.0±0.1.

[10] Feed concentrated glucose stock (400 g/L) to fermentation broth when the sugar level decreases below 10 g/L.

[11] Take sample twice a day to monitor cell growth and titrate substrate and products.

4. Sampling

[1] Collect 2x2 mL cells from fermenters

[2] Centrifuge the cells at 14,000 rpm for 10 mins at 4 ^{o}C.

[3] Add the supernatant into a new 2 mL tube.

[4] Centrifuge the supernatant at 14,000 rpm for 10 mins at 4 ^{o}C.

[5] Add the supernatant into a new 2 mL tube.

[6] Test glucose, products, and amino acid with 2 mL supernatant using HPLC.

[7] Store the other 2 mL supernatant at -80 ^{o}C

APPENDIX X List of publications

Journal Publications

[1] C. Ma, J. Ou, N. Xu, J.L. Fierst, S.T. Yang, X.M. Liu. “Rebalancing redox to improve biobutanol production by *Clostridium tyrobutyricum*”. Bioengineering, vol. 3, 2015.

[2] C. Ma, J. Ou, S. McFann, M. Miller, X.M. Liu. "High production of butyric acid by Clostridium tyrobutyricum mutant". Front. Chem. Sci. Eng., vol. 9, 369-375, 2015.

[3] C. Ma, K. Kojima, N. Xu. "Comparative proteomics analysis of high n-butanol producing metabolically engineered *Clostridium tyrobutyricum*". J. Biotechnol., vol. 193, pp. 108-119, 2015.

[4] J. Ou, C. Ma, N. Xu, Y. Du, X.M. Liu. "High Butanol Production by Regulating Carbon, Redox and Energy in Clostridia". Front. Chem. Sci. Eng., vol. 9, pp. 317-323, 2015.

[5] N. Xu, C. Ma, W. Sun, Y. Wu, X.M. Liu. “Achievements and perspectives in Chinese hamster ovary host cell engineering”. Pharmaceutical Bioprocessing, vol. 3, pp. 285-292, 2015.

[6] S. McFann, L. Mathews, M. Leffler, C. Dietrich, A. Crumbley, Chao Ma, and X.M. Liu. “Metabolic Flux Model to optimize n-butanol production by *Clostridium tyrobutyricum*”. JOSHUA, vol. 12, pp. 29-34, 2015.

[7] R. Lind, C. Ma, X.M. Liu. “Production of Butyric Acid by Metabolically Engineered *Clostridium tyrobutyricum*”. Joshua, vol. 11, pp. 4-7, 2014.

[8] H. Bowers, K. Triplett, G. Lim, N. Xu, C. Ma, and X.M. Liu. “High-Level Expression of Targeted Anti-Cancer Biopharmaceuticals Using CHO Cell”. Joshua, vol. 11, pp. 8-11, 2014.

[9] C. Lu, C. Ma, and X.M Liu. “Minireview: High-Productivity and Low-Cost Biobutanol Production by Integrated Process Development”. International Journal of Innovative Research in Science & Engineering, vol. 1, 2014.

Presentations

[1] C. Ma, J. Ou, X.M. Liu. Metabolic Engineering of *C. tyrobutyricum* for High n-Butanol Production by Rebalancing Carbon and Redox. AIChE Annual Meeting, Salt Lake City, UT, November 2015.

[2] C. Ma, J. Ou, X.M. Liu. Analysis of Amino Acids Metabolism in Butanol Fermentation by *Clostridium tyrobutyricum*. AIChE Annual Meeting, Salt Lake City, UT, November 2015.

[3] J. Ou, C. Ma, X.M. Liu. Omics Guided Rationally Metabolic Engineering of *Clostridium tyrobutyricum*. AIChE Annual Meeting, Salt Lake City, UT, November 2015.

[4] N. Xu, C. Ma, Y. Yang, X.M. Liu. Comparative Proteomic Analysis of Host and High Biopharmaceuticals Producing CHO Cell Lines. AIChE Annual Meeting, Salt Lake City, UT, November 2015.

[5] S. McFann, L. Mathews, C. Mayhugh, J. Robinson, C. Ma. X.M. Liu. Constraint-Based Metabolic Model Elucidates Energy, Reducing Power, and Carbon Flux Distribution in *Clostridium tyrobutyricum* for Optimization of n-Butanol Production. AIChE Annual Meeting, Salt Lake City, UT, November 2015.

[6] L. Mathews, C. Dietrich, M. Leffler, W. Smith, C. Ma, X.M. Liu. Process Optimization to Improve Butyric Acid Production with *Clostridium tyrobutyricum*. AIChE Annual Meeting, Salt Lake City, UT, November 2015.

[7] C. Ma. X.M. Liu. Comparative Proteomics Analysis of High Butyrate and Butanol Producing Clostridium tyrobutyricum Mutants. AIChE Annual Meeting, Atlanta, GA, November 2014.

[8] C. Ma, S.T. Yang, and X.M. Liu. Genomic and Proteomic Analysis to Characterize Butyric Acid Fermentation by Metabolically Engineered Clostridium tyrobutyricum. AIChE Annual Meeting, Atlanta, GA, November 2014.

[9] C. Ma, N. Xu, L. Zhou, S.T. Yang, and X.M. Liu. How to Increase Butanol Production by Metabolic Cell-Process Engineering of *Clostridium tyrobutyricum*. AIChE Annual Meeting, Atlanta, GA, November 2014.

[10] C. Ma, N. Xu, X.M. Liu. Improve Biobutanol Production by Integrated Carbon and Redox Rebalance in *Clostridium tyrobutyricum*. AIChE Annual Meeting, Atlanta, GA, November 2014.

[11] K.S. Venkatesh Babu, C. Ma**,** X.M. Liu. Process Engineering of *Clostridium tyrobutyricum* to Improve Butyric Acid Production. AIChE Annual Meeting, Atlanta, GA, November 2014.

[12] R. Lind, C. Ma, and X.M. Liu. Butanol Production Improvement by Metabolically Engineered *Clostridium tyrobutyricum* ATCC 25755. AIChE Southern Regional Conference, Puerto Rico, March 2014.

[13] C. Ma, N. Xu, and X.M. Liu. Application of Omics technologies in n-biobutanol production by metabolically engineered *C. tyrobutyricum*. AIChE Annual Meeting, San Francisco, CA, November, 2013.

[14] N. Xu, C. Ma, and X.M. Liu. Proteomics: Mechanism of Biosimilar Quality Regulation in Three CHO Host Cells. AIChE Annual Meeting, San Francisco, CA, November, 2013.

[15] E. Parcher, C. Ma, X.M. Liu. Biobutanol Production Using *Clostridium tyrobutyricum* By Integrating Metabolic Engineering and Process Development. AIChE Annual Meeting, San Francisco, CA, November, 2013.

[16] B. Artale, C. Ma, and X.M. Liu. Metabolic engineering of *Clostridium tyrobutyricum* to improve biofuel production by boosting reducing power. AIChE Annual Meeting, San Francisco, CA, November, 2013.

[17] C. Ma, X.M. Liu. How to balance the productions of butyric acid and butanol by metabolic engineering of *C. tyrobutyricum*. ACS Annual Meeting, New Orleans, LA, April 2013.

[18] C. Ma, X.M. Liu. How to increase the butonal production by metabolic engineering of *C. tyrobutyricum*, SEC Symposium, Atlanta, GA, February, 2013.

[19] M. Bakies, C. Ma, X.M. Liu. C4 biofuel and high value biochemical production using metabolically engineered clostridia. AIChE Annual Meeting, Pittsburgh, PA, 2012.